ABSTRACT

SHARMIN, NADIA. Performance Optimization of LNAPL Three Phases Extraction by Prefabricated Vertical Wells (PVWS). (Under the direction of Dr. M. A. Gabr).

The use of petroleum products has sometimes been implemented with inadequate storage and disposal practices, which led to widespread contamination of the subsurface environment. Liquid petroleum products having a density less than water are referred to as Light Non Aqueous Phase Liquids (LNAPL), and are commonly found at the interface of unsaturated and saturated zones. LNAPL fluctuate with groundwater table and form a 'smear zone' occupied by ganglia. Remediation of these residual ganglia is extremely challenging even with today's advanced technology.

Research presented herein is focused on investigating the extraction of multiphase subsurface organic contamination using in situ approach termed Well Injection Depth Extraction (WIDE). The research encompasses field and modeling studies. The field study, performed at a former air force base in Ohio, included monitoring system performance, in terms of extracted liquid and gas phases, over 185 operating hours on 38 separate days. The modeling study consisted of three parts: i) groundwater modeling, ii) contaminant transport modeling, iii) multiphase flow and transport modeling. The modeling study attempted to characterize phase transfer mechanism as a function of air permeability and suction head, study the mechanics involved with controlled lowering/raising of groundwater table through system optimization, and investigate effect of subsurface hydrogeologic parameters (permeability, porosity) on the ability to extract LNAPL source

and the magnitude of the residual phases. Modeling results were also used in an optimization scheme to investigate schedules for lowering of groundwater table and extraction efficiency.

The results from this study document field data on system performance for extraction of LNAPLs in a subsurface with lenticular morphology. The field results were used to calibrate the models used in the analytical studies. Results from the analytical studies explained phenomena related to various phase extraction based on well spacing, and impact of subsurface parameters on residual LNAPL distribution and preferential phase for extraction. The optimization analyses provided a framework for establishing a process for systematic lowering of groundwater table to target residual phase with volatilization, and optimize well spacing for maximum removal of contaminant mass.

Performance Optimization of LNAPL Three Phases Extraction by Prefabricated Vertical Wells (PVWs)

by
Nadia Sharmin

A dissertation submitted to the Graduate Faculty of
North Carolina State University
in partial fulfillment of the
requirements for the Degree of
Doctor of Philosophy

Civil Engineering

Raleigh, North Carolina

2009

APPROVED BY:

Dr. Mohammed A. Gabr Chair of Advisory Committee	Dr. Roy H. Borden
Dr. M. Shamimur Rahman	Dr. G. Kumar Mahinthakumar

DEDICATION

This work is dedicated to my wonderful parents,

for reasons too numerous to mention

BIOGRAPHY

Nadia Sharminn was born in Dhaka, Bangladesh on January 6, 1978. She graduated from Viquarunnisa Noon Scool and College in 1994 and subsequently enrolled in the Civil Engineering Program at Bangladesh University of Engineering and Technology (BUET). Following graduation, Nadia secured a lecturer position with Ahsanullah University of Science and Technology and initiated her graduate education at BUET. Nadia received her Masters of Science Degree in Civil Engineering from BUET in August 2004 and started her Ph.D. at North Carolina State University during the fall semester of 2004. As a Ph.D. candidate, Nadia was a research and teaching assistant. She enjoyed every moment of her Ph.D. life in North Carolina.

ACKNOWLEDGEMENTS

First and foremost, I would like to express my sincere thanks to my Advisor Dr. Mohammed Gabr. I have learnt a lot from him both academic and otherwise, and I consider myself fortunate for getting the opportunity to work under his supervision. This piece of work would be impossible for me without his help and guidance.

Dr. G.. Kumar Mahinthakumar was an excellent resource during the optimization analysis component of my research. Special thanks to him for his support and inspiration during the terminal stage of this research.

I would like to thank Dr. Roy H. Borden, Dr. Shamim Rahman and Dr. John Havlin for taking part in my graduate career as a member of my doctoral committee. I sincerely appreciate your time and effort.

I would like to thank the Army Corps of Engineers for their support. The research presented herein was partially sponsored by the Army Corps of Engineers and their feedback is highly appreciated.

I am grateful to my mentor Dr. Sahadat Hossain for providing me guidance ever since I was preparing to apply for graduate studies. I am indebted to Dr. Feroze Ahmed, my M.Sc. supervisor for his encouragement.

Many many thanks to my sister Shaila Urmi who from day one saw me graduating and leaving her and in a way is a proxy for my mother. Thanks to my brother in law Mahmood for creating a home for me away from my own. Very special thanks to my nephew Arshaan, who never allowed me a single moment to miss anyone or anything.

I could not have reached this point in my life without the care, never ending support and guidance of my parents, Azizul Haque and Selima Begum. I am indebted to them for their endless love, affection and sacrifices. Thanks also to my brother Neil for his encouragement.

Last, but by no means least, thanks go to my husband Rashed for his endless sacrifice, patience and counting days of my return to him.

TABLE OF CONTENTS

LIST OF TABLES

LIST OF FIGURES

1. INTRODUCTION

BACKGROUND

Petroleum liquids are the nucleus of modern civilization. However, the use of petroleum products has sometimes been practiced with inadequate storage and disposal that led to widespread contamination of the subsurface environment. The United States Environmental Protection Agency (EPA) estimates that roughly 11 million gallons of gasoline per year are lost due to leaking from underground storage tanks (Brauner et al. 1996). In North Carolina, over 2000 petroleum contamination incidents from underground storage tanks have been identified. (Water Resources Grant Proposal 1997).

Petroleum products, having a density less than water, are referred to as Light Non Aqueous Phase Liquids (LNAPL). LNAPL can be present in subsurface in all four phases (free product, dissolved, vapor and sorbed), each of which adds its own distinct complication to implementing effective remediation technique. Hydrocarbon contamination of soil and water by LNAPL in the subsurface has been the focus of much attention for the past 20 years (e.g. Reddi et.al. 1998, Gordon et. al. 2002, Ewing et. al. 2002, Adamski et. al. 2005). LNAPL pools formed at the interface of unsaturated and saturated zones fluctuate with groundwater table and form a `smear zone' that is occupied by LNAPL ganglia or blobs (Reddi, 1998). Eventually LNAPL residual globules represent potential long term source for continued groundwater contamination. Recovery of these residual ganglia has made LNAPL remediation extremely challenging and adds

uncertainties to the possible achievement of specified end points of remediation.

PROBLEM STATEMENT

David Miller, co-founder of Geraghty and Miller, suggested “trying to clean up an aquifer is like trying to get all the soap out of a sponge”. Taking this comment further, American Petroleum Institute (API) believes that complete remediation of LNAPL contaminated aquifer means squeezing oil soaked sponge an extended period of time. To date, a variety of technologies have been used in an attempt to remediate LNAPL-contaminated sites. The remediation of such aquifers by the conventional pump-and-treat methods has been shown to be extremely inefficient as the pump and treat processes can not provide hydraulic gradients large enough to overcome the capillary forces trapping the ganglia within the pore spaces (Pennel, 1996, Reddi, 1998). In this case, water may flow around the ganglia within the pores. Commonly, traditional pump and treat systems exhibit tailing and rebounding effect in LNAPL contamination cases.

Other possible approaches for LNAPL removal from saturated zone include chemical oxidation, steam injection, and in situ bioremediation and alternated electron where as bioventing can be employed in a vadose zone. Air sparging is also a potentially effective means of treating LNAPL, as this method promotes both biodegradation and volatilization. However, the possibility of spreading the contaminant in significantly stratified subsurface limits the use and versatility of air sparging.

In summary, an effective remediation approach of LNAPL not only encompasses a

specific method or mechanism, but also equally important is how such mechanism is deployed. In addition, the flexibility with which a given phase of LNAPL contamination can be targeted at a given time, taking geologic and groundwater conditions into account, is a condition needed by agencies and organizations looking to further develop the contaminated sites for commercial purposes.

Research presented herein is focused on investigating the extraction of multiphase LNAPL contamination using prefabricated vertical wells (PVWs) installed on relatively close spacing (typically on the order of 2 m.) The research encompasses field and modeling studies. The field study, performed at a former air force base in Ohio, includes monitoring system performance in terms of extracted liquid and gas phases. The modeling study consists of three parts: i) groundwater modeling, ii) contaminant transport modeling, iii) multiphase flow and transport modeling. The modeling effort attempts to characterize phase transfer mechanism as a function of air permeability and suction head, study the mechanics involved with controlled lowering/raising of groundwater table through system optimization, and investigate effect of key subsurface hydrogeologic parameters and boundary conditions on the ability to extract LNAPL source and the magnitude of the residual phases. Modeling also included an optimization scheme to investigate schedules for lowering of groundwater table, and schemes for spatial distribution of the PVWs for effective extraction process of a given phase.

OBJECTIVE

The overall objective of the research is to expand our knowledge in the area of LNAPL remediation and the mass transfer using an in situ remediation system that relies on prefabricated wells installed on a close spacing (1-3 m). The research work encompasses field and modeling studies. The primary research objectives are:

1) Implement and operate pilot-scale field test pad to monitor and characterize system performance in terms of extracted liquid and gas phases resulting from LNALP contamination,
2) Investigate effect of subsurface hydrogeologic parameters on the ability to extract LNAPL source, and changes in the magnitude of the residual phases. These parameters include extraction rates, hydraulic conductivity (referred to as permeability,) irreducible water content, LNAPL and gas contents, LNAPL thicknesses, and loadings from hydrocarbon for both soluble and gas phases.
3) Explain the phase transfer mechanism during the extraction process as a function of permeability and suction head as well as domain boundary conditions,
4) Study the mechanics involved with the ability to systematically control the lowering/raising of groundwater table through optimization of system operation,

5) Develop a scheme to maximize the extraction of a specific contamination phase by providing optimized spatial location of PVWs and investigate parameters affecting extraction rates.

SCOPE OF THE THESIS

The dissertation work is presented in four technical papers with equations included within the text, but tables, figures and references are presented at the end of each paper (included as chapters). In the first Chapter, the introduction and objectives of the research are defined followed by literature review. The first paper thereafter details the field demonstration testing component of this research along with the multiphase flow and transport model. The multi phase model focuses on the remediation time for each contamination phases: LNAPL, vapor, and soluble phase. The second paper is focused on developing and validating a model, and conducting a sensitivity analysis of parameters affecting multiphase flow and transport processes. Impact of hydrogeologic parameters and well spacing on phase transfer and remediation process are investigated. The third paper discusses a finite element modeling that is developed to study the impact of the extraction process, using PVWs, on the groundwater head distribution and contaminant transport. An optimization process is employed to develop an operating schedule for control of groundwater elevations within the remediation zone. The fourth paper presents optimization analysis to establish a frame work regarding the development of a spatial configuration for PVWs forming the WIDE system and investigate aspects related to

mass transfer during the extraction process.

The last chapter summarizes the components of the research detailed in the four papers, describes the conclusions and contributions to the state of the art, and provides recommendations for future research.

Appendix A, B, C and D present the detail boring logs for field soils, the equations of multiphase flow, the input to the multiphase model, and a sample of optimization program respectively.

REFERENCES

Adamski, M., Kremesec, V., Kolhatkar, R., Pearson, C., Rowan, B.(2005). "LNAPL in fine-grained soils: Conceptualization of saturation, distribution, recovery, and their modeling". *Ground Water Monitoring and Remediation*. 25(1): 1069-3629

Brauner, J. S & Killingstad, M. (1996)."In situ Bioremediation of Petroleum Aromatic Hydrocarbons".http://www.cee.vt.edu/ewr/environmental/teach/gwprimer/btexbio/btexbio.html

Ewing, J. E., Dwarakanath, V., Gordon, K. D., Meinardus, H. W., Ginn, J. S. (2002). "Evaluation of LNAPL recovery using soil vapor extraction, Proceedings of the Third International Conference on Remediation of Chlorinated and Recalcitrant Compounds". *Proceedings of the Third International Conference on Remediation of Chlorinated and Recalcitrant Compounds*. 1705-1713

Gordon, K. D., Jin, M., Meinardus, H. W., Ginn, J. S. (2002) "Multi-phase fluid flow evaluation of lnapl recovery using containment trenches". *Proceedings of the Third International Conference on Remediation of Chlorinated and Recalcitrant Compounds*. 1689-1696

Pennell, K. D., Abriola, L. M., Loverde, L. E. (1996). “Use of surfactants to remediate NAPL-contaminated aquifers”.*ASCE Specialty Conference, Proceedings, Non-Aqueous Phase Liquids (NAPLs) in Subsurface Environment: Assessment and Remediation.* 221-232

Reddi, L. N., Menon, S., Pant, A. (1998). “Pore-scale investigations on vibratory mobilization of LNAPL ganglia”. *Journal of Hazardous Materials.* 62(3): 211-230.

Water Resources Grant Proposal. (1997). “Limiting Factors in the Bioremediation of Soil and Groundwater Contaminated With Aromatic Hydrocarbons”. *http://water.usgs.gov/wrri /96 grants/seir13nc.htm*

2. LITERATURE REVIEW

BACKGROUND

Technologies to remediate LNAPL, even as recently as the 1980, have considered "pancake" conceptualization for LNAPL distribution and migration in subsurface (Remediation Technologies Development Forum 2005). The 80's "pancake" model envisioned LNAPL as a single phase fluid and the pores fully saturated with LNAPL floating on water table (or capillary fringe) which is completely recoverable. Based on Dullian's (1979) "Porous Media: Fluid Transport and Pore Structure" concept, Parker et al. (1990) and Farr et al. (1990) modified the single mobile phase "or pancake' concept to "multiphase model". The LNAPL "multiphase model" included the critical influence of capillarity. The new hypothesis considered LNAPL to coexist with water and air in the "LNAPL saturation zone". Figure 2-1 illustrates the presence of LNAPL in porous media (API 2003).

Research to remediate LNAPL reveals that as LNAPL is depleted by dissolution or 'pump and treat' remediation technology, its saturation decreases. The LNAPL pathway becomes smaller, and tortuous, with depletion which reduces its mobility. Eventually the non wetting fluid LNAPL breaks into immobile and isolated blobs or ganglia and is entrapped by water as wetting fluid. Entrapment of LNAPL at residual saturation, fluctuating groundwater table, the wide range of solubility and viscosity of LNAPL components, and stringent end points of remediation specified by regulatory

agencies have made LNAPL remediation challenging (API 2003).

LNAPL PHASE DISTRIBUTION IN SUBSURFACE

Upon release to the environment, LNAPL migrates vertically until residual saturation depletes the liquid or until the capillary fringe is reached (Norris et al 1993). Newell et al. (1993) published that LNAPL constituents can be in four phases in subsurface. The phases are:

1) Air Phase-vapor in the pore space
2) Aqueous Phase-dissolved in water
3) Liquid Phase-free or mobile phase non aqueous LNAPL
4) Adsorbed Phase-sorbed to subsurface solid

In the unsaturated zone, LNAPL may exist in all four phases. In the saturated zone, LNAPL may exist in aqueous, free phase and adsorbed phases. Figure 2-2 shows the partitioning of LNAPL among the four phases potentially available in the unsaturated zone.

LNAPL AND WATER SATURATION DISTRIBUTION

The apparent thickness of LNAPL obtained from monitoring well is more than that of the actual free product in field. (Scheigg 1985). An idealized conceptual relationship between free-product thicknesses in the well and in the soil is shown in Figure 2-3. The upper surface of the LNAPL layer is termed the “air-oil interface (Z_{ao})”

and the lower surface of the oil is termed as “oil-water interface (Z_{ow})”. The actual elevation of the potentiometric surface cannot be measured directly in the well, but can be calculated by equation 1.

$$z_{aw} = \left(1 - \frac{r_o}{r_w}\right) z_{ow} + \frac{r_o}{r_w} z_{ao} \qquad \textbf{Equation (1)}$$

where

ρ_o= density of LNAPL

ρ_w= density of water

The LNAPL saturation distribution in the porous vadose-saturated zone over the depth interval between the LNAPL/water interface and the air/LNAPL interface is a function of the water-LNAPL capillary pressure (LNAPL is generally the non-wetting fluid compared to water). The distribution of the LNAPL saturation above the air/LNAPL interface is a function of the LNAPL-air capillary pressure, where LNAPL is the wetting fluid compared to air. The complete LNAPL saturation profile can be obtained from having both the water-LNAPL and LNAPL-air capillary pressure curves. (Ballestro, 1995, Bedient, 1999; Science Advisory Board, British Columbia, 2006; API 2003).

API publication number 4729 developed the LNAPL and water saturation distribution theory on the basis of work done by Van Genuchten. Van Genuchten (1980) related the water saturation (S_w) to suction pressure head (h) through the following

equation:

$$S_w(h) = S_{wr} + (1 - S_{wr})\left[\frac{1}{1+(ah)^n}\right]^m \qquad \textbf{Equation (2)}$$

Where Swr = irreducible water saturation

α and n are Van Genuchten model parameters, and,

m = 1-1/n

Equation 2 can be written as

$$\Theta_w(h) = \left(\frac{S_w(h) - S_{wr}}{1 - S_{wr}}\right) = \left[\frac{1}{1+(ah)^n}\right]^m \qquad \textbf{Equation (3)}$$

Where Θ_w = air-water reduced saturation

Equation 3 scales the water saturation in 0 to 1 range. Using Leverett assumptions for the LNAPL-water pair, the water saturation can be represented in equation 4. Equation 5 shows the total fluid (water and LNAPL)-air saturation distribution at any depth z (Van Genuchten 1980). The symbols used in equation 4 and 5 are as follows:

$S_w(z)$= water saturation

$S_o(z)$= LNAPL saturation

$S_{ors}(z)$= Residual LNAPL saturation in the saturated zone

$S_{orv}(z)$= Residual LNAPL saturation in the vadose zone

$S_t(z)$= Total fluid (LNAPL and water) saturation

S_{wr} = Irriducible water saturation

For LNAPL-water pair

$$S_w(z) = S_{wr} + (1 - S_{wr} - S_{ors})\left[\frac{1}{1+(a_{ow}(z - z_{ow}))^n}\right]^m \qquad \textbf{Equation (4)}$$

Where z_{ow} = LNAPL-water Interface

α_{ow} = Scaling parameter in LNAPL-water interface

For Total fluid (LNAPL and water)-air pair

$$S_t(z) = S_{wr} + S_{orv} + (1 - S_{wr} - S_{orv})\left[\frac{1}{1+(a_{ao}(z - z_{ao}))^n}\right]^m \qquad \textbf{Equation (5)}$$

Where z_{ao} = Air-LNAPL Interface

α_{ow} = Scaling parameter in Air-LNAPL interface

$S_t(z)= S_w(z)+ S_o(z)$

For $z< z_{ao}$

$$S_t(z)= 1$$

For $z< z_{ow}$

$$S_w(z)= 1- S_{ors}(z)$$

A qualitative example of LNAPL saturation distribution with respect to depth is

presented in Figure 2-4. The dashed line on the left of Figure 2-4 shows the residual LNAPL distribution. The residual LNAPL distribution (within the free product LNAPL layer) corresponds to the amount of free product LNAPL that would become immobile with free LNAPL recovery. Capillary forces trap LNAPL only as the LNAPL saturation is reduced (API 2003).

REMEDIATION OPTIONS

Active and passive remediation technologies for LNAPLs are generally classified into in-situ and ex-situ approaches. In contrast to a passive system, an active system seeks to mobilize the plume toward extraction points strategically placed to capture the mobilized contaminants. In the case of the subject site, a main objective of the active remediation system is to reduce the amount of free products, or LNAPL, within the subsurface to the extent possible as free products act as a continuous contamination source. The active system addressed here is the WIDE for soil flushing, while passive systems discussed are bioremediation, air sparging and bioventing.

The soil flushing processes normally refers to the in-situ extraction of contaminants and utilizes water, with or without chemical additives, as the primary washing fluid. Chemical additives including surfactants, acids, and solvents, are used to promote desorption and solubilization. The conventional soil flushing process involves a number of steps, with the hydrogeologic conditions of the contaminated area being extremely important to the success of the process. These steps are:

1) Solubilization and mobilization of the contaminants,

2) Extraction of the contaminants from the subsurface,

3) Contaminant treatment and/or disposal

As such, soil flushing is considered an active remediation approach whereby a gradient is induced through the system to mobilize the contaminants toward extraction points. In comparison, a passive system mostly relies on the site's natural gradient for mobilization of contamination toward a system whereby a form of oxidation or chemical/biological conversion is induced. For example, a remediation curtain can be installed down gradient of a migrating plume. Such a curtain may include microorganisms for bioremediation or reactive material for oxidation and degradation of contaminants. A passive remediation curtain can also be enhanced with air sparging and bioventing processes. For relatively small sites, a passive option may be deployed for site-wide coverage of the plume instead of merely relying on interception of down gradient migration (in this case passive refers to relying on natural gradient to mobilize the contaminants.).

In the case of the test site, one may estimate a flow rate for passive treatment system considering the following assumptions:

i. 30.48 m wide PVWs installation with appropriate spacing,

ii. a natural gradient of less than 0.01 (as is the case at the site),

iii. an average hydraulic conductivity of $1.4x10^{-6}$ cm/s and,

iv. A continuous sand lens that is 0.08 m in thickness and residual saturation of 0.4.

In a best-case scenario, approximately 378 L/year of free product may reach the passive treatment system – assuming no retardation of contaminant movement in comparison to groundwater. This value is reasonable in view of the approximately 113.4-151.2 L of free product volume that is collected per year at the test site by purging the wells. For an active remediation system where a gradient is induced, the flow rate and extracted volume can be one order of magnitude higher depending on the induced hydraulic gradient and the number of operating h per year.

WIDE System

The use of Prefabricated Vertical Wells (PVWs) within the WIDE field serves to control the hydraulic head distribution within the domain of installation such that gradient for gas and liquid flow is increased, and therefore mobilization of the plume toward extraction wells is induced. By virtue of applying vacuum head and distributing it within a subsurface domain, interphase mass transfer and equilibrium among phases are altered for the benefit of mobilization and mass extraction. The extraction of the soluble phase also enhances dissolution throughout the domain (within the solubility limit). Research data so far show that the hydraulic head is affected over 30.48 m away from the active PVWs. As applied vacuum pressure is in most cases less than the vapor pressure of the extracted contaminant, stripping occurs within the subsurface and even within the liquid

holding vacuum tank depending on the contact time.

It is important to however note that the sustainable extraction rates, on a long term basis, may be impacted by the presence of entrapped residual saturation, held for example by capillary action, adsorption kinetics, or by sequestration of contaminants due to sorption and partitioning. Cagle et al. (1997) reported the results of a case study in which the objective was to extract jet fuel from clay soils at the Naval Air Facility, El Centro, California. The authors used fluid injection with vacuum extraction (FIVE) as an alternative method of treating the site soils without disrupting the existing fuel farm's operation. They recommended a combination of approaches including multiphase extraction, air injection/pneumatic soil fracturing, and bioremediation. It is of interest to note that in Cagle's et al study, the rate of hydrocarbon biodegradation was estimated to range from 1.6 to 39 mg/kg/day. In the case of the WIDE active approach, a step of bioventing/air extraction process may be needed to address the residual phase. As site conditions change, whereby some of the residual phase contaminants are released (as may be evident from re-appearance of free product in wells), the active extraction process can then be re-implemented.

Bioremediation

It is generally believed that the feasibility of *in situ* bioremediation of high levels of organic compounds is questionable. Robertson et al (1996) indicated that NAPL's toxicity inhibits microorganisms and prevent their growth, which, in turn lengthens the

acclimatization period prior to biodegradation taking place. Steffensen et al (1995) indicated that biodegradation is critically dependent on the particular physico–chemical characteristics of a NAPL and site soils. It is also the case that entrapped residual NAPL may be biodegradation-resistant due to the presence of toxic compounds, or unavailability of nutrients. Peignenburg et al (1996) specified that methods of predicting rates of biodegradation in the field seem to be lacking.

Xie et al. (2003) generally discussed the difficulty of remediation of jet fuel due its composition being a mixture of many individual hydrocarbons (with the aromatic fraction being the most toxic). The authors utilized a sequential process of chemical oxidation followed by bioremediation to investigate the efficacy of such a process on degrading jet fuel. Their data indicated that aerobic microbial removal rates of all fractions of JP-4 were slower than chemical oxidation. The authors concluded that aromatic fractions were well degraded using the pre-chemical oxidation but minimally affected by microbial treatment. Xie et al. (2003) indicated that pre-chemical oxidation, with Potassium Permanganate for example, may enhance the bioremediation process but also noted that toxicity of pre-chemical oxidation inhibited microbial metabolism. They indicated that toxicity of pre-chemical treatment may explain why biological removal of aromatics was not effective. The authors presented the following equation for estimating contaminant concentration rate with time (t), based on apparent degradation rate constant for the substrate (k_{app}) and initial concentration (Co).

$$\mathbf{Ln}(C) = k_{app}\, t - \mathbf{Ln}\,(Co) \qquad \textbf{Equation (6)}$$

It is interesting to note that the apparent rate constants ranged from 0.001 d^{-1} to 0.013 d^{-1} for the live microcosm without pre-chemical oxidation. Xie et al. (2003) stated that "2 – 3 half-lives are desired to obtain reliable first-order rate constants. In our experiment, however, degradation of (Equivalent Carbon) EC fractions did not typically reach that level." The authors suggested that actual reaction rate constant (k) values can be obtained for a specific process using the following equation:

$$K_{app} = k/(1 + q_{sw}K_d + q_{gw}K_H) \qquad \textbf{Equation (7)}$$

The authors specified q_{sw} equal to 0.36 g/mL and q_{gw} of 0.43 mL/mL for biological microcosms, respectively. K_H and K_d are Henry's constant [L^3/L^3], and mass distribution coefficient between the sediment and solution [L3/M], respectively. These coefficients are evaluated for specific EC fractions.

Wiedemeier et al (1996) presented natural attenuation rates for soluble BTEX phase based on a data set from a JP-4 jet fuel spill at Hill Air Force Base. The rates ranged from 0.006 to 0.038 1/d, with most rates near 0.02 1/d. Carberry et al. (2001) indicated that in situ biodegradation rate of NAPL is best correlated with the molecular weight of the petroleum contaminants. They reported a rate constant of 0.012 1/d based on the results from 4 test sites of leaking underground fuel tanks.

To put these data in perspective, one may consider the solubility of the JP-4 to be 57 mg/L and apply bioremediation to the soluble phase in order to achieve 0.005 mg/L. In this case an estimate based on data presented by Xie et al. (2003) will result in a time range of 718 to 9,340 days to achieve the desired level. This estimation is based on the assumption that biological agents are able to reach the substrate and assuming conditions similar to those addressed in Xie et al.(2003) study, but does not address the degradation of the NAPL itself (as a free product).

Air Sparging

Air sparging is a process by which air is injected into the subsurface to strip volatile organic compounds (VOCs) from liquids and solids. In this case, positive pressure is used for inducing gas distribution within a zone of concern. The stripped compounds are then removed through vapor extraction to control the migration of VOCs. The combined process is commonly referred to as Air Sparging/Soil Vapor Extraction (AS/SVE). Positive injection of air may also have the secondary effect of increasing dissolved oxygen concentration to stimulate an aerobic degradation process. In general there is a dearth of data in literature regarding the efficiency of air sparging on the removal of NAPLs in general, and Jet fuel in particular. Johnston et al (2002) reported the results of pilot-scale field study in which air sparging with a vapor extraction system was used to remove weathered gasoline from a sandy aquifer. Their data indicated that air moved by the air sparging process contributed the majority of the petroleum

hydrocarbons removed; indicating that air sparging has increased the mass extracted by a factor of 1.9 as compared to removal by vapor extraction only. Air sparging was also effective in removing residual NAPL from below the water table.

Adam et al. (2000) indicated that air sparging can be used to effectively remediate dissolved and free phase benzene based on results from a controlled laboratory study. Waduge et al (2004) performed a laboratory study to investigate extraction efficiency using AS/SVE for various NAPL entrapment conditions. Their results indicated that a randomly distributed NAPL source with a low saturation gave the lowest removal efficiency due to small NAPL–air contact surface area. On the other hand, the authors indicated that removal efficiency of 91% was obtained for the case where the NAPL was placed in a homogenous fine sand matrix. This efficiency was interestingly higher than the case when NAPL was placed within a coarse grain matrix. These findings were however contrary to those reported by Braida et al. (2000) who indicated that more than 50% reduction in the removal rate of benzene was found when sand grain size was decreased from 30/50 to 70/100 (30/50 indicates particles passed a No. 30 sieve but were retained on a No. 50 sieve; mean particle size is 0.305mm for 30/50 and 0.168 mm for 70/100.) The discrepancy in these reported results highlight the role interfacial surface area (the area available for mass transfer) plays in affecting the remediation efficiency.

Monitored Natural Attenuation

After eighteen months of active remediation of JP-4, Cho et al (1997) reported the

results of a site study that was conducted to evaluate the effectiveness of natural attenuation in controlling exposure to hazards associated with residual saturation. According to the authors, the estimated yearly loading of BTEX compounds and MTBE into the receptor was trivial even without considering biological degradation. The biodegradation of hydrocarbons dissolved in groundwater was estimated from changes in groundwater chemistry. Data indicated that concentrations of target components in permanent monitoring wells continued to decline with time. The authors concluded that no further active remediation was required based on their monitored data.

CASE STUDIES FOR LNAPL REMEDIATION

Several studies have been conducted with regards to multiphase LNAPL remediation. Many of the field sites on which research has been conducted are current and/or former disposal sites at Air Force Bases, petroleum refineries, manufactured gas plant sites, underground storage tank sites, production spills, and pipeline ruptures. LNAPL's complex behavior necessitates innovative technology and model study/development. Application of multiple treatment methods is common to remove various phases of LNAPL. This section reviews both field and numerical case studies for LNAPL recovery from subsurface.

Missouri Refinery Site

Khaitan et al. (2005) discussed the remediation of a closed refinery site in

Missouri using several technologies to efficiently carry out the remediation process. The refinery was closed in 1982. More than 7,200,000 L of free product have been recovered at this site. Even in 2004, the pump-and-treat was continued to cease off-site migration. Pump-and-Treat in conjunction with air sparging, phytoremediation and monitored natural attenuation were used to remediate BTEX compounds. Result shows that air sparging increased biodegradation 80% at areas of high hydraulic conductivity soils whereas that increased 14% in areas with low hydraulic conductivity. In higher hydraulic conductivity area, air sparging accelerated natural attenuation, and pump and treat provided plume control.

Result shows that pump and treat was an extremely time consuming process in LNAPL remediation. The authors concluded that Pump-and-Treat with air sparging was initially effective but eventually time consuming and cost ineffective. Air sparging efficiency was low in low permeability soil.

Utah Hill Air Force Base

Operable unit 1 (OU1) at Hill Air Force Base, Utah, was highly contaminated with LNAPL. Ewing et.al (2002) presented a simulation study to evaluate the feasibility of Soil Vapor Extraction (SVE) system at OU1. In the same year and using the same site, Gordon et al. (2002) performed another simulation study to evaluate multiphase fluid flow of LNAPL recovery using trenches. Ewing's simulation study using AIRFLOW/SVE showed that SVE is effective for closely spaced wells. The maximum extraction rate was

limited to no more than 9900 L/min; and the results indicated less than 20% of the total LNAPL mass removal at the end of 10^{th} year of operation.

A second simulation study, conducted by Gordon et al. (2002), using UTCHEM software, showed the effectiveness of containment trenches for LNAPL removal. The hydraulic conductivity of the soil was $3.5x10^{-2}$ cm/s. Result showed that the trench recovered approximately 10% of the total LNAPL. Gordon et al. (2002) also investigated the sensitivity of LNAPL removal to aquifer hydraulic conductivity. One scenario was a homogeneous, isotropic permeability field of $2x10^{-3}$ cm/s, and the other assumed a homogeneous, isotropic permeability field of $2x10^{-2}$ cm/s. For the containment trench removal method Gordon e al. (2002) stated that "although the permeability of the aquifer does have an effect on the recovery of LNAPL, this effect is relatively small and will not have a significant impact on the dewatering or LNAPL recovery process."

Brookline Petroleum Release Site

A bioslurping pilot study was conducted at a petroleum release site in Brookline, Massachusetts, to remove free product and to reduce soluble phase concentrations of petroleum. Approximately 14 kg/day was the average vapor emission rate. The result indicated non-uniform zone of vacuum influence/radius of influence in all directions. The conclusion from this research is "two-phase extraction appears to be a very effective remedial technology for removing LNAPL" (Cresap 1999).

Taiwan Contaminated Site Simulation and Optimization

Yen et al. (2003) performed a two stage analytical framework involving a combined simulation/regression/optimization modeling approach to optimize the pumping volume for LNAPL using BIOSLURP (2004) computer program. The model was calibrated and verified from the field results of test site contaminated with 65% gasoline and 35% diesel, located in Tainan, Taiwan. The area of concern for free product recovery was approximately 1200 m^2. The shallow, unconfined local aquifer consisted of fine sand with a thin interlay of silt and clay. The hydraulic conductivity of the shallow aquifer was $1.8x10^{-3}$ cm/s (1.55 m/day) and porosity was 0.35. The model was calibrated in terms of the oil thickness in field after operating for one day. The author mentioned that the Bioslurp model calibration was performed by first using measured or assumed parameter values, then running the model and manually adjusting the parameter values until the observed and simulated values were in acceptable agreement. The final calibrated parameters, listed in Appendix II, of the paper shows that even the measured parameter hydraulic conductivity ($1.8x10^{-3}$ cm/s to $5.8x10^{-3}$ cm/s) and porosity (0.35 to 0.37) were altered to match with the field result. The range of the assumed parameters was not compared with those reported in literature.

LINDO software package and regression model were used for the optimization analysis with the objective to maximize the oil and gas recovery and minimize water recovery. Soluble phase extraction was not considered in the analysis. The simulation was

performed with 10 wells. The three constraints were system response, clean up level and operating capacity and non-negativity constraints related to number of wells and positive volume of LNAPL, water and gas. The optimization was performed for 5, 7 and 12 days of running period assuming the same flow rate which is not mentioned in the paper. The main finding of Yen et al. (2003) was that for the contaminated site 7-day operational time period between two consecutive remediation efforts could be a near optimal solution.

REFERENCES

Adams, J.A., and Reddy, K.R. (2000). "Removal of dissolved- and free-phase benzene pools from ground water using *in situ* air sparging." *Journal of Environmental Engineering*. 126: 697-707.

American Petroleum Institute (API) 4729 (2003). "Models for Design of Free Product Recovery Systems for Petroleum Hydrocarbon Liquids, Regulatory Analysis and Scientific Affairs Department".

Braida, W. and Ong, S.K. (2000). "Influence of porous media and airflow rate on the fate of NAPLs under air sparging." *Transport in Porous Media.* 38: 29-42.

Bedient, P. B., Rifai, H. S. and Newell, C. J. (1999). "Groundwater contamination transport and remediation." *Sources and Types of Groundwater Contamination*. Upper Saddle River, NJ: Prentice Hall. 75-111.

Cagle, G.A., Guerrero, J.A., Everds, P. and Gonzales, M. (1997). "Combining *in situ* technologies in low-permeability soil, a case study," *Proceedings of the 1997 ASCE Annual Fall National Convention.* Minneapolis, MN. (October): 297-311.

Carberry, J.B. and Wik, J. (2001) “Comparison of *ex-situ* and *in situ* bioremediation of unsaturated soils contaminated by petroleum.” *Journal of Environmental Science and Health - Part A Toxic/Hazardous Substances and Environmental Engineering*. 36(8):1491-1503.

Cho, J.S., Wilson, J.T., DiGiulio, D.C., Vardy, J.A., and Choi, W. (1997). “Implementation of natural attenuation at a JP-4 jet fuel release after active remediation.” *Biodegradation*. 8: 265-273.

Cresap, G. H. Jr. (1999). “Case study: Application of short-duration, periodic bioslurping at a petroleum hydrocarbon release site Hazardous and Industrial Wastes”. *Proceedings of the Mid-Atlantic Industrial Waste Conference.* 159-168.

Dullian, F.A.L. (1979). “Porous Media: Fluid Transport and Pore Structure”. *Academic Press (1st Edition).*

Ewing, J. E., Dwarakanath, V., Gordon, K. D., Meinardus, H. W., Ginn, J. S. (2002). “Evaluation of LNAPL recovery using soil vapor extraction, Proceedings of the Third International Conference on Remediation of Chlorinated and Recalcitrant Compounds”. *Proceedings of the Third International Conference on Remediation of Chlorinated and Recalcitrant Compounds.* 1705-1713

Farr, A.M., Houghtilan, R.J., and McWhorter, D.B. (1990). "Volume Estimation of Light Nonaqueous Phase Liquids in Porous Media". *Ground Water*. 28(1): 48-56.

Gordon, K.D.,Jin, Minquan; M, Hans W., Ginn, J. S. (2002). "Multi-phase fluid flow evaluation of lnapl recovery using containment trenches". *Proceedings of the Third International Conference on Remediation of Chlorinated and Recalcitrant Compounds*. 1689-1696

Johnston, C.D., Rayner, J.L., and Briegel, D. (2002). "Effectiveness of *in situ* air sparging for removing NAPL gasoline from a sandy aquifer near Perth, Western Australia." *Journal of Contaminant Hydrology*. 59: 87-111.

Khaitan, S., Kalainesan, S., Erickson, L.E., Kulakow, P., Martin, S., Karthikeyan, R., Hutchinson, S.L.L., Davis, L.C., Illangasekare, T.H., Ng'oma, C. (2005). "Remediation of Sites Contaminated by Oil Refinery Operations". *Environmental Progress, American Institute of Chemical Engineers.* 25(1):20-31

Newell, C. J., Steven D. A., Ross, R. R. and Huling, S. G. (1995)." Light Non Aqueous Phase Liquids, Groundwater Issue". *EPA/540/S-95/500*

Norris, H., Brown, M., Semprini, W., Kampbell, R., Bouwer, Borden, Vogel, Thomas,

Ward. (1993). “Handbook of Bioremediation”. *Robert S. Kerr Environmental Research Laboratory*.

Parker, J.C. and Lenhard, R.J. (1990**).**Vertical integration of three-phase flow equations for analysis of light hydrocarbon plume movement”. *Transport in Porous Media*.5(2):187-206.

Peignenburg, W.J.G.M. and Damborsky, J. (1996). “Biodegradability Prediction.” Dordrecht, The Netherlands.

Robertson, B.K. and Alexander, M. (1996). “Mitigating toxicity to permit bioremediation of constituents of nonaqueous phase liquids.” *Environmental Science Technology*. 30: 2066–2070.

Scheiegg, H.O. (1985). “Consideration on water, oil and air in porous media”. Water Science and Technology. 17:467-476.

Steffensen, W.S. and Alexander, M. (1995). “The effect of competition for available nutrients in systems containing mixtures of substrates.” *Applied Environmental Microbiology*. 61: 2859–2862.

van Genuchten, M. Th. (1980). “A closed-form equation for predicting the hydraulic conductivity of unsaturated soils”. *Soil Science Society of America Journal*. (44):892-898.

van Genuchten, M. Th., and Wierenga, P. J. (1980). “Mass transfer studies in sorbing media 1. Analytical solution”. *Soil Science Society of America Journal.* (40):473-480.

Wiedemeier,T. H., Swanson, M. A., Wilson, J.T., Kampbell, D. H., Miller, R. N. and Hansen, J. E. (1996) “Approximation of biodegradation rate constants for monoaromatic hydrocarbons (BTEX) in ground water.” *Ground Water Monitoring & Remediation.* 16(3): 186-194.

Waduge, W.A.P., Soga, K. and Kawabata, J. (2004). “Effect of NAPL entrapment conditions on air sparging remediation efficiency.” *Journal of Hazardous Materials.* 110: 173-183.

Xie, G. and Barcelona, M. J. (2003). “Sequential chemical oxidation and aerobic biodegradation of equivalent carbon number-based hydrocarbon fractions in jet fuel.” *Environmental Science and Technology.* 37 (20) (Oct): 4751-4760.

Yen, H. Y., Chang, N. B. (2003). ‘‘Using the bioslurping model to assess the light

hydrocarbon recovery in contaminated unconfined aquifer. I: Simulation analysis.'' *Practice Periodical of Hazardous, Toxic, and Radioactive Waste Management.* 7(2) (April):114-130.

Yen, H. Y., Chang, N. B. (2003). ''Using the bioslurping model to assess the light hydrocarbon recovery in contaminated unconfined aquifer. II: Optimization ation analysis.'' *Practice Periodical of Hazardous, Toxic, and Radioactive Waste Management.* 7(2) (April):131-138.

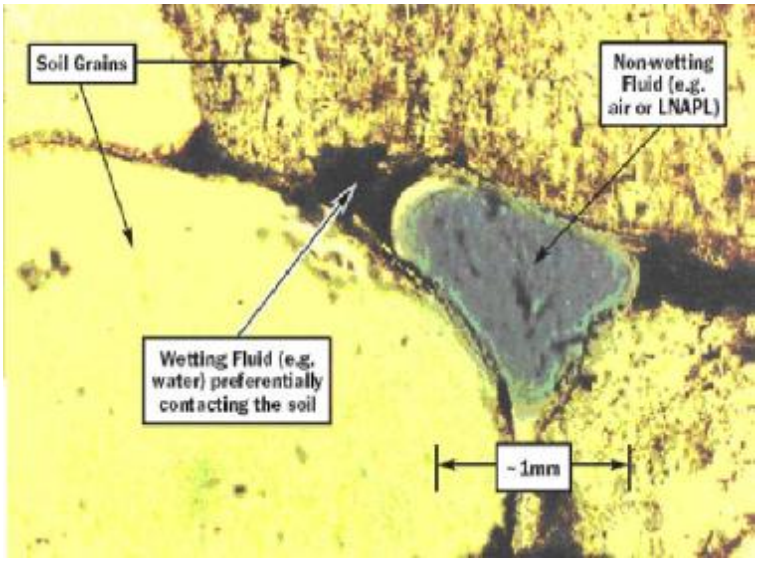

Figure 2-1 Multiple fluids in the pore space of a granular porous media.

(API 2003)

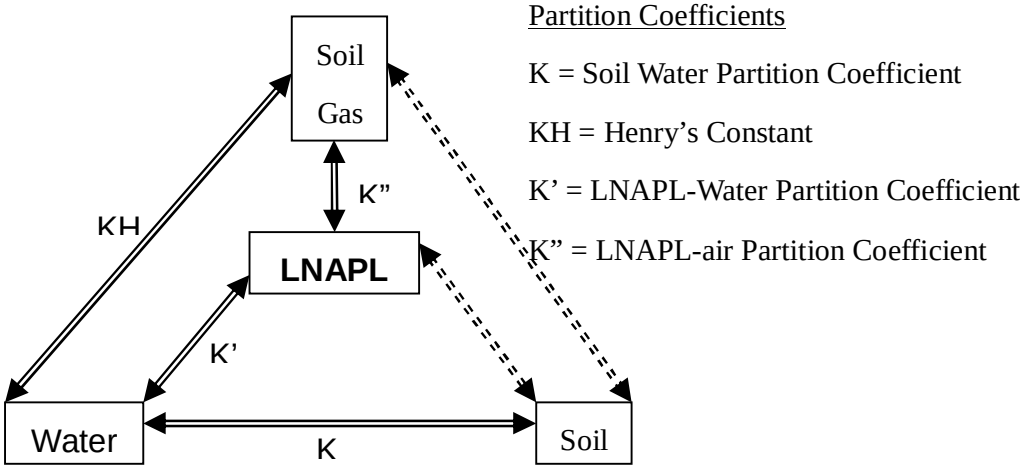

Figure 2-2 Partitioning of LNAPL among the four phases found in the unsaturated zone.

(Newell, et al., 1995)

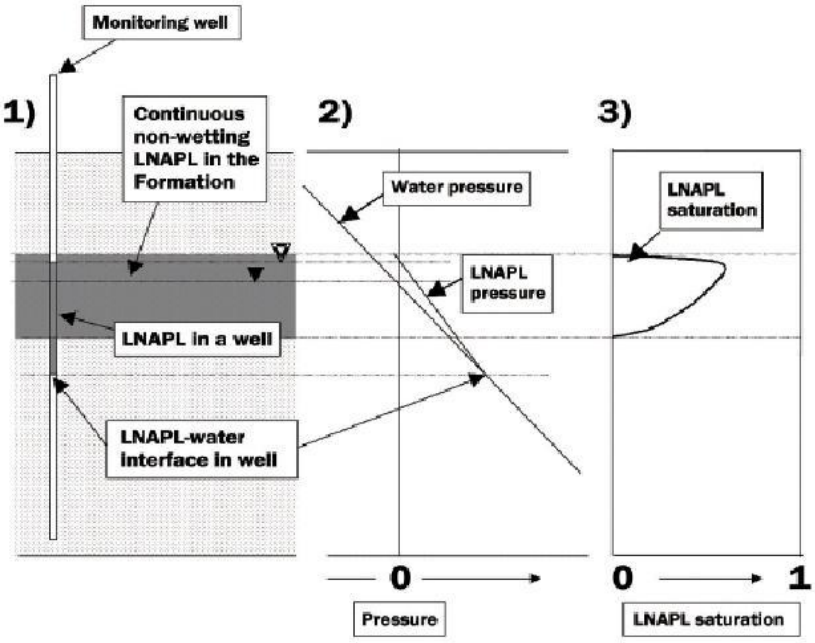

Figure 2-3 Idealized conceptualization of LNAPL in a well and adjacent formation.

(API 2003)

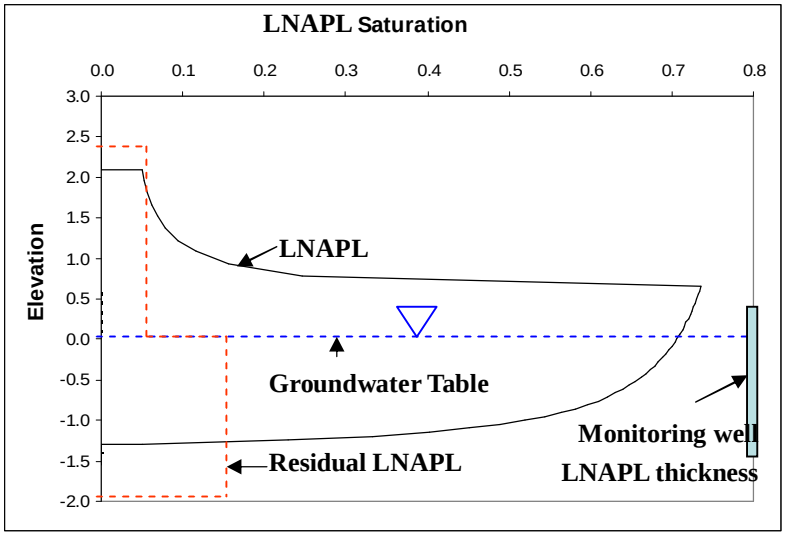

Figure 2-4 Qualitative LNAPL distribution in subsurface.

(API 2003)

3. CASE STUDY OF MULTIPHASE EXTRACTION OF LIGHT NON-AQUEOUS PHASE LIQUID (LNAPL) USING PREFABRICATED VERTICAL WELLS

To be submitted to the Canadian Geotechnical Journal

Case Study of Multiphase Extraction of Light Non-Aqueous Phase Liquid (LNAPL) Using Prefabricated Vertical Wells

N. Sharmin, M. A. Gabr and J. D. Quaranta

ABSTRACT

An essential step in the remediation of light non-aqueous phase liquid (LNAPL) is the extraction of the free phase that acts as a source in the subsurface. In addition to the extraction of the liquid phase, the remediation of the entrapped residual globules necessarily encompasses the extraction of soluble phase, air circulation for promoting the mass transfer to the gas phase, the extraction of organic vapors, and bioventing. The paper describes a case study in which the well injection depth extraction (WIDE) system, a hybrid subsurface flushing/vapor-gas extraction system, is used for the extraction of LNAPL (jet fuel, JP-4) at a former air force base. Field testing consisted of 185 operating h on 38 separate days. A total of 133 L of free phase liquid is removed from the subsurface in conjunction with 467 kg of organics in the vapor phase as volatilization took place due to the application of vacuum heads exceeding the JP-4 vapor pressure. The average LNAPL extraction rate is 0.72 L/h and the average extracted mass in the gas phase is 2.54 kg/h. Approximately, 25000 L of contaminated groundwater are also extracted by the system. The average extraction rates varied between 75 L/h and 285 L/h. Multiphase transport modeling is performed using the computer program, BIOSLURP, to provide an analysis of the extraction process in liquid, gas, and soluble phases, and

provide an indication of the extraction time to an end point of remediation. The model is calibrated using field data to match the extracted free phase and aqueous phase volumes. Model results indicate that the 292 L of free phase LNAPL can be recovered in 19.5 days (based on 8 h of operation in a day). Results indicate that under an applied vacuum head ranging from 410 to 330 mm of mercury (1 cm Hg = 1.33 KPa), the concentration in the vapor phase at the location of the pad is at or below regulated threshold values after 2.5 years of extraction. The results from the model also indicate that the soluble phase in the groundwater at the end of 4.25 years of system operation is below 0.005 ppm. A cost comparison with similar systems' performance reported in literature is presented.

KEYWORDS: Light Non-Aqueous Phase Liquid (LNAPL); Multiphase contaminant transport; Remediation technique in low permeability soil; Well injection depth extraction (WIDE); Wide-cut contaminant remediation.

INTRODUCTION

The difficulty in achieving complete remediation of light non-aqueous phase liquid (LNAPL) in subsurface soil profiles arises mainly from the complex entrapment of LNAPL in the heterogeneous media, with such entrapment being in the saturated and unsaturated modes. The contamination of interest at the test site is mainly jet fuel (JP-4.) A remediation system for jet fuel can be viewed as operating in either passive or active

modes. A passive system relies on the site's natural gradient for mobilization of the contamination toward the system whereby an oxidation/conversion mechanism is induced. An example of a passive system is air spargning or bioremediation. In contrast to a passive system, an active system seeks to mobilize the plume toward extraction points strategically placed to capture and remove the mobilized contaminants. The most common active system is the 'pump and treat' approach. However these systems have traditionally shown tailing and rebounding effects over time (see for example Travis et al. 1990, Haley et al. 1991, and Bartow et al. 1995). The active system addressed in this case study is WIDE. A brief review of three examples of passive systems for remediation of jet fuel contaminated sites (namely bioremediaiotn, air sparging and natural attenuation) is presented for comparison.

WIDE System

The WIDE system and its application has been previously described (e.g. Gabr et al. 1995, Kunberger et al. 2003, and Warren et al. 2006). The major elements of the WIDE technology include: i) PVWs, ii) groundwater and a soil vapor vacuum extraction system, iii) a liquid injection system, and iv) an above-ground treatment system. A PVW, 100 mm wide by 4 mm thick, is manufactured as a composite system comprised of an inner core, an outer permeable filter jacket, and, at specified positions, an impermeable barrier sleeve.

WIDE system controls the hydraulic head distribution within the field of installation such that gradient for gas and liquid flow is increased and therefore

mobilization of the plume toward extraction points is induced. By virtue of applying vacuum head and distributing it within a subsurface domain, interphase mass transfer and equilibrium among phases is altered for the benefit of mobilization and mass extraction. As vacuum pressure exceeds the vapor pressure of the LNAPL, stripping may occur within the subsurface and even in the liquid tank, depending on the contact time. The flushing process of the soluble phase also enhances dissolution throughout the domain (within solubility limit.). Similar to the general case of pump and treat systems, sustainability of multiphase extractions rates, on a long term basis, will be impacted by the presence of entrapped residual saturation, held for example by capillary action or adsorption kinetics such as sequestration of contaminants by sorption and partitioning. Cagle et al. (1997) reported the results of case study remediating jet fuel in clay soils at the Naval Air Facility, El Centro, California. They recommended a combination of approaches including multiphase extraction, air injection/pneumatic soil fracturing, and bioremediation. The rate of hydrocarbon biodegradation was estimated to be 1.6-39 mg/kg per day. As site conditions however change whereby some of the residual phase contaminants are released (as may be evident from monitored product thickness in wells), the active extraction process can be re-implemented.

Bioremediation

The feasibility of *in situ* bioremediation of high levels of organic compounds is questionable. Robertson et al. (1996) indicated that NAPL's toxicity inhibits microorganisms and prevent their growth, which, in turn lengthens the acclimatization

period prior to biodegradation taking place. Steffensen et al. (1995) indicated that biodegradation is critically dependent on the particular physio–chemical characteristics of a NAPL and contaminated site soils. It is also the case that entrapped residual NAPL may be biodegradation-resistant due to the presence of toxic compounds, or unavailability of nutrients. Peignenburg et al. (1996) specified that methods of predicting rates of biodegradation in the field seem to be lacking.

Xie et al. (2003) generally discussed the difficulty of remediation of jet fuel due its composition being a mixture of many individual hydrocarbons (with aromatic fraction being the most toxic.) The authors utilized sequential chemical oxidation and bioremediation to investigate the efficacy of the process on degrading jet fuel. Their data indicated that aerobic microbial removal rates of all fractions of JP-4 were slower than chemical oxidation. The authors concluded that aromatic fractions were well degraded using the prechemical oxidation but minimally impacted by microbial treatment. Xie et al. (2003) indicated that prechemical oxidation with Potassium Permanganate, for example, may enhance the bioremediation process but also noted that toxicity of prechemical oxidation inhibited microbial metabolism. They indicated that toxicity of prechemical treatment may explain why biological removal of aromatics was not effective. Xie et al. (2003) stated that "2-3 half-lives are desired to obtain reliable first-order rate constants. In our experiment, however, degradation of (Equivalent Carbon) EC fractions did not typically reach that level." Wiedemeier et al. (1996) presented natural attenuation rates for soluble BTEX phase based on a data set from a JP-4 jet fuel spill at

Hill Air Force Base. Carberry et al. (2001) indicated that *in situ* biodegradation rate of NAPL is best correlated with the molecular weight of the petroleum contaminants. It should be noted that biodegradation is the only feasible biological agent which able to reach the substrate which can be challenging in predominately clay soils.

Air Sparging

Air sparging is a process by which air is injected into the subsurface to strip volatile organic compounds (VOCs) from liquids and solids. In this case, positive pressure is used for impacting gas distribution within a zone of influence. Burns et al. (2001) presented comprehensive study of bubble size and distribution with injection pressure for effective stripping. Generally, the stripped compounds are removed through vapor extraction process using a vacuum system to control the migration of VOCs. The combined process is commonly referred to as Air Sparging/Soil Vapor Extraction (AS/SVE). Positive injection of air may also have the secondary effect of increasing dissolved oxygen concentration to simulate an aerobic degradation process. In general there is a dearth in literature regarding the efficiency of air sparging on the removal of NAPLs in general and jet fuel in particular. Johnston et al. (2002) reported the results of pilot-scale field study in which air sparging with a vapor extraction system were used to remove weathered gasoline from a sandy aquifer. Their data indicated that air moved by the air sparging process contributed the majority of the petroleum hydrocarbons removed. The authors indicated that air sparging increased the mass extracted by a factor of 1.9 as compared to removal by vapor extraction only. Air sparging was also effective in

removing residual NAPL from below the water table.

Adam et al. (2000) indicated that air sparging can be used to effectively remediate dissolved and free phase Benzene based on results from a laboratory study. Overall, their study showed that air sparging can be used to effectively remediate dissolved- and free product phases of benzene. Waduge et al. (2004) performed a laboratory study to investigate extraction efficiency using AS/SVE for various NAPL entrapment conditions. Their results indicated that a randomly distributed NAPL source with a low saturation gave the lowest removal efficiency due to small NAPL–air contact surface area. On the other hand, the authors indicated that efficiency of 91% was obtained for the case where the NAPL was placed in a homogenous fine sand matrix. This efficiency was higher than the case when NAPL was placed within coarse grain matrix. These results are however contrary to those found by Braida et al. (2000) who reported that more than 50% reduction in the removal rate of benzene was found when sand grain size was decreased from 30/50 to 70/100 (30/50 means particles passed No. 30 sieve but retained on #50 sieve; mean particle size is 0.305mm for 30/50 and 0.168 mm for 70/100). The discrepancy in these reported results highlights the role interfacial area available for mass transfer plays in affecting the remediation efficiency.

Monitored Natural Attenuation

After eighteen months of active remediation of JP4, Cho et al. (1997) reported the results of a site study that was conducted to evaluate the impact of natural attenuation to control exposure to hazards associated with residual saturation. The estimated yearly

loading of BTEX compounds and MTBE into the receptor was trivial even without considering biological degradation. The biodegradation of hydrocarbon dissolved in groundwater was estimated from changes in groundwater chemistry and data indicated that concentrations of target components in permanent monitoring wells continued to decline. The authors concluded that no further active remediation is required based on their monitored data.

Work in this paper documents a case study describing field performance and modeling of PVWs for *in situ* extraction of LNAPL, namely jet fuel (JP-4), at the former Lockbourne Air Force Base (AFB). The modeling effort aims at extrapolating data from field measurement to estimate end points of remediation for groundwater and soil media. The field installation includes a prototype test pad measuring 12.8 m by 44 m a 17,000 L/min air compressor powering a 5.08 cm diameter eductor vacuum system, and a surface piping network consisting of 25 rows, each row encompassing 7 or 8 PVWs. Liquid rates and total organic concentrations in the air stream are monitored and used to evaluate the system performance.

Residual NAPL zones existing in the subsurface can act as continual sources and therefore it is difficult to reach target maximum contaminant levels (MCLs) during a field experiment. Predictive analyses are performed to model the subsurface hydraulic domain and gain insight into the system performance of multiphase contaminant extraction and remediation. There are few models available in literature for representing the transport of three phases in the subsurface. NAPL Simulator by Guarnanccia et al. (1997).is one

possible model that contains mathematical representation for multiphase flow, interphase mass transfer, and constituent mass transport, However, it was developed mainly for near-surface, granular soils. Modeling in this study is performed using the computer program BIOSLURP (2004) and aims at providing information on remediation time for free, vapor and soluble phase. The multiphase flow equations describe three mobile phases, which including soluble phase, NAPL, and gas. The interphase mass-transfer process defines how NAPL contaminants partition between phases. Results of the WIDE system performance for removal of Jet Fuel and associated cost are compared with those from similar projects at Pope and Shaw air force bases.

FIELD CASE STUDY

Construction of the WIDE system began August 29, 2005, followed by the system start-up and commissioning. The construction operation entailed several steps prior to installation. Construction began with a site layout survey, followed by site preparation and earthwork staging. The site survey indicated that the WIDE field should be positioned over an area that was identified via SCAPS data (Site Characterization and Analysis Penetrometer System) performed by the Army Corps of Engineers', as shown in Figure 3-1. Following the survey, scraping and leveling the site soils was performed. A geosynthetic fabric was installed and was overlain by approximately 76.2 mm of crushed concrete to stabilize the site's soft soil for construction traffic. The system fabrication, construction, and installation were performed by the Nilex Corporation, Denver, CO.

Specific details regarding the configuration of the installed WIDE system are presented in Table 3-1.

The field installation and assembly were completed in three days using a crew of one equipment operator and two field technicians. After installation of the individual PVWs, a wedge-shaped steel tip was mounted to the mandrel and used to compact the soil around the annulus opening (created by the insertion/extraction of the mandrel) in order to close the gap near the surface. (Note: The gap below the surface closes due to effective stress). The compaction using the wedge-shaped tip was followed by a dynamic roller compactor that was driven along each row of PVWs in order to seal the surface. At selected locations, dry bentonite powder was poured around the compacted annulus to further ensure a tight seal between the soil and the PVWs. The pad encompasses 25 rows, each consisting of 7 or 8 PVWs, as schematically shown in Figure 3-2.

The vacuum system uses compressed air to produce a vacuum head that is applied to the manifold and piping network. The air compressor supplies approximately 8,780 L/min to produce a vacuum-induced air flow rate to the manifold piping of approximately 991-1,133 L/min.

Recorded data include: i) the applied vacuum head, ii) air flow (motive + field vacuum), iii) extracted liquid (i.e., groundwater and free phase JP-4) rate, iv) chemical concentrations of hydrocarbons, and v) operational time. The waste stream was routed to a blow-down, liquid/gas separation tank. The gas vapors produced from the system were released into the atmosphere after frequent sampling, as per the NIOSH (The National

Institute for Occupational Safety and Health) Method 1501. The contaminated groundwater and free phase JP-4 generated by the system were routed to a storage tank. Initially, the waste stream was hauled off site for disposal but then a water-oil separator with a skimmer was added toward the end of the project to save on disposal cost. A process flow diagram that outlines the arrangement of the equipment for use during the field operation is presented in Figure 3-3.

SUBSURFACE CONDITIONS

The site soils are characterized as glacial till with shale fragments, clay, silt, and sand with locally isolated layers of silt, sand, and gravel. These isolated layers are poorly connected, suggesting a lenticular morphology. Hence, the extraction of the site's contaminant (i.e., the jet fuel, JP-4) is further compounded by such heterogeneity, which not only affects the mobilization of JP-4, but also its entrapment on both the micro (inter-particle) and macro (intra-layer) scales.

The site is of generally flat topography, with the groundwater's natural gradient less than 1% based on elevations obtained from well data. On-site groundwater was detected in a gray/brown, medium density, silty sand layer located 4.88 to 5.49 m below ground level. The hydraulic conductivity values reported in the past (Kunberger et al. 2003), based on groundwater well testing and laboratory hydraulic conductivity testing, range from $8x10^{-6}$ cm/s to $2x10^{-4}$ cm/s.

A soil investigation was conducted at the site using boring logs and geoprobe

soundings. Table 3-2 presents the physical characteristics of the site soils obtained from laboratory testing on recovered specimens. The natural water content of the test specimens obtained from the site ranges from 11% to 22%. The plasticity index (PI) varies from 5.5% to 8.5% with an average liquid limit of 21%. The specific gravity was measured to be in between 2.7-2.73. Grain size distribution was determined for specimens obtained from a depth of 5.18 to 6.1 m below the ground surface. Based on grain size distribution according to ASTM D 422-63 samples from depth of 5.18 to 6.1 m, approximately 25% of the soil grains are classified as fines (smaller than 0.074 mm). In addition, 60% to 65% of the particles at that depth are of sand size (i.e., greater than 0.2 mm). Figure 3-4 shows an idealized subsurface profile based on the results of the site investigation and laboratory testing.

Site Contamination

The contamination of interest at the test site is JP-4. Information regarding the history of JP-4 indicates that it is a kerosene-gasoline mix. It is also known as *wide-cut* fuel because it is made from a wide range of hydrocarbon products. Xie et al. (2003) state that JP-4 is a mixture comprised of over 100 hydrocarbons. For this reason, the Total Petroleum Hydrocarbon Criteria Working Group (TPHCWG) lump JP-4 petroleum hydrocarbons into groups based on their equivalent carbon numbers (Edwards et al. 1997). JP-4 has a vapor pressure of 91 mm Hg at 20^{o}C. Its solubility in water is 57 mg/L at 20^{o}C (Chemical Rubber Company 1984). Its specific gravity is approximately 0.78 to

0.8. Based on available information, approximately 85% of JP-4 is saturated low molecular weight aromatic hydrocarbons. Given the site geology, areas of entrapment can range from residual saturation within capillary zones to high saturation in the form of isolated pools within high permeability subsurface lenses.

A limited site investigation was conducted at the test site mainly to characterize the solid phase (i.e., the soil) of the organics contamination. The work was performed by Belasco Drilling using a continuous direct push 65 cm diameter SIMCO 2400 geotechnical soil sampler in conformance with the ASTM D 6282-98 Standard Guide for Direct Push Soil Sampling for Environmental Site Characterizations. Sampling was performed 3.66 to 7.62 m below ground level. The soil samples were recovered using acetate tubes. Five locations were tested within the test pad (see Figure 3-2). Laboratory testing of the recovered soil samples includes characterization of chemical constituents within the following classifications: Diesel range organics (DRO), gasoline range organics (GRO), and kerosene range organics (KRO). The testing was performed by the REIC Laboratory of Beaver, West Virginia using the EPA method SW 8015B for total petroleum hydrocarbons (TPH).

Figure 3-5 shows the combined concentration of DRO, GRO, and KRO as a function of depth. The concentration follows the approximate geologic characteristics of lenticular morphology. This geology can be seen at a depth of 4.57 m from ground surface where the maximum concentration obtained was 10,530 mg/kg north of row 5 (Figures 1 and 2). At the same depth, but at location 2 north of row 18 (Figures 1 and 2), a value of

154 mg/kg was estimated. This difference in concentration of the two orders of magnitude can be explained by the absence/presence of sand/silt seams, which may act as reservoirs for contamination depending on the groundwater level and contamination mobility.

Table 3-3 shows sample location, number, and depth as well as data for contamination in terms of mass of the contaminant in mg/kg of soil. The majority (8 out of 12) of the characterized samples yielded concentrations equal to or less than 700 mg/Kg, as shown in Table 3-3, with the higher concentrations obtained at the approximate location of the subsurface sand/silt lens. The average for all data is 1720 mg/kg, but this average is not necessarily a meaningful quantity in this case, given that higher concentrations were detected in the proximity of the sand seams. Table 3-3 also shows volatile organic compounds (VOC) data at the testing locations monitored using a handheld photo-ionization detector (PID). VOC values generally greater than 500 ppm (on volume basis) indicate the presence of free phase JP-4 at the sampling location.

Monitored Data

During the course of the WIDE operation, a number of subsurface parameters were monitored. Among these parameters were the fluctuation in the groundwater table levels and the thickness of JP-4 at the well locations. Groundwater samples were obtained, and the concentration of BTEX (benzene, toluene, ethylbenzene, and m, p and o xylene) compounds was measured in the laboratory. Monitored well data reported in this paper are from LMW-4. As shown in Figure 3-1, LMW-4 is located outside the test pad,

approximately 2.44 m southeast of its far edge (close to Row# 1). Grab samples were obtained during the system operation using sampling methods and protocols established in the Ohio EPA Technical Guidance Manual for Hydrogeologic Investigations and Ground Water Monitoring (1995). Chemical laboratory analysis involved the evaluation of the contaminant mass in the extracted air and liquid samples. Blank and repetitive tests were performed for validation and reproducibility of the data. For the groundwater, the test method used was EPA Method 8021A Volatiles by Gas Chromatograph using Photoionization and Electrolytic Conductivity Detectors in Series. For air sampling, the selected method was the NIOSH Method 1501 for Aromatic Hydrocarbons. The LNAPL was characterized based on the free phase volume recovered.

SYSTEM PERFORMANCE

Field testing included 185 operating h on 38 separate operating days. During this period, free phase LNAPL as well as soluble and gas phases, as indicated by monitored liquid rates and total organic concentrations in the air stream, were removed from the subsurface. Air emissions were based on the total of gasoline, kerosene and diesel range organics (i.e., GRO, KRO, and DRO).

Groundwater Extraction Flow Rates

Field extraction was undertaken on a row-by-row basis, with each row being run for a specific time, typically 1 h/d. Each row contained either seven or eight individual

PVWs. In two of the operating days, multiple rows were operated simultaneously, but the majority of the operating time was on a single-row basis in an attempt to extract the available free phase JP-4 as well as maximize mass concentration in the air phase. Overall, the flow rate ranged from approximately 75 L/h to 285 L/h. Groundwater extraction flow rates varied with time and the location of a given row; an average extraction flow rate of approximately 135 L/h was obtained for the overall system operation. Figure 3-6 illustrates the cumulative groundwater flow volume as a function of operating time. Figure 3-6 also shows a gradual increase in the slope of the extraction rate as the cumulative operating time increases. Such an increase can be attributed partly to the formation of a stable filter at the soil/geotextile interface, but was observed primarily as the groundwater elevation rose as a consequence of rainstorm events.

JP-4 Extraction Flow Rates

As with groundwater extraction, the extraction of JP-4 was performed on a row-by-row basis, with only two days of multiple row operation. Figure 3-7 illustrates the total extracted free JP-4 volume as a function of operating time. The density of JP-4 is 0.80 kg/L; the liquid volume of the data shown in Figure 3-7 corresponds to a total volume of approximately 133 L, which is equivalent to approximately 109 kg. The extracted liquid volume of the JP-4 is later viewed in conjunction with the volatilized mass, because significant volatilization occurs due to the applied vacuum head being higher than the JP-4 vapor pressure.

The removal of JP-4 is shown as a step function simply because multiple extraction periods of zero-free JP-4 occurred between those of active-free phase removal. This variation is most likely due to the relative location of JP-4 with respect to the subsurface layers, the degree of saturation, residual saturation, and the depth of extraction focus. Because JP-4 has a density that makes it lighter than water, it is subject to depth variations based on groundwater fluctuations. The presence of a subsurface layer interface (a lens with relatively high permeability and glacial till with low permeability) within this fluctuation range further complicates the extraction process. The extraction of the JP-4 was most effective when the groundwater table was at the relatively thin, silty sand lens that represents an area of preferential flow. Because the sand lenses are discontinuous throughout the site, there is a need for a row-by-row active operation such that once the JP-4 that is available due to gradient-induced flow is removed at a given location, a shut-down period allows for a recharge while the extraction continues at a different location within the PVWs network.

Emission Rates

In addition to the extraction of JP-4 in the free phase, extraction occurred in the air phase. Such extraction targets the volatilized JP-4 within the soil pores with the application of vacuum heads that exceed the vapor pressure of the product (91 mm of Hg, or approximately 1.23 m, of water at 20^{o}C). The concentration of organics in the air stream was monitored using a handheld PID. A calibration study was performed to

establish the relationship between gas concentrations obtained by the PID and those obtained from sampling using carbon cartridges; correlation data are shown in Figure 3-8. Based on these data, the mass extracted in the air stream and computed based on PID readings was increased by a factor of 1.5. Laboratory testing and analyses of the air samples were performed by REIC.

Figure 3-9 illustrates the cumulative mass of JP-4 extracted over time in the air phase. These values are based on an average concentration obtained by the PID during the run times. The upward trend in the slope of the air emissions corresponds, in terms of time, to the increase in the slope of the groundwater extraction (Figure 3-6). Initially, the extraction rate in the air stream was 2 kg/h but later increased to 3 kg/h. Over the course of the operation, the air emissions JP-4 mass that was removed was 467 kg, with an average rate of approximately 2.54 kg/h. Generally, the higher removal rates in the air stream were correlated to a lower elevation of groundwater.

Monitoring Well Data

Figure 3-10**,** 3-11 and 3-12 illustrate the variations in the groundwater depth, free-product thickness, and BTEX concentration as a function of time for monitoring well LMW-4. Figure 3-10 shows a rise in the groundwater table elevation over the period of operation of almost 1.1 m. This variation is reasonable for a seasonal groundwater fluctuation and is due to melting snow and an increase in rainfall events during the months of March and April, 2006.

The variation in free-product thickness, as seen in Figure 3-11, is attributed to the rising groundwater table. This variation in plume thickness is due to the release of LNAPL trapped in the pores and also due to the effects of operation of the extraction system. Mobilization of the free JP-4 can occur due to the hydraulic gradient created by the system operation, which causes flow toward the pad. It was observed that the plume thickness increased on days following active extraction. Both in Figure 3-11 and Figure 3-12, the open circle symbols indicate days of system operation and, as such, do not have relative y-axis values. The "before" system operation data are indicated by "day 0" values.

Figure 3-12 presents concentrations of BTEX compounds as a function of time based on the results of tests performed on samples obtained from LMW-4. The monitored data over the time of operation indicate a maximum concentration of 0.56 mg/L for benzene and 0.55 mg/L for ethylbenzene at the LMW-4. These BTEX concentrations are not expected to decrease as long as JP-4 (LNAPL) is present in the subsurface, because re-equilibration among the phases will continue to occur until the JP-4 (LNAPL) source is removed.

MULTIPHASE TRANSPORT MODEL

Modeling is used to study the mobilization of the contaminant's three phases (soluble, free or liquid, and gaseous) with the application of the vacuum head and extraction flow rate. The modeling encompassed two steps. The first was to calibrate the

model by comparing the extracted liquid rates and volume to field values. Once model calibration is achieved, the multiphase flow model is used to investigate remediation times, taking into account the trapped JP-4 (LNAPL) in the soil pores.

Model Description

The computer software used for the multiphase flow and transport model is BIOSLURP, developed by RASI (Resources and System International, Inc). BIOSLURP is a commercially available code and is based on continuum analyses of the flow domain using the finite element approach. The advantage of this program is its ability to simulate the vacuum-enhanced recovery of multiphase (soluble, free or liquid, and gaseous) organics, which is the process employed by the PVWs implemented in the field. This software uses the Van Genuchten constitutive model along with fluid scaling parameters to compute water and free phase volumes (BIOSLURP, Technical Documentation and User Guide). In addition, the water, free or liquid JP-4, and gas transmissivities are continuously updated during the simulation, depending on the hydraulic head and matric suction conditions.

Model Configuration

Two configurations are assumed for the modeling effort. The first utilized the pad as implemented in the field for model calibration, and the second utilized a domain representative of one row of PVWs, assuming repeatability of the configuration. Figure 3-

13 displays schematically the basic steps of the modeling effort.

The domain for the model calibration is shown in Figure 3-14. A total aerial domain of 65.8 m x 39 m was discretized using 3,139 nodes. A uniform nodal spacing of 0.91 m was used in both the x and y directions. In Figure 3-14, the solid circles represent the location of the PVWs, and the solid black lines alongside the solid circles represent the alignment of rows. The solid triangle represents the location of monitoring well LMW-4 (Figure 3-1). The liquid (the free phase on top of the groundwater) elevation was set at a depth of 4.88 m (16 ft) below the ground surface, as was approximately measured in the field.

Because BIOSLURP solves from the left node to the right node, the test pad was modeled as a mirror image of the site to obtain a stable numerical solution. The thick solid line along the boundary of the test pad represents a constant head boundary. All boundaries were treated as no flow for the free phase. Along the four boundaries, the gas pressure was assumed to be atmospheric.

For estimation of end point of remediation, the modeling domain was reduced to 1.83 m x 12.8 m; representing one row that includes 7 PVWs with a zone of influence that is 1.83 m (a repeating unit of such configuration will represent the pad). A uniform nodal spacing of 0.91 m was used in both the x and y directions with a total number of nodes equal to 39 nodes. This approach for modeling the domain was necessary to in order to run the simulation in a reasonable computation time (run duration is about 5 h in this case).

Model Input Parameters

The soil properties needed for the flow simulation are: saturated hydraulic conductivity in the principal flow directions, soil porosity, irreducible water content, and Van Genuchten retention parameters (α and n.) As mentioned earlier, the hydraulic conductivity values of the test pad site reported in the past (Kunberger et al. 2003), based on groundwater well testing and laboratory hydraulic conductivity testing, range from 8 x 10^{-6} cm/s to 2 x 10^{-4} cm/s. The conceptual model for the multiphase transport is based on a single-layer soil with $8x10^{-6}$ cm/s of hydraulic conductivity.

The porosity of the soil was calculated from the water content and specific gravity and is equal to 0.45. The maximum residual free JP-4 (LNAPL) saturation was considered to be 15% in the saturated zone and 5% in the unsaturated zone. The Van Genuchten retention parameters, α and n, were according to Carsel et al. (1988). The data for the modeled soil are presented in Table 3-4 with reference to the source of the assumed value; these values were selected to be representative, as possible, the site soils and grain size distribution. The bottom boundary of the model (the aquifer bottom) is assumed level and sealed.

Fluid Properties

The fluid properties required by BIOSLURP are: the specific gravity ratio, ρ_{ro} (i.e., the ratio of the free LNAPL specific gravity to the water specific gravity), the dynamic viscosity ratio, η_{ro} (i.e., the ratio of the free LNAPL dynamic viscosity to the

water dynamic viscosity), and the surface tension of water; the surface tension of the free LNAPL; and the free LNAPL-water interfacial surface tension. These fluid properties are presented in Table 3-5 at an assumed temperature of 20^{o}C.

Physicochemical Properties of Contaminant

Contaminant transport is assumed to be governed by both advection and dispersion with possible retardation due to sorption. For dispersion, the longitudinal dispersivity is assumed based on the 1.83 m spacing between two PVWs. Anderson (1984) indicated that the longitudinal dispersivity is generally about one-tenth of the distance of a transport experiment. The longitudinal dispersivity is taken as 10% of 1.83 m (0.183 m). Because the flow vector is mainly in the horizontal direction, the transverse dispersivity has been chosen as 10% of the longitudinal dispersivity. The fraction of the sorption sites that are in contact with mobile water is considered to be 100%. The solubility of benzene (chosen to represent JP-4) is assumed to be 1,780 mg/L (Bedient et al. 1999). The benzene mole fraction in hydrocarbon is taken as 1%. The pure phase density of benzene is assumed equal to 867 kg/m^3. The concentration of benzene in the groundwater is taken as 0.3 mg/L, which is the average value measured from the monitoring well. The physicochemical properties for benzene are presented in Table 3-6.

MODELING RESULTS

Model Validation

The first objective of the modeling effort is to replicate the initial hydraulic head distribution within the flow domain. The average JP-4 thickness during March and April, 2006 in the LMW-4 and P6 (Piezometer # 6) was 0.23 m. No flow boundaries for the free JP-4 were assumed along the four sides of the model test pad, as indicated on Figure 3-14.

The model was calibrated for the extraction rate (for both water and free JP-4) for row #13 (Figure 3-2) to obtain volume and rate as monitored in the field. Data from row # 13 was selected for use in calibration since this row extracted maximum amount of free product and therefore provides the most performance data. Field testing shows that row #13 extracted 2,425 L of water and 25 L of JP-4 over a period 21.5 h. The total run time for row #13 in the field was 21.5 h in 12 days, which provides 1.79 h/d of operation on average. The average groundwater and free JP-4 extraction rates for row #13 were 125 L/h and 2 L/h, respectively. The field vacuum head ranged between 410 to 330 mm, based on data from the vacuum gauges. Accordingly, the first and last PVWs of the model row are assigned 410 mm and 330 mm vacuum heads, respectively. The vacuum heads in between the PVWs were assumed to vary linearly, and were computed accordingly.

Figure 3-15 and Figure 3-16 compare the field and model results obtained for groundwater and free phase JP-4 (LNAPL) volume recovery, respectively. Four operation times were simulated: 2, 4, 6 and 8 h of system operation/d. The model was run to match

the total extracted volume, regardless of the number of operating h/d, by adjusting the number of days to the simulation, as illustrated in Figures 15 and 16. For example, if the number of operational hours used in the field is 2 h/d, then the model was run for 10.75 days (21.5/2 = 10.75) to obtain the same volume of liquid as for the 21.5 h of run time. If the number of hours is 4 h/d, the model was run for 5.4 (21.5/4 = 5.4) days to obtain the field volume, as described above. A similar technique was used for the computation of the free phase JP-4 (LNAPL), as shown in Figure 3-16. It is expected that long term system operation time will be 8h/d, which will be used in the prediction of the end points of remediation.

The model shows that field results match well when the model was run approximately 2 h/d for a duration of 10.75 days, which simulates the 21.5 h operational time used in the field. That is, this scenario approximates the field case. The data in Figure 3-15 and Figure 3-16 show that other scenarios are also possible. For example, when operating 4 h/d at the average flow rate of 125 L/h, the field volumes are replicated using a model run time equal to 5.4 days (21.5/4 = 5.4). These analyses show that the model boundary conditions, initial head distributions and magnitude, and hydrogeologic parameters are reasonable, and that they yield results representative of the field conditions. Further model analyses based on 8 h/day of operation are stated below.

Predicted Remediation Time

After the model was calibrated, it was used to estimate the remediation time for

0.08 m of JP-4 thickness over a 1.83 m x 12.8 m area within row #13, as shown in Figure 3-17. The 0.08 m of free JP-4 (LNAPL) profile distribution in the subsurface is presented in Figure 3-18. The distribution was calculated using an Excel spreadsheet, developed by Charbeneau (2000) and based on the Brooks-Corey and Van Genuchten approaches to the creation of the soil-water-LNAPL characteristic curve in the vadose-saturated zone. The results of the distribution presented in Figure 3-18 are based on the assumed subsurface and fluid parameters presented in Table 3-6. Figure 3-18 shows that for the subsurface characteristics, the effective free JP-4 (LNAPL) layer saturation is 36.3%, based on the Van Genuchten model. This saturation yields 292 L of LNAPL that are available for extraction under an induced gradient.

The analyses assumed row #13 was operated 8 h/d. Removal time for the gaseous phase through soil vapor extraction under the applied vacuum head, and the time required to achieve drinking water standards for soluble phase benzene were estimated. The initial extraction flow rates for the model were 2 L/h for the free phase and 125 L/h for the soluble phase.

In this case, and given the model parameters, 292 L of free JP-4 (LNAPL) can be recovered in 19.5 days (based on 8 h of operation in a day) with an effective rate of 1.87 L/h. These flowrates are adjusted by the model to account for the changes in degree of saturation with extraction process.

In addition to the mass transfer from the free LNAPL phases, the transport model was simulated using an initial soluble phase and gas phase concentration of 0.3 ppm.

These values were selected respectively based on monitoring well and air sampling data done initially for the project at the beginning of the system operation. Figure 3-19 (left vertical axis) presents the variation of soluble phase concentration at point O (Figure 3-17). The drinking water standard for benzene is 0.005 ppm (ATSDR 1988), which is US EPA-defined threshold concentration. At the end of 4.25 years of system operation, the maximum benzene concentration is 0.002 ppm.

As the gas extraction is decoupled from the aqueous and free phase transport, the gas extraction rate is assumed to be equal to 10,273 L/min. The applied vacuum varied between 410 and 330 mm of mercury, depending on the PVW location. Figure 3-19 (right vertical axis) presents the maximum concentration in the vapor phase, 0.38 ppm at point O (Figure 3-17), is achieved after 2.5 years of vapor extraction. The threshold value for benzene in the gaseous phase is 0.5 ppm (ATSDR 1988). At the end of the gas and soluble phase removal below threshold value, simulation result shows that 8 L, 1% of the total volume (802.5 L) of oil still remained left as free LNAPL.

O&M COMPARISON

The WIDE system performance values are compared with results from one similar completed JP-4 environmental remediation projects Shaw AFB (IT Corporation 1998), as reported by the Federal Remediation Technologies Roundtable (FRTR). The details of the site used for this comparison is presented in Table 3-7. The Shaw AFB site is located in the coastal plains geologic zone in South Carolina with relatively shallow water table

depth less than 1.52 m below ground surface. The subsurface soils are sand and silts, compared to predominantly glacial till inter-bedded with sand/silt lenses at the subject site. The remediation system at Shaw consisted of skimmer pumps with target pump rate of 227 to 454 L/h. The system was however replaced with skimmer bailers placed in the wells to reduce operating costs. The cumulative mass removed versus O&M cost is shown Figure 3-20 for the two sites (Lockbourne and Shaw). Based on the data presented, the O&M cost of WIDE is comparable to the cost incurred for clean up at Shaw AFB.

SUMMARY AND CONCLUSION

The work reported herein documents the performance of WIDE technology for the *in situ* extraction of subsurface contamination. System performance for the extraction in LNAPL in various phases was presented in terms of monitored liquid rates and total organic concentrations in the air stream. Field testing consisted of 185 operating hours on 38 separate days over an 18-month period from mid-October 2005 until early April 2007. Predictive analyses were performed to model the multiphase contaminant transport process. The model was calibrated using field data and was then used for estimation of time required to attain an end point of remediation. Based on the data presented in this study, the following conclusions are advanced:

i. A total of 133 L of free JP-4 was removed from the subsurface in conjunction with 467 kg of organics in the vapor phase as volatilization took place

due to the application of vacuum heads exceeding the JP-4 vapor pressure. This mass is equivalent to a LNAPL liquid volume of approximately 567 L. The average LNAPL extraction rate was 0.72 L/h, and the average extracted mass in the gas phase was 2.54 kg/h.

ii. If free JP-4 is present, it is usually indicated by relatively high PID readings (approximately >500 ppmv), but typically within 1 to 2 h the PID readings are significantly reduced.

iii. In general, the higher liquid removal rates were achieved when the groundwater table was elevated. The average extraction rates varied between 75 L/h and 285 L/h.

iv. The model results indicate that 292 L of free JP-4 can be recovered in 19.5 days (based on 8 h of operation in a day). Under an applied vacuum head varying between 410 and 330 mm of mercury (1 cm Hg = 1.33 KPa)

v. The concentration in the vapor phase at the location of the pad is below regulated thresholds values after 2.5 years of extraction. The results of the model indicate that the soluble phase in the groundwater at the end of 4.25 years of system operation is at or below 0.005 ppm.

vi. The O&M cost versus time for the WIDE was comparable to that estimated for work at Shaw AFB. The average O&M cost was approximately $20/lb of extracted mass for system at both Lockbourne and Shaw AFB.

The difficulty of achieving complete remediation at the test site arises mainly

from the nature of the “wide cut” JP-4 contamination as well as from complex entrapment of jet fuel in the heterogeneous subsurface system with such entrapment being in saturated and unsaturated modes. An essential step to the remediation effort at the test site is the extraction of the free product acting as a source in the subsurface. In addition, an approach to remediating the entrapped residual globules should encompass vapor and liquid extraction, air circulation for promoting mass transfer to gas phase, vapor extraction for removal of organic vapors, and bioventing (increase dissolved-oxygen concentration for subsurface microbial populations to degrade organic compounds).

ACKNOWLEDGEMENTS

Many individuals and organizations contributed to the project's overall accomplishments. The Principal Investigators wish to specifically thank Mr. Kevin Jasper, P.E., Corps of Engineers, for his unwavering programmatic support. Mr. Roy Spears, Department of Energy, provided extensive support through site visits and equipment infrastructure for the project. Mr. Tom Learner, Nashville District, was instrumental in assisting with field work, especially during milestone steps such as system installation, sampling, etc. Mr. John Sneberger, Environmental Support Services, was the field technician on the project. The research team wishes to acknowledge the individuals, organizations, and agencies that contributed to the three phases of this work:

US Army Corps of Engineers

Louisville District	Nashville District	Huntington District
Kevin Jasper, P.E.	Thomas Lerner, P.G.	Dave Meadows, P.E.
Jay Trumble, P.E.	Lauren Heffelman	Frank R. Albert, Jr., P.E.
Doug Meadors, P.E.		

Rickenbacker International Airport

Paul Kennedy

National Environmental Education and Training Center (NEETC)

David Mallino

The air and liquid samples were analyzed by Research Environmental and Industrial Consultants, Inc.

REFERENCES

Adams, J.A., and Reddy, K.R. (2000). "Removal of dissolved- and free-phase benzene pools from ground water using *in situ* air sparging." *Journal of Environmental Engineering*. 126: 697-707.

Anderson, M. P. (1984). "Movement of contaminants in groundwater: Groundwater transport-advection and dispersion." *Groundwater Contamination, Studies in Geophysics*. Washington DC: National Academy Press. 37-45.

ASTM D 6282-98. (2008). *Standard guide for direct push soil sampling for environmental site characterizations.* http://www.astm.org/DATABASE.CART/HISTORICAL/D6282-98.htm (May16).

ASTM D422 – 63. (2007). *Standard Test Method for Particle-Size Analysis of Soils.* http://www.astm.org/Standards/D422.htm (October, 2008)

ATSDR (Agency for Toxic Substances and Disease Registry). (1988)."Benzene toxicity standard and regulations." <www.atsdr.cdc.gov/HEC/CSEM/benzene/standards_regulations.html> (June 2007).

Bartow, G. andDavenport, C. (1995). "Pump-and-Treat Accomplishments: A Review of the Effectiveness of Ground Water Remediation in Santa Clara Valley, California," *Ground Water Monitoring Review*. 140-146.

Bedient, P. B., Rifai, H. S. and Newell, C. J. (1999). "Groundwater contamination transport and remediation." *Sources and Types of Groundwater Contamination*. Upper Saddle River, NJ: Prentice Hall. 75-111.

BIOSLURP. (2004). *Technical documentation and user guide*. Resources and System International, Inc. Blacksburg, VA.

Braida, W. and Ong, S.K. (2000). "Influence of porous media and airflow rate on the fate of NAPLs under air sparging." *Transport in Porous Media*. 38: 29-42.

Burns, S. E. and Zhang, M. (2001). "Effects of system parameters on the physical characteristics of bubbles produced through air sparging," *Environmental Science and Technology. 35(1) (January):204-208.*

Cagle, G.A., Guerrero, J.A., Everds, P. and Gonzales, M. (1997). "Combining *in situ* technologies in low-permeability soil, a case study," *Proceedings of the 1997 ASCE Annual Fall National Convention.* Minneapolis, MN. (October): 297-311.

Carberry, J.B. and Wik, J. (2001) “Comparison of *ex-situ* and *in situ* bioremediation of unsaturated soils contaminated by petroleum.” *Journal of Environmental Science and Health - Part A Toxic/Hazardous Substances and Environmental Engineering*. 36:1491-1503.

Carsel, R. F. and R. S. Parish. (1988). “Developing joint probability distribution of soil water retention characteristics”. *Water Resources Research*. 24(5)(May): 755-769.

Charbeneau, R. J. (2000). “Groundwater hydraulics and pollutant transport.” *Spreadsheet Calculations of LNAPL Distribution*. Long Grove, IL: Waveland Press, Inc. 550-555.

Chemical Rubber Company (CRC). (1984). CRC handbook of chemistry and physics. Ed. Robert C. Weast. 65th ed. Boca Raton, FL: CRC Press, Inc.

Cho, J.S., Wilson, J.T., DiGiulio, D.C., Vardy, J.A., and Choi, W. (1997). “Implementation of natural attenuation at a JP-4 jet fuel release after active remediation.” *Biodegradation*. 8: 265-273.

Guarnaccia, J., Pinder, G. and Fishman, M. (1997). “NAPL: Simulator Documentation,” *EPA/600/R-97/102*. National Risk Management Research Laboratory United States Environmental Protection Agency, OK.

"Density of air." <http://en.wikipedia.org/wiki/Air_density> (2008).

Edwards, D. A., Andriot, M. D., Amoruso, M. A., Tummey, A. C., Bevan, C. J., Tveit, A., Hayes, L. A., Youngren, S. H., Nakles, D. V.(1997). "Development of fraction specific reference doses (RfDs) and reference concentrations (RfCs) for total petroleum hydrocarbons." Amherst, MA: Amherst Scientific Publishers.

Gabr, M. A., Bowders, J. J., and Woksien, S. (1995). "Prefabricated vertical drains (PVDs) for enhanced soil flushing." *Geoenvironment 2000*. New Orleans: 1250–1264.

Haley, J.L., Hanson, B., Enfield, C., and Glass, J. (1991). "Evaluating the effectiveness of ground water extraction systems." *Ground Water Monitoring Review.*119-124.

IT Corporation. (1998). "Groundwater Containment at Sites SD-29 and ST-30, Shaw AFB, South Carolina." http://costperformance.org/profile.cfm?ID=260&CaseID=260. (2008).

Johnston, C.D., Rayner, J.L., and Briegel, D. (2002). "Effectiveness of *in situ* air sparging for removing NAPL gasoline from a sandy aquifer near Perth, Western Australia." *Journal of Contaminant Hydrology.* 59: 87-111.

Kunberger, T., Quaranta, J. D. and Gabr, M. A. (2003). "Remediation of former Lockbourne Air Force Base using well injection depth extraction (WIDE)." *12th Panamerican Conference on Soil Mechanics & Geotechnical Engineering*. Cambridge, MA. (June): 1575-1581.

Lyman Warren, J., Reehl William, F., Rosenblatt and David H. (1993). "Handbook of Chemical Property Estimation Methods." McGraw-Hill, New York.

Ohio EPA. (1995). Chap. 10 in *Technical guidance manual for hydrogeologic investigations and ground water monitoring*.

Oostrom, M., White, M. D., Lenhard, R. J., Geel, P. J. V. and Wietsma T. W. (2005). "A comparison of models describing residual NAPL formation in the vadose zone." *Vadose Zone Journal.* 4:163–174.

Peignenburg, W.J.G.M. and Damborsky, J. (1996). "Biodegradability Prediction." Dordrecht, The Netherlands.

"Petroleum contaminated soil." <http://www.com.state.oh.us/SFM/pub/bust_1301_7-9-16.pdf> (Dec. 5, 2007).

Robertson, B.K. and Alexander, M. (1996). "Mitigating toxicity to permit bioremediation

of constituents of nonaqueous phase liquids." *Environmental Science Technology*. 30: 2066–2070.

Steffensen, W.S. and Alexander, M. (1995). "The effect of competition for available nutrients in systems containing mixtures of substrates." *Applied Environmental Microbiology*. 61: 2859–2862.

Travis, C.C. and Doty, C.B. (1990). "Can contaminated aquifers at superfund sites be remediated?" *Environmental Science and Technology*. 24(10):1464-1466.

Waduge, W.A.P., Soga, K. and Kawabata, J. (2004). "Effect of NAPL entrapment conditions on air sparging remediation efficiency." *Journal of Hazardous Materials*. 110: 173-183.

Warren, K. A., Gabr, M. A. and Quaranta, J. D. (2006). "Field study to investigate WIDE technology for TCE extraction." *Journal of Geotechnical and Geoenvironmental Engineering* 132 (9) (Sept): 1111-1120.

Wiedemeier,T. H., Swanson, M. A., Wilson, J.T., Kampbell, D. H., Miller, R. N. and Hansen, J. E. (1996) "Approximation of biodegradation rate constants for monoaromatic hydrocarbons (BTEX) in ground water." *Ground Water Monitoring &*

Remediation. 16(3): 186-194.

Xie, G. and Barcelona, M. J. (2003). "Sequential chemical oxidation and aerobic biodegradation of equivalent carbon number-based hydrocarbon fractions in jet fuel." *Environmental Science and Technology*. 37 (20) (Oct): 4751-4760.

Yen, H.K., Chang, N.B. and Lin, T.F. (2003). "Bioslurping model for assessing light hydrocarbon recovery in contaminated unconfined aquifer. I: Simulation analysis". Practical Periodical of Hazardous, Toxic, and Radioactive Waste Management. 7 (2): 114-130.

Table 3-1 Details of WIDE Components.

Item	**Data**
System footprint	12.8 m wide x 44 m long
PVWs	
Total # PVWs installed	188
Spacing	1.83 m on center
Installation depth	6.1 m BGL (Below Ground Level)
Sheathed interval	3.96 m BGL
Unsheathed interval	2.13 m
Surface piping size	2.54 cm dia. PVC
Geotextile	Typar 4457
Apparent opening size	120 US sieve
Mass of filter	1.3 Newton/m^2

Table 3-2 Physical Characteristics of the Site Soils.

Depth (m)	**Specific gravity**	**Liquid limit (%)**	**Plasticity index (%)**	**Soil type (Plasticity chart)**
3.66-4.88	2.7	23.3	8.5	Sandy and silty clays
4.88-4.95	2.73	Non-plastic		Silty sand
4.95-5.49	2.7	19.3	5.5	Silty clays
5.49-10.67	2.7	20.4	6.4	Clayey silts and sands

Table 3-3 Summary of Sample Locations and Depth using PID Data.

Location #	Sample designation	Depth (m)	Moisture content (%)	On-site PID data (ppm is volume-based)	TPH (mg/Kg)
1	DP-601-8	2.44	NT	VOC=2050 ppm LEL=7%	NT
	DP-601-14	4.27	14	VOC=185 ppm LEL=4%	3780
	DP-601-19	5.79	11	No Test Data	256.5
	DP-601-23	7.01	14	No Test Data	335.9
2	DP-602-15	4.57	16	VOC=90.8 ppm, LEL=0%	154.0
	DP-602-19	5.79		No Test Data	NT
	DP-602-26	7.92	12	No Test Data	281.2
3	DP-603-17	5.18	17	VOC=1099 ppm	3948.0
4	DP-604-10	3.05	15	VOC=2017 ppm, LEL=7%	359.6
	DP-604-15	4.57	17	VOC=2030 ppm, LEL=9%	10530
	DP-604-19	5.79	12		24.5
5	DP-605-10	3.05	19	VOC=234 ppm LEL= 7%	200.7
	DP-605-16	4.88	19	No Test Data	666.4
	DP-605-20	6.10	18	No Test Data	112.4

Table 3-4 Input Subsurface Characteristics.

Groundwater table depth (from ground surface)	4.95 m
Soil type[a]	Gray/brown silty sand (SM)
Water content, %[a]	22.8
Permeability, cm/s[a]	8×10^{-6}
Specific gravity, Gs[a]	2.73
Residual water saturation[b]	0.09
Maximum residual free JP-4 saturation[b]	0.15
Unsaturated zone maximum residual saturation[b]	0.05
Van Genuchten, α, 1/m[c]	3
Van Genuchten, n[c]	1.2

[a]Field and Laboratory Measured

[b]Petroleum contaminated soil, Charbeneau et al. (2000)

[c]Carsel et al. (1988).

Table 3-5 Input Fluid Parameters

Name of fluid properties	Numerical value
Density of JP-4 (jet fuel or LNAPL)[b]	800 kg/m^3
Density of air (20^{o}C)[a]	1.2 kg/m^3
Free JP-4 -to-water dynamic viscosity ratio, η_{ro}[b]	0.9
Surface tension of water, σ_w[b]	.072 (N/m)
Air-free JP-4 surface tension, σ_o[b]	0.025 (N/m)
LNAPL-water interfacial surface tension, σ_{ow}[b]	0.053 (N/m)
Air-to-water dynamic viscosity ratio[b]	0.018

[a]http://en.wikipedia.org/wiki/Air_density

[b]Oostrom et al. (2005)

Table 3-6 Physicochemical Properties for Benzene

(Lyman et al.1993)

Free JP-4 -water nonequilibrium mass transfer coefficient[a] 1/m	1.25
Air-free JP-4 nonequilibrium mass transfer coefficient[a] 1/m	1.25
First order decay coefficient for benzene in water phase 1/d	0.005
Henry's coefficient	0.24
Distribution coefficient for benzene, cc/gm	0.83
Diffusion coefficient of benzene in water, m^2/d	0.0001
Diffusion coefficient of benzene in air, m^2/d	0.76

[a] defined in Yen et al. (2003)

Table 3-7 Federal Remediation Technologies Roundtable (FRTR) Compared Sites

Site Name/Location	**Soil Lithology**	**Date**	**Contaminant & Contaminant Phase**
Site SD-29 and ST-30; Shaw AFB, South Carolina, US Air Force	Sands & Silts.	March 95 to February 96	JP-4, Liquid (product
Former Lockbourne, AFB, Columbus, ohio	Silty to clayey fine-grained sands.	October 2005-January 2007	JP-4, Air and Liquid (product)

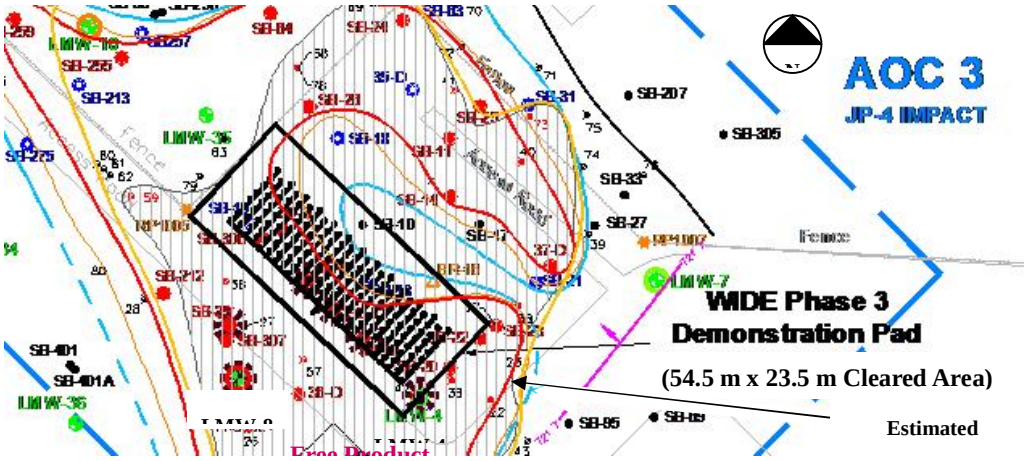

Figure 3-1 WIDE system at former Lockbourne AFB.

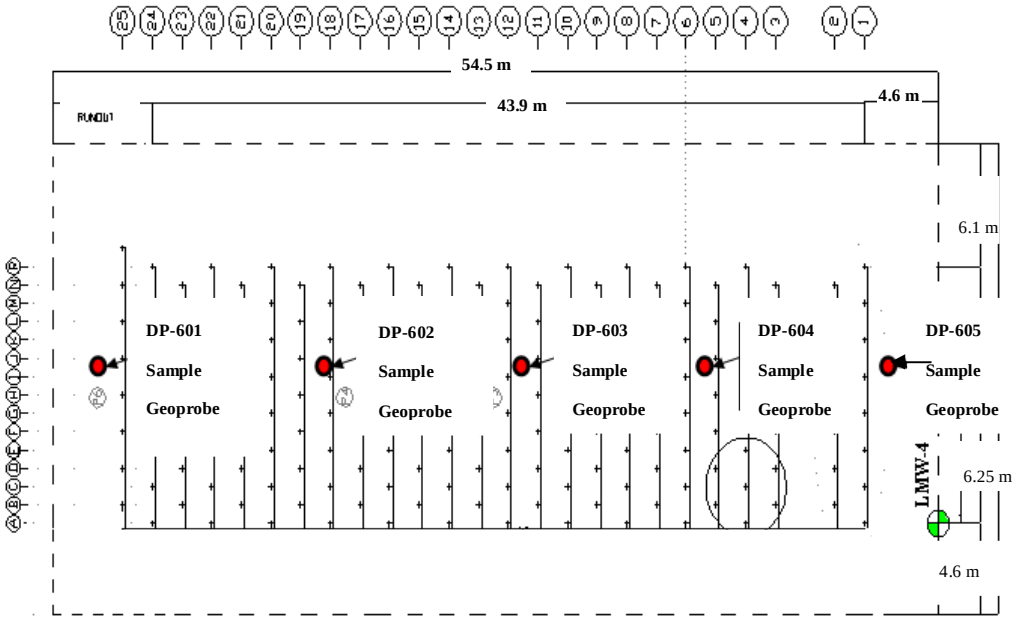

Figure 3-2 Schematic plan view of test pad and location of soil logs.

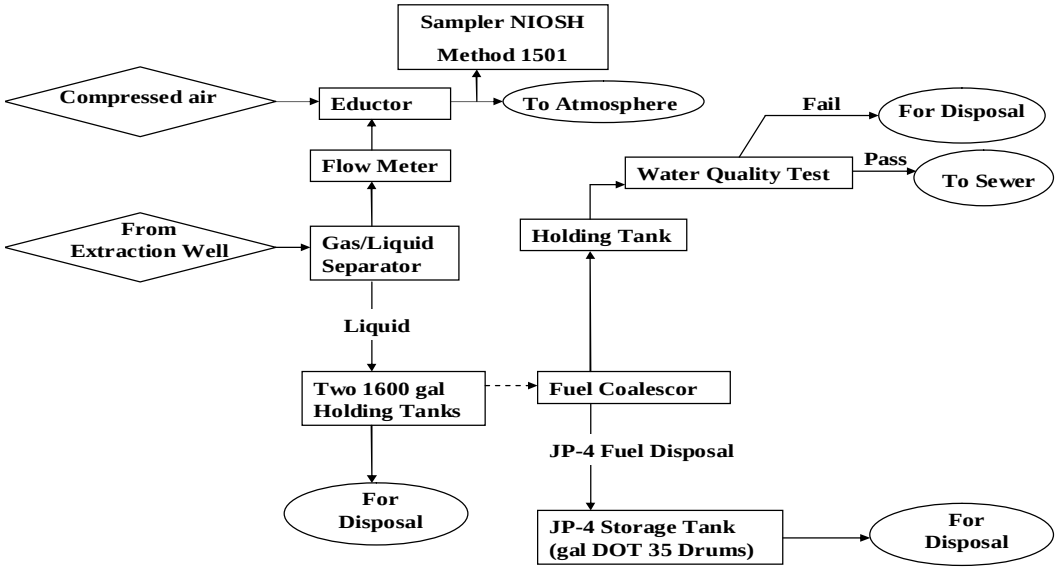

Figure 3-3 Flow process diagram of proposed WIDE field operation.

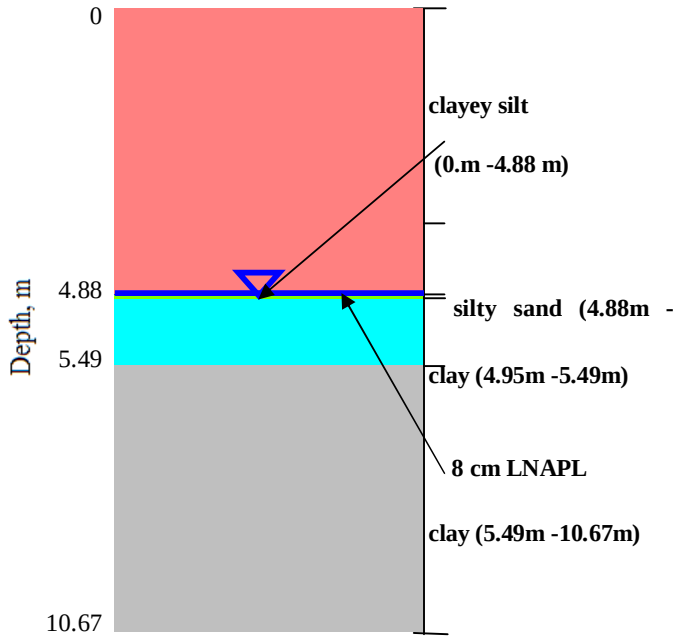

Figure 3-4 Vertical soil profile in addition to Table 3-2.

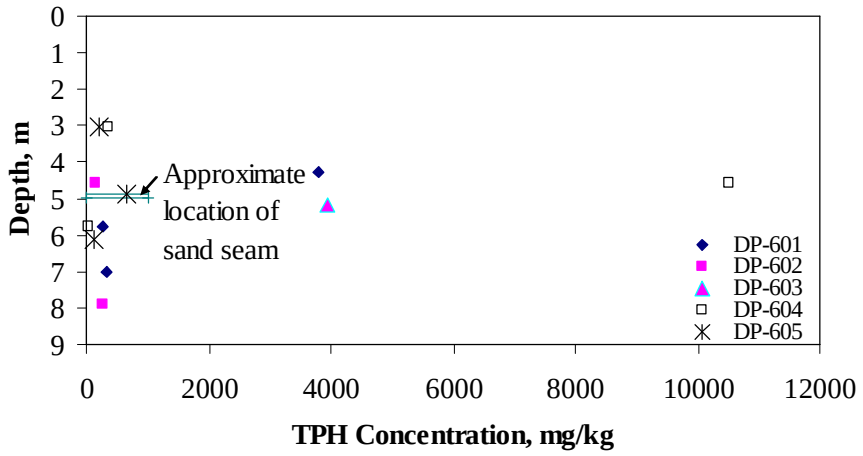

Note: Contaminants shown are DRO, GRO and KRO; and locations are shown in Figure 3-2.

Figure 3-5 Distribution of TPH contamination with depth, as obtained from the extraction of the solid phase.

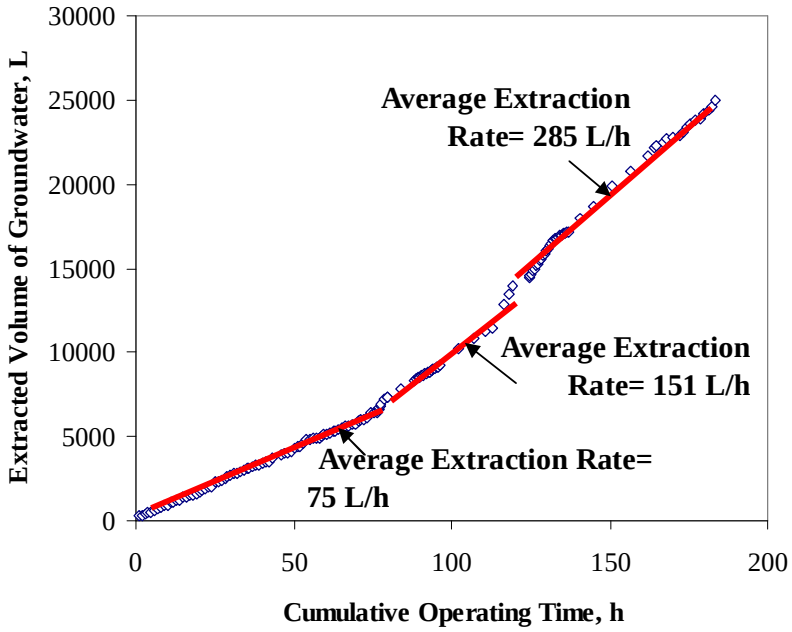

Figure 3-6 Cumulative extracted groundwater as a function of operating time.

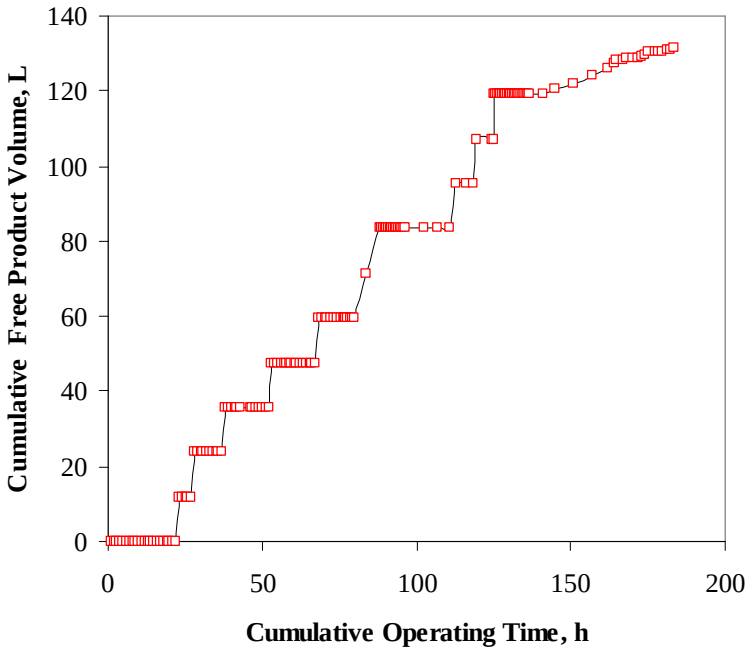

Figure 3-7 Cumulative extracted free JP-4 volume as a function of operating time.

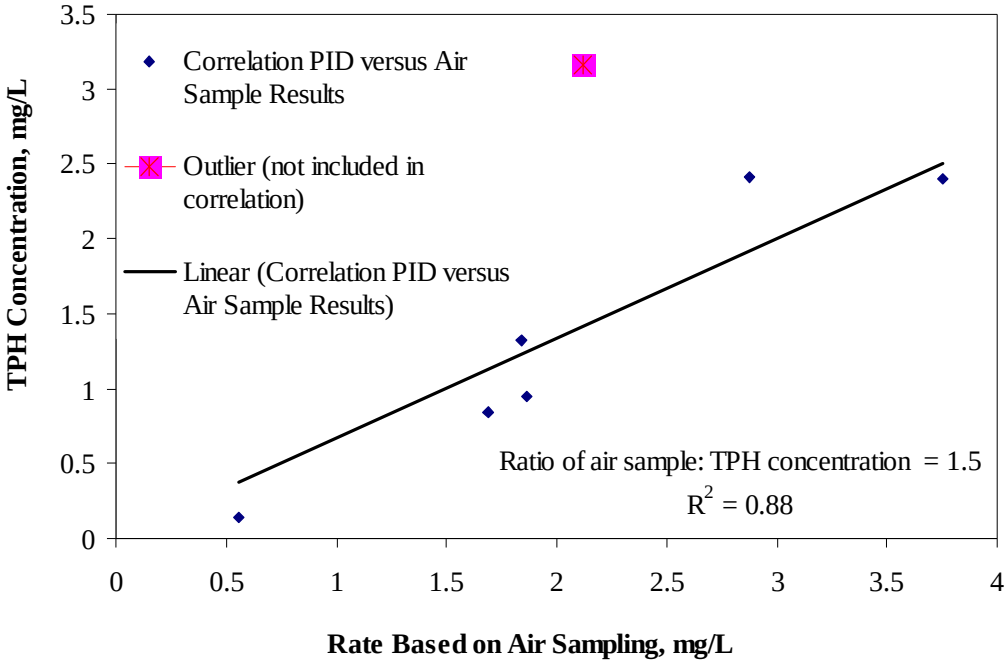

Figure 3-8 Relationship between PID data and concentrations obtained from sampling using carbon cartridges.

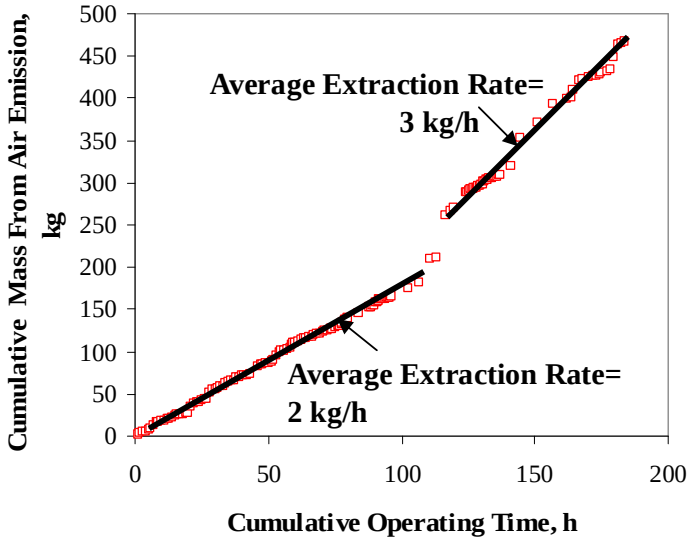

Figure 3-9 Cumulative mass of JP-4 vapor removed as a function of operating time.

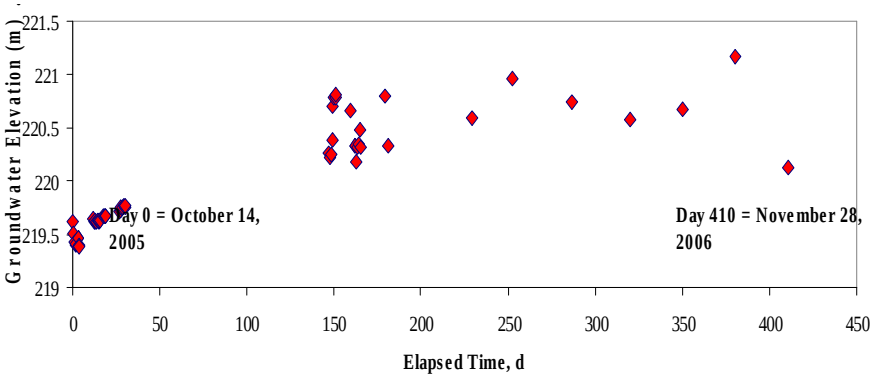

Figure 3-10 Variations in groundwater depth as a function of time for LMW-4.

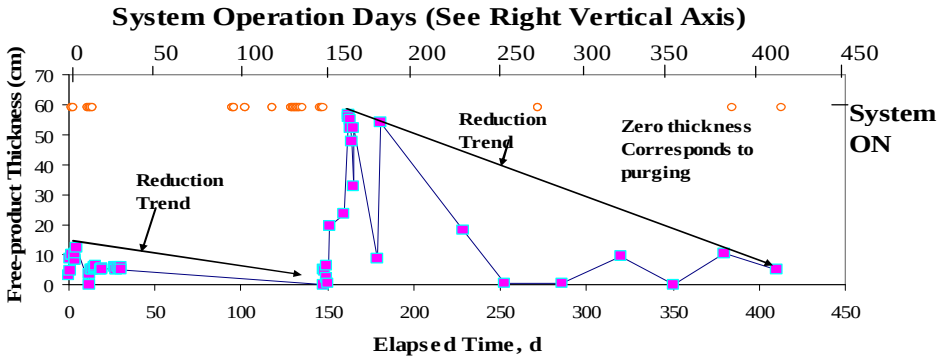

Figure 3-11 Variations in JP-4 plume thickness as a function of time for LMW-4.

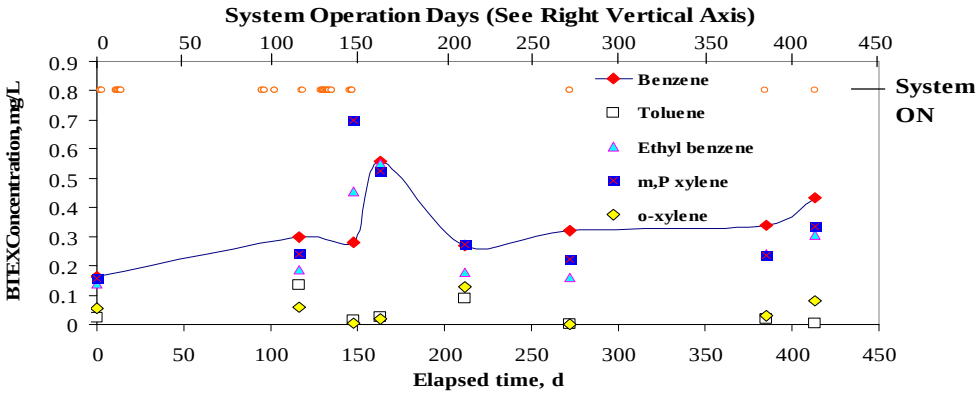

Figure 3-12 BTEX concentration variations as a function of time for LMW-4.

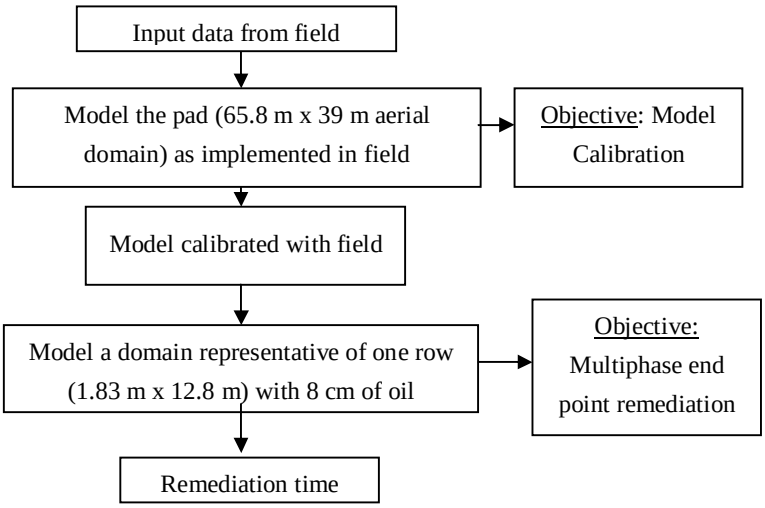

Figure 3-13 Flowchart showing the basic steps of modeling effort.

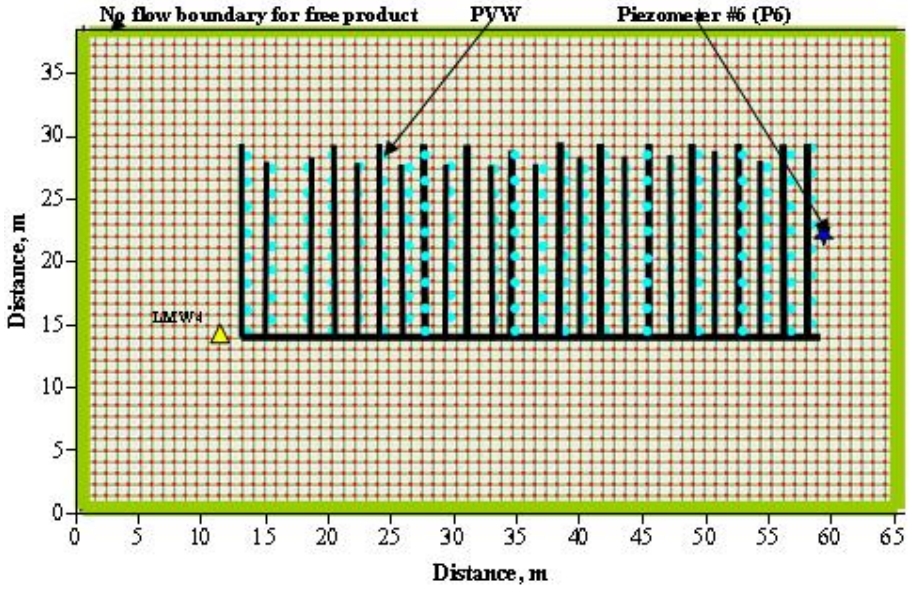

Figure 3-14 Plan view of test pad.

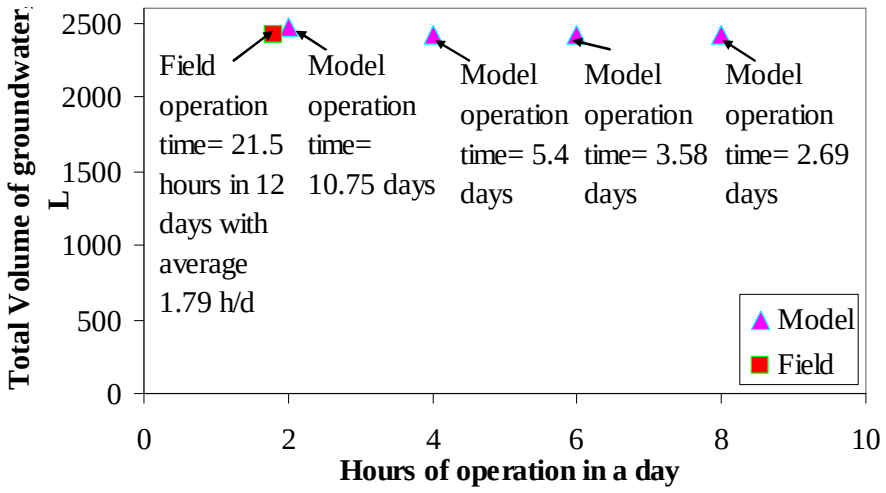

Figure 3-15 Comparison of extracted total volume of groundwater for field and model.

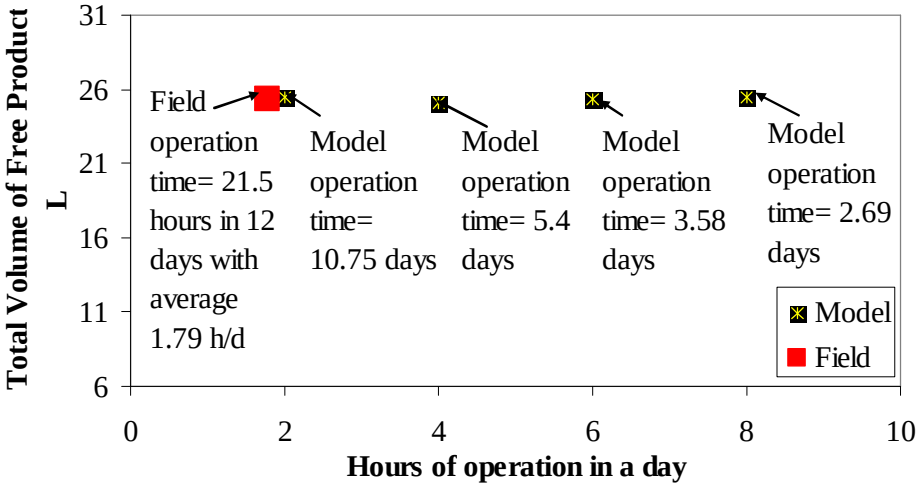

Figure 3-16 Comparison of extracted total volume of free phase JP-4 (LNAPL) for field and model.

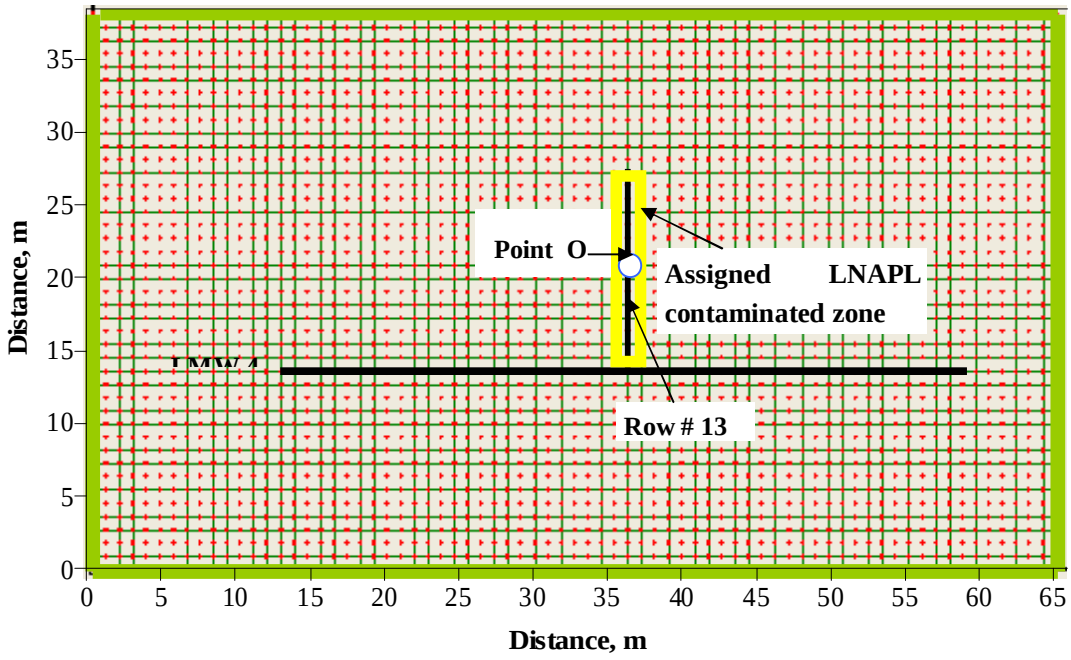

Figure 3-17 Assigned LNAPL contaminated zone.

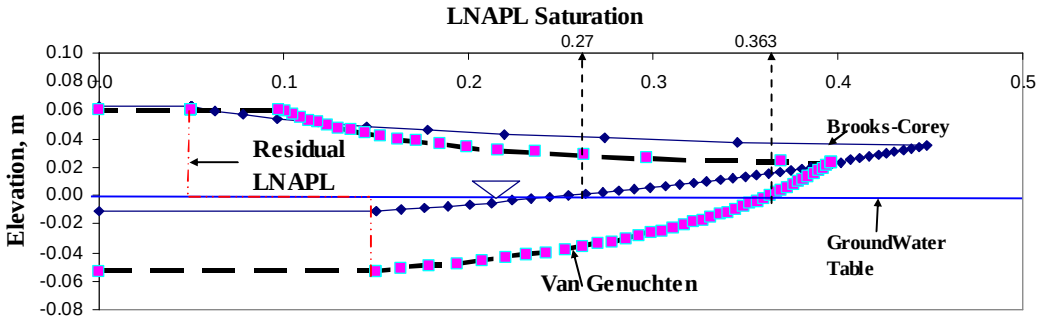

Figure 3-18 Liquid JP-4 distribution in subsurface (based on 0.08 m or 3-inch thickness of free product).

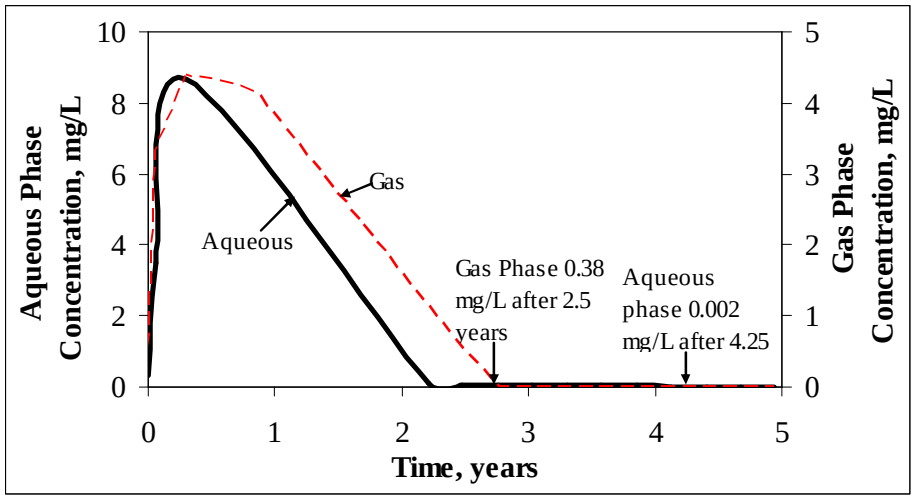

Figure 3-19 Aqueous (soluble) and gas phase variation with time.

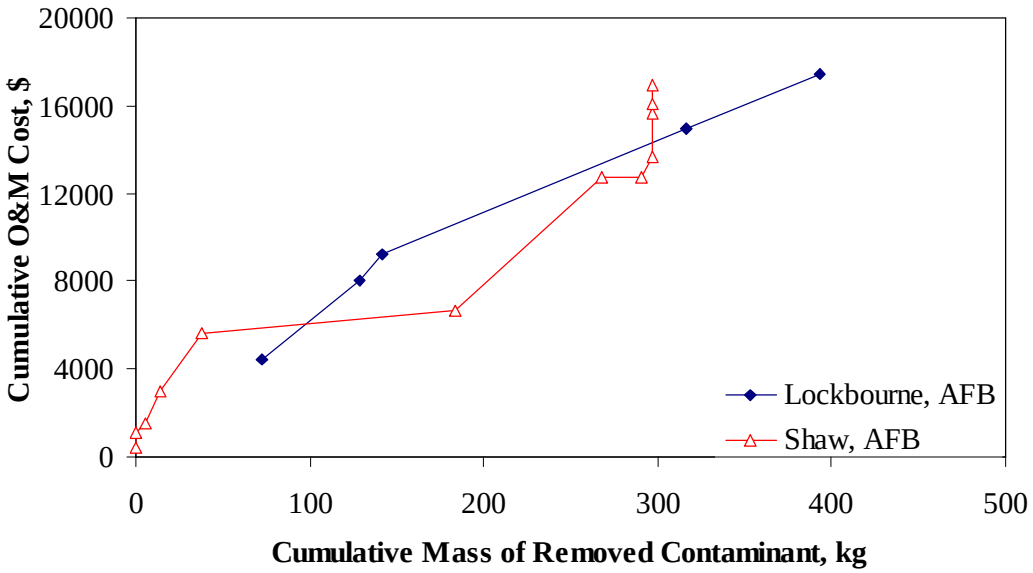

Figure 3-20 Cumulative O&M costs vs. cumulative extracted mass.

4. PARAMETERS AFFECTING MULTIPHASE LNAPL RECOVERY USING PREFABRICATED VERTICAL WELLS (PVWS)

To be submitted to the Canadian Geotechnical Journal

PARAMETERS AFFECTING MULTIPHASE LNAPL RECOVERY USING PREFABRICATED VERTICAL WELLS (PVWs)

N. Sharmin and M. A. Gabr

ABSTRACT

This paper integrates parameters calibration and analysis to explore the mechanics involved with extraction of LNAPL using prefabricated vertical wells installed on a relatively close spacing. The analyses are performed using the computer program BIOSLURP and were mainly focused on free LNAPL recovery. The modeling study included two components; firstly validating the hydraulic and hydrogeologic parameters by calibrating the model with the field results and secondly, a parametric study varying the key parameters of the calibrated model. Five key parameters were varied to determine the effect on the LNAPL flow and transport behavior, these are water extraction rate, irreducible water, LNAPL and gas content, both monitoring well and actual LNAPL thickness and impact of loading from hydrocarbon for both soluble and gas phase. Analyses results indicated that injection/extraction operational mode is undesirable if LNAPL recovery is the primary focus due to having the wetting flood bypassing the LNAPL under the induced gradient. It was found that LNAPL removal percentage is not dependent on the water to LNAPL extraction rates as long as free LNAPL exists in the subsurface. The LNAPL percent removal rate varied from 65% to 20% due to the variability of entrapped mass as hydraulic conductivity and porosity were

varied. In addition, the magnitude of irreducible LNAPL content has significant influence on the extraction efficiency. Increasing irreducible LNAPL from 5% to 20% decreases the percent removal from 52% to 0.2% for 0.08 m LNAPL assuming constant head boundary condition. For the same soil type, lower initial LNAPL thickness decreases LNAPL removal efficiency. Results showed that the reduction of initial actual LNAPL thickness from 0.08 to 0.03 m decreased the free LNAPL removal from 65 to 35% for sand.

KEYWORDS: Light Non-Aqueous Phase Liquid (LNAPL); Multiphase contaminant transport; Prefabricated Vertical Wells (PVWs); Remediation technique in low permeability soil; Simulation and optimization.

INTRODUCTION

The behavior of an immiscible hydrocarbon plume, such as Light Non Aqueous Phase Liquids (LNAPL), is different from those of dissolved contaminant plume in the subsurface. LNAPL in the subsurface generally forms a visible, separate oily phase and float on top of the groundwater table (Bedient et al. 1997). As many of the spills occurred several decades ago, there is usually insufficient information regarding the volume and extent of a given spill, and therefore it is difficult to characterize the performance of engineered remediation system. It is of interest to note that review of available literature did not yield information on a one remediation system that has been successful in

removing 100% of free LNAPL from the subsurface. This is mainly due to the trapping of residual LNAPL blobs in individual pores with groundwater level variation, and the complex behavior of LNAPL within soil/aquifer matrix.

The most common *in-situ* remediation system is the 'pump and treat' approach. However these systems have traditionally shown tailing and rebounding effects over time (see for example Travis et al. 1990, Haley et al. 1991, and Bartow et al. 1995). The Well Injection Depth Extraction (WIDE) system introduced by Gabr et al. (1997) has attempted to provide an approach to enhance the extraction process. By virtue of installing prefabricated vertical wells on a close spacing, the hydraulic head distribution within the remediation field is controlled such that gradients for gas and liquid flow is increased, and mobilization of the plume toward extraction points is enhanced. By virtue of applying vacuum head and distributing it within a subsurface domain, interphase mass transfer and equilibrium among various phases of LNAPL are altered for the benefit of mobilization and mass extraction.

In comparison to *in situ* active extraction of substance contaminant process, a common approach that can be classified as rather passive is bioremediaiotn. The feasibility of *in situ* bioremediation of high levels of organic compounds is however questionable. Robertson et al. (1996) indicated that NAPL's toxicity inhibits microorganisms and prevent their growth, which, in turn lengthens the acclimatization period prior to biodegradation taking place. Steffensen et al. (1995) indicated that biodegradation is critically dependent on the particular physio–chemical characteristics of

a NAPL and contaminated site soils. It is also the case that entrapped residual NAPL may be biodegradation-resistant due to the presence of toxic compounds, or unavailability of nutrients. Peignenburg et al. (1996) specified that methods of predicting rates of biodegradation in the field seem to be lacking.

Another approach reported in literature is air sparging (a process by which air is injected into the subsurface to strip volatile organic compounds (VOCs) from liquids and solids). In this case, positive pressure is used for impacting gas distribution within a zone of influence. Adam et al. (2000) indicated that air sparging can be used to effectively remediate dissolved and free phase Benzene based on results from a laboratory study. Besides laboratory studies, mathematical modeling is playing a major role in explaining, analyzing and understanding remediation of petroleum hydrocarbons in groundwater environments (Langley et al. 2005).

The aim of work in this paper is to investigate parameters related to mass extraction and phase transfer of subsurface LNAPL contamination during operation of prefabricated vertical wells installed on a close spacing. The model, developed using finite element based program, is calibrated using data from a field study. A parametric study is performed to ascertain system performance aspects. Parameters considered in the analysis included liquid extraction rate, LNAPL thickness within the subsurface, phase transfer coefficients and irreducible water, LNAPL and gas contents. In addition, the overall recovery efficiency of LNAPL is assessed in viewed of the varied.

MULTIPHASE MODEL

A two-dimensional finite element analysis model is developed using BIOSLURP, by RASI (Resource and System International, Inc). BIOSLURP is a commercially available code for continuum analyses of the multiphase flow domain. The transport module simulates the aqueous and gas phase transport, and computes and updates the temporal and spatial variation of the contaminant concentration for the inter-phase mass transfer (extraction mode) for each time step during the simulation. The advantage of this program is its ability to simulate recovery of multiphase (soluble, free or liquid and gaseous) organics, which is the process employed by the prefabricated wells implemented in the field. As the extraction process leads to desaturation, an estimate of liquid and gas head distributions is obtained; software flow module continuously updates the distribution of the LNAPL specific volume in the subsurface domain accordingly, and defines its temporal and spatial variation for the transport module.

Multiphase flow

A brief description of the fundamental mass conservation equations implemented in BIOSLURP for water, LNAPL and gas were described by Katyal et al. (1988) and Yen et al. (2003). The vertically integrated volume balance equation for the water, oil, and gas phases are displayed in Equation 1, 2 and 3 (Katyal et al. 1988, Yen et al. 2003), where V_w=specific volume (L) of water; V_o=specific volume (L) of NAPL; and V_a=specific volume (L) of gas. $Tw_{i\ j}$ =water transmissivity tensor; To_{ij}= oil transmissivity tensor; and

Ta_{ij}=gas transmissivity tensor; Rp=source/sink rate (LT^{-1}); p=w, o, and a for the water, oil, and gas phase respectively; Z_{ao} = air-oil interface and Z_{ow} = oil-water interface.

$$\frac{\partial Vw}{\partial t} = \frac{\partial}{\partial x_i}[Tw_{ij}\frac{\partial Zaw}{\partial x_j}] + R_w$$

Equation (1)

$$\frac{\partial Vo}{\partial t} = \frac{\partial}{\partial x_i}[To_{ij}\frac{\partial Zao}{\partial x_j}] + R_o$$

Equation (2)

$$\frac{\partial Va}{\partial t} = \frac{\partial}{\partial x_i}[Ta_{ij}\frac{\partial Zaa}{\partial x_j}] + R_a$$

Equation (3)

Constitutive Relationship

In BIOSLURP program, relationships between phase saturations and pressures are described by a three-phase extension of the Van Genuchten (1980) model, which takes into account the effects of LNAPL entrapment. Prior to the occurrence of oil at a given location, the system is treated as a two-phase air-water system described by the Van Genuchten (1980) function as follows (Katyal et al. 1988 and Yen et al. 2003):

$$\overline{S}_w = \left[1 + (a y_{aw})^n\right]^{-m}$$

Equation (4)

Where

$\bar{S}_w = \frac{(S_w - S_m)}{(1 - S_w)}$ is the effective water saturation,

S_m is the irreducible water saturation,

$y_{aw} = h_a - y_w$ is the air-water capillary pressure,

α [L^{-1}] and n are porous medium parameters, and

$m = 1 - \frac{1}{n}$

Following the occurrence of oil at a location, the system is then described by the three phase relations as shown in equations 5, 6 an7 (Katyal et al. 1988 and Yen et al. 2003):

$$\bar{\bar{S}}_w = \left[1 + \left(a \frac{s_w}{s_{ow}} y_{ow}\right)^n\right]^{-m}$$

Equation (5)

$$\bar{S}_t = \left[1 + \left(a \frac{s_w}{s_o} y_{ao}\right)^n\right]^{-m}$$

Equation (6)

Where

$\bar{\bar{S}}_w$ is the apparent water saturation,

$\overline{S}_t$ is the effective total liquid saturation,

$y_{ow} = y_o - y_w$ is the oil-water capillary pressure,

$y_{ao} = h_a - y_o$ is air-oil capillary pressure,

s_w is the surface tension of water,

s_o is the surface tension of oil,

s_{ow} is the oil-water interfacial surface tension.

The apparent water saturation is given by

$$\overline{\overline{S}}_w = \overline{S}_w + \overline{S}_{ot}$$

Equation (7)

Where

$\overline{S}_{ot}$ is the effective trapped oil saturation, can be estimated using an empirical relationship given by Land (1968). The vertical integration of phase saturation profiles gives specific volume of water, V_w and specific volume of oil V_o.

$$V_w = \int_{Z_L}^{Z_u} f S_w(Z) dz$$

Equation (8)

$$V_o = \int_{Z_{ow}}^{Z_u} fS_o(Z)dz$$

Equation (9)

Where,

Z_{ow} = oil-water interface

Zu = top elevation of the capillary fringe

LNAPL-layer relative permeability

LNAPL phase distribution in subsurface can be defined by a relative permeability curve (Figure 4-1) based on Land (1968) and Williams et al. (1971). Newell et al. (1995) surmized that relative permeability (ratio of effective permeability of the medium to a fluid at partial saturation to the permeability at 100% saturation) can describe different types of multiphase flow regimes (all of which may exist at any particular site):

Zone 1: LNAPL occurs as a potentially mobile, continuous phase and saturation is high. Water is restricted to small pores. The relative permeability of water is low. Such conditions may be observed within large mobile product accumulations.

Zone II: Both LNAPL and water occur as continuous phases, but, generally, do not share the same pore spaces. However, the relative permeability of each fluid is greatly reduced by the saturation of the other fluid. Such conditions may be representative of zones of smaller mobile product accumulations at the water table.

Zone III: LNAPL is discontinuous and trapped as residual in isolated pores. Flow is almost exclusively related to the movement of water, not LNAPL. Examples of such conditions may be found within zones of residual LNAPL retained below the water table.

Transport model

The vertically integrated transport equation for species α in the saturated zone soluble phase is displayed in Equation 10 (Katyal et al. 1988, Yen et al. 2003).

$$\frac{\partial C_{am}}{\partial t_i}[V_{wm} + frB_l K_d] = \frac{\partial}{\partial x_i}(V_{wm} D_{mij} \frac{\partial C_{am}}{\partial x_j}) - Q_{wi} \frac{\partial C_{am}}{\partial x_i} - q_s (C_{as} - C_{am}) B_l - l_{am} B_l + B_l H_{ga} + I_{m\text{-}im} B_l + I_{m\text{-}g} B_l$$

Equation (10)

where V_w=specific volume of water; V_{wm}=specific volume of water in the mobile phase $\cong V_w S_m$; Q_{wi} and Q_{wj}=horizontal, vertically integrated flux ($L^2 T^{-1}$) assuming linear adsorption ($P=k_d C$), decay losses $\lambda_{\alpha m}$ [T^{-1}] and the contaminant load from a hydrocarbon source to the mobile phase $H_{g\alpha}$ [L^{-1}]. Similarly, the vertically integrated transport equation for species α in the unsaturated zone gas phase is displayed in Equation 11 (Katyal et al. 1988, Yen et al. 2003).

$$\frac{\partial}{\partial t}[V_a C_{aa}] = \frac{\partial}{\partial x_i}[V_a D_{aij} \frac{\partial (C_{aa)}}{\partial x_j}] - \frac{\partial}{\partial x_i}[Q_{azj} C_{aa}] + b_{ui} H_{\partial a} + l_{aa} B_{ui} - I_{g-mw} B_{ui} - I_{g-imw} B_{ui} - Q_a C_{aas}$$

Equation (11)

where Va=specific volume of air in the unsaturated zone; Daij=hydrodynamic dispersion tensor in the gas phase; $H_{\partial a}$=contaminant load from a hydrocarbon source into the gas phase; Q_{azj}=vertically integrated gas flux; B_{ui}=unsaturated zone thickness; $\lambda_{\alpha a}$=decay term for the unsaturated zone; and the last term is the source/sink for the gas phase.

SOIL CHARACTERISTICS PARAMETERS

Extensive studies have been performed by the United States Department of Agriculture and the United States Environmental Protection Agency (EPA) to determine the soil-water retention parameters based the Brooks and Corey (1966) and the Van Genunchten model (1980) approaches, respectively. These studies provided estimates of the model's parameters and their variation based on readily obtainable soil texture information. Rawls et al. (1982) and Rawls et al. (1993) summarized the USDA data, while Carsel et al. (1988) presented the EPA data. Carsel et al.(1988) used a data base for the 12 Soil Conservation Service (SCS) textural classifications as obtained from measurements reported in SCS Information Reports. These reports generally contained soil data for the predominant soil series within a state. A total of 42 books representing 42 states were used to develop the database. Carsel et al.(1988) used a multiple regression

equation developed by Rawls et al. (1985) to estimate the retention parameters for the Brooks and Corey Model and the corresponding Van Genunchten parameters from equation 12 and 13 (Charbennau, 2000).

$$l = n - 1$$

Equation (12)

$$y_b = \frac{1}{a}$$

Equation (13)

where

ψ_b= Displacement pressure head, m

λ = Pore size distribution index

α [L^{-1}] and n are the Van Genuchten porous medium parameters

In Table 4-1, the first six columns and 2nd to 13th rows presents the average soil texture data and Van Genuchten model parameters obtained from Carsel et al. (1988) study. The 7th Column displays the specific volume for different soil types, calculated for 1.44 m of monitoring well thickness using Equation 9 and the parameters obtained from Carsel et al. (1988) for as corresponding soil. The 1.44 m of LNAPL well thickness was a value monitored during a field study related to this project (Sharmin et al. 2009). The last row (14th row) shows the soil texture data obtained for a test soil (soil encountered during the field study) to obtain 0.08 m specific volume of oil in the test pad area corresponding to 1.44 m of monitoring well thickness (using Equation 9). The validity of Equation 9 is

checked using Charbeneau's (2000) approach for estimation of free product volume. Figure 4-2 presents the calculated specific volume thickness corresponding to 1.44 m of monitoring well thickness, which is identical that estimated by Charbeneau (2000). Results for different types of soils are also presented in this figure. It is of interest to note that this paper used Van Genuchten parameters, while Charbenaeu (2000) used Brooks and Corey parameters.

TEST SITE DESCRIPTION

Field testing was performed in Lockbourne, Ohio (Sharmin et al. 2009) as a part of this research program. The field site was contaminated with BTEX (Benzene, Toluene, Ethylbenzene and Xylene), Jet Propellant 4 (JP-4), and Jet A petroleum hydrocarbon from leaking underground storage tanks and failure in the underground piping system. The prefabricated vertical wells (PVWs) were installed at the sites and operated for 38 days in an 18 months period at the field test site (see Sharmin et al. 2009 for details).

Site Conditions

The site soils are characterized as glacial till with shale fragments, clay, silt, and sand with locally isolated layers of silty sand. These isolated layers are poorly connected, suggesting a lenticular morphology and are approximately 0.08 m in thickness. Hence, the extraction of the LNAPL at this site is further compounded by such heterogeneity which not only impacts the mobilization of LNAPL but also its entrapment on micro

(intra particles) and macro (intra layers) scales.

Groundwater on site was detected in a gray/brown, medium dense, silty sand layer 4.88-5.49 m below ground level. The site is of generally flat topography with the groundwater's natural gradient less than 1% based on elevations from well data. The hydraulic conductivity values reported in the past, based on groundwater well testing, ranged from 8×10^{-6} cm/s to 2×10^{-4} cm/s (Kunburger et. al. 2003, Sharmin et. al. 2008).

PVWs Implementation

The field experiments of the *in situ* pilot-scale remediation system included 188 PVWs. The test pad included an area measuring 13m by 44m, surface piping network consisted of 25 rows – each encompassing 7 or 8 PVWs, and a 17 m^3/min air compressor powering a 5cm (2-inch) diameter eductor vacuum system. The PVWs were installed 6.1 m (Below Ground Level) deep in a grid pattern of offset rows that were spaced approximately 1.83 m apart. Each PVW was sheathed with an impermeable sleeve to a depth of 3.96 m (Below Ground Level). A 1.5 m^3 tank was used as a means for applying vacuum pressure to the piping network, and temporarily store extracted fluids. The extracted liquid was transferred to two 6 m^3 liquid holding tanks for subsequent disposal. The system is operated in dual-phase extraction (DPE) mode to remove various combinations of contaminated groundwater, separate-phase petroleum product, and hydrocarbon vapors. Figure 4-3 shows the test pad setup with PVWs in field. Box 1 in Figure 4-3 displays that the PVWs in two consecutive rows are placed such that 1 PVW

of a row is placed in between two PVWs of the other row to ensure coverage of the contaminated area under remediation.

MODEL CALIBRATION

Grid and Boundary Conditions

An aerial domain of 3.66 m by 7.31 m was discretized using 4753 nodes. A uniform nodal spacing of 0.08 m was used both in x and y direction. BIOSLURP allows a PVW to be assigned only at nodes. The model grid spacing was selected such that the spacing between two nodes would be less than the width (0.1 m) of the PVW. Figure 4-4 shows the model test grid. The solid lines in all four sides of the model represent the boundary. In this case, a no flow boundary represents a repeating unit of the PVW modeled domain. A constant head boundary represents injection units surrounding the extraction domain.

Model Parameters

As mentioned earlier, the hydraulic conductivity values of the test pad site reported in the past (Kunberger et al. 2003), based on groundwater well testing and laboratory hydraulic conductivity testing, range from 8×10^{-6} cm/s to 2×10^{-4} cm/s. Although relatively low in magnitude, this hydraulic conductivity is the typical value for the silty sand seam at the test pad site. The porosity of the soil was calculated from the water content and specific gravity and is equal to 0.45.

LNAPL Phase

Field results (Sharmin et al. 2009) indicate that extraction of the free phase is most effective when the groundwater table is within the relatively thin, silty sand lens. The LNAPL saturation is higher in soils with a larger pore size, such as sand, than in soils with a smaller pore size, such as silt (Remediation Technologies Development Forum, 2005). The conceptual model for the multiphase transport is developed based on a single-layer soil with $8x10^{-6}$ cm/s of hydraulic conductivity (the lowest of the field range). This is mainly due to model limitation of not allowing modeling of multi-layers. The free product thickness in the model is taken as 0.08 m to represent the field saturation with the area of maximum condition. As discussed earlier, the 0.08 m of LNAPL thickness has been obtained from 1.44 m of monitoring well thickness using Equation 9. The associated parameters for the test site are presented in 14th row of Table 4-1.

Fluid Properties

The fluid properties required by BIOSLURP are: the specific gravity ratio, ρ_{ro} (i.e., the ratio of the free LNAPL specific gravity to the water specific gravity), the dynamic viscosity ratio, η_{ro} (i.e., the ratio of the free LNAPL dynamic viscosity to the water dynamic viscosity), the surface tension of water; the surface tension of the free LNAPL; and the free LNAPL-water interfacial surface tension. These fluid properties are presented in Table 4-2 at an assumed temperature of 20^{o}C.

Transport Properties

Soluble phase transport is assumed to be governed by both advection and dispersion with retardation due to sorption. For dispersion, the longitudinal dispersivity is assumed based on the 1.83 m spacing between two PVWs. Anderson (1984) indicated that the longitudinal dispersivity is generally about one-tenth of the distance of a transport experiment. The longitudinal dispersivity is taken as 10% of 1.83 m (0.183 m). Because the flow vector is mainly in the horizontal direction, the transverse dispersivity has been chosen as 10% of the longitudinal dispersivity. The fraction of sorption sites that are in contact with mobile water is considered to be 100%. The solubility of benzene (chosen to represent JP-4) is assumed to be 1,780 mg/L (Bedient et al. 1999). The benzene mole fraction in hydrocarbon is taken as 1%. The pure phase density of benzene is assumed equal to 867 kg/m^3. The concentration of benzene in the groundwater is taken as 0.3 mg/L, which is the average value measured from the monitoring wells on site.

A list of the soil properties, fluid properties, and physicochemical properties for Benzene required to generate the model test grid are presented in Table 4-2.

Location of PVWs and Flowrates

Figure 4-3 shows the PVW placement pattern in field. Table 4-3 shows groundwater and LNAPL flowrates monitored on March 25, 2006 for the consecutive operation of row# 2, 3 and 4. Table 4-3 also includes groundwater and LNAPL flowrates obtained on different days of operation for row # 21. Row # 21 has been chosen as it

yielded a variety of groundwater and LNAPL extraction rates. On the days of row# 21 operation, the adjacent rows 22 or 20 were not operated. Therefore, in terms of PVW placement, two types of analyses were performed using the grid presented in Figure 4-4. i) Consecutive operation of row# 2, 3 and 4 in a day (March 25, 2006 in field). The placement of PVWs is as shown in Figure 4-4 and ii) Operation of Row # 21 for multiple days (October 18, 2005; February 25 and March 12, 2006). All the positions of the rows are presented in Figure 4-3. As mentioned earlier, each of the rows was composed of 7 or 8 PVWs. The last two columns of Table 4-3 show the extraction flowrate for LNAPL and groundwater for PVWs of the different rows on multiple days of operation. Figure 4-5 schematically summarizes the steps followed to calibrate the model for flow analysis.

Model Calibration: Flow Analysis

The model calibration for flow analysis was performed in three steps. The first is to replicate the specific volume of LNAPL within the flow domain. The second is to compare the extraction flowrate for both groundwater and LNAPL with field flowrate, and the third is to compare the hydraulic head distribution obtained from model versus field.

The average LNAPL thickness in the field was 0.08 m which was mainly in the 0.08 m thick silty sand lens. The program requires an input value of extraction flowrate for both groundwater and LNAPL. However as the program runs, these flowrate values are rebalanced depending on the unsaturated permeability changes, with the change in

degree of saturation for both water and LNAPL in the soil pores. Katyal et al. 1988 and Yen et al. 2003 described the phase transmissivities for water-oil and gas respectively as:

$$Tp_{ij} = \int_{Z_L}^{Z_u} k_{rp} Ksp_j dz$$

Equation (14)

$$Ta_j = \int_{Z_L}^{Z_u} k_{ra} Kso_{ij} dz$$

Equation (15)

Where, K_{rp}=relative permeability of phase P; Ksw_{ij} =saturated hydraulic conductivity tensor; Kso_{ij} =($RD_{ro}Ksw_{ij}/n_{ro}$), Ksa_{ij}=($RD_{ro}Ksw_{ij}/n_{ra}$); Zu and Z_L=lower and upper integration limits for the water and LNAPL phases; Zs=ground surface elevation; n_{ro}=LNAPL to water dynamic viscosity ratio; n_{ra}=air to water dynamic viscosity ratio; RD_{ro} = relative density of LNAPL.

A series of various combinations of irreducible water contents and Van Genuchten parameters α and n were used to calibrate the model in terms of extraction flowrate. The model was calibrated for field extraction rates (for both water and LNAPL) obtained for row #2,3,4 and 21. The average groundwater and LNAPL extraction rates for these rows are presented in Table 4-3. As each row is composed of 7 or 8 PVWs, and equal flowrate was assumed per each PVW and applied to the model. For example, if a row has 7 PVWs, the total flowrate of that row is Q_{field}, the model input for each PVW was q_{input}= Q_{field} /7. The computed output extraction flowrate was compared with the field average total flowrate for each row.

Figure 4-6 plots the specific volume corresponding to monitoring well LNAPL thickness of 1.44 m along with permeability as function irreducible water content. The data are shown for the test soil along with computed values for parameters from the data base for various soils reported in Table 4-1. The test soil is classified as silty sand and results show good agreement with permeability and irreducible water content (obtained using Van Genuchten parameters) when compared to the range of soils for the LNAPL thickness used in the analysis.

Figure 4-7(a) and 4-7(b) compare the field and model volume recovery rate, obtained for groundwater and LNAPL respectively, for consecutive operation of rows (2,3,4). Additionally, Figure 4-8(a) and 4-8(b) compare the field and model results obtained for groundwater and LNAPL volume recovery rate, respectively, for a single row operation with various combination of input flowrate for LNAPL and groundwater, as presented in last two columns of Table 4-3. In both cases a 15% maximum residual LNAPL saturation, and 5% maximum residual water saturation, were used as input parameters in the model. These input values provided flowrates comparable to field values. It should be noted that while these parameters were selected to match field data, they fall within the range of recommended values in literature (Carsel et al. 1988, Charbennau 2000). A comparison between groundwater and LNAPL flowrates also shows the validity of the assumed relative permeability versus saturation curve concept presented in Figure 4-1. Initial higher LNAPL extraction rates e.g. data in Figure 4-7(b) induced increasing groundwater extraction rate with time (Figure 4-7(a) and Figure 4-8(a)

respectively). Higher LNAPL extraction rate led to lower saturation and decreased the relative permeability for LNAPL, which, in turn, caused higher saturation and increasing relative permeability for groundwater.

Data in Figure 4-9 further supports the concept of relative permeability relationship (Figure 4-1). Model simulation are performed for 0.08 m, 0.05 m and 0.03 m specific volume of LNAPL for consecutive operation of PVWs representing rows # 2,3 and 4. For all three specific volumes, the extraction rate for LNAPL was maintained at 24 L/h for 1.5 h as monitored in the field. As shown in Figure 4-9 groundwater extraction rate increases with the lower amount of assumed LNAPL due to the change in pore saturation phase (lower LNAPL specific volume means higher groundwater saturation). This behavior is important to note when reviewing field data whereby more extraction of contaminated groundwater is not desirable.

The model is also validated by comparing the groundwater heads obtained from model and field monitoring Well (LMW-4 in Figure 4-3). The location of hydraulic head monitoring point of the model is presented in Figure 4-4. Figure 4-10 shows the change in head (from original static level) as a function of operating time. Result shows that, based on the model parameters, the model is capable of replicating the field data in terms of groundwater heads. The flowrate of groundwater in the field was 81.4 L/h and 124.05 L/h for 2 and 1 h (Figure 4-10) operating time, respectively, while the LNAPL extraction rate was 3.15 L/h when the system was operated for 1 h. The 2 h system operation did not extract any LNAPL which explains the higher head difference due to then the larger

groundwater flowrate.

Model Calibration: Transport Analysis

The test grid for groundwater flow analysis along with the calibrated parameters is used for transport analysis. For transport analysis, the average groundwater and free JP-4 extraction rates are assigned as 125 L/h and 2 L/h, respectively (Gabr et al. 2008). In the flow analysis, 1/7th or 1/8th of the total flowrate of each row was assigned at each PVW (based on the number of PVWs in a row).

The analysis is performed to estimate the soluble and vapor phase concentrations. For soluble concentration, the liquid extraction was performed under atmospheric pressure. For vapor phase concentration, external vacuum was applied. The field vacuum head ranged between 310 to 410 mm of Hg, which were the values monitored in the field from vacuum gauges. The vacuum head was set to 410 mm of Hg for the base case of the study. Since the program output does not include the extracted mass directly, the mass was calculated based on the balance of concentration in each of the three phases (air, soluble and solids) as well as amount of extracted LNAPL.

The contaminant load from a hydrocarbon source to the mobile phase H_{ga} (Equation 10) and contaminant load from a hydrocarbon source into the gas phase $H_{\partial a}$ (Equation 11) are two key parameters whose value is not well defined in literature. These values are akin to mass transfer coefficients but not at equilibrium conditions. BIOSLURP Technical documentation was the only source of these values. These two

parameters are therefore calibrated with respect to the field results. Since benzene is one of the most toxic compounds of concern in the waste stream, it was used for this calibration. Field results show that the average benzene concentration is 0.3 mg/L (Sharmin et al. 2009) in aqueous phase for a sample collected after 0.25 h of system operation. Accordingly, setting the contaminant load from a hydrocarbon source to the mobile phase H_{ga} = 0.331 1/m, the model output shows that the benzene concentration is 0.3 mg/l in extracted groundwater after 0.25 h of run time.

On the other hand, the average total petroleum hydrocarbon (TPH) in gas phase was 473 mg/L when the system was operated for 0.5 h (Sharmin et al. 2009). Simulation shows that if the contaminant load from a hydrocarbon source to the gas phase is set to $H_{\partial a}$ = 7.45 1/m, the benzene concentration in air is 1.6 mg/L in extracted vapor after 0.5 h of run time; which is replicating the field estimated value of 1.53 mg/L.

PARAMETRIC STUDY

Based on input parameters evaluated during the calibration phase, a parametric study is conducted by varying five of the key parameters to determine their effect on the LNAPL flow and transport. These parameters are water extraction rate, irreducible water content, LNAPL and gas contents, both monitoring well and actual LNAPL thicknesses, and loadings from hydrocarbon for both soluble and gas phases. The parametric analyses were performed for four different types of soil in order to analyze the impact of permeability variation and associated porosity and irreducible water content on LNAPL

removal. The input parameters representing the different soil types are presented in Table 4-1.

In addition, the impact of constant head, and no flow, boundary conditions are investigated. The no flow boundary and constant head boundary represents extraction only and injection-extraction scenarios respectively. The no flow boundary represents PVWs line in the middle of the pad that is assumed to be repeated in both directions at a spacing equal to the width of the domain. The constant head boundary represents the state where the PVWs are alternatively used for extraction and injection process.

Grid for Parametric Analysis

A total aerial domain of 2.44 m by 2.44 m was discretized using 1600 nodes. A uniform nodal spacing of 0.06 m was used both in x and y direction. The model grid spacing was selected such that the spacing between two nodes would be less than the width (0.1 m) of the PVW. Therefore, the model test grid would simulate the volume of soil impacted by the PVW operation. Figure 4-11 shows the model test grid with a PVW at center (1.189 m by 1.189 m).

Impact of Boundary Conditions

The simulation was performed for constant head and no flow boundaries. The analysis was performed for sand, sandy loam, loam, and field soil because of their wide range of permeability and associated hydraulic and hydraogeologic properties, as

presented in Table 4-1. Figure 4-12 shows the percent removal of LNAPL as a function of boundary condition. Figure 4-12 shows that using constant head boundary impacts LNAPL removal for the case of low permeability (field soil and loam) but not for sand soils. For sand with permeability 8.25×10^{-3} cm/s, the LNAPL removal rate is same for both constant head and no flow boundary conditions, where as for the field soil, with permeability 8×10^{-6} cm/s, the LNAPL removal percentage decreases by a factor of approximately 4 when a constant head versus no flow boundary is used. Continuous flow in constant head boundary induces more wetting fluid (water) which entraps the non-wetting fluid (LNAPL) in the soil pores. The surplus of wetting fluid reduces the mobility of non-wetting fluid which eventually reduces the LNAPL recovery. The finding is an argument against injection/extraction operational mode if LNAPL recovery is the primary focus.

Impact of Water Extraction Rate

The average groundwater and LNAPL extraction rates are 17.86 L/h and 0.285 L/h for a single PVW, respectively which makes the ratio of groundwater flowrate to LNAPL extraction flowrate equals to 62.5. The ratio of water to LNAPL flowrate was varied from 100 to 1, keeping the LNAPL extraction flowrate at 0.285 L/h, for all type of soil.

Data in Figure 4-12 shows that the LNAPL removal percentage is same for variable water extraction rate as long as LNAPL volume and residual saturation

parameters, for LNAPL and water remain unchanged, for a particular type of soil. The percent removal however varies widely for different soil types, because of their different hydraulic properties, with 80% for sand versus 25% for the field soil assuming no flow boundary.

Impact of LNAPL Thickness

Figure 4-2 provided data on free product volume assuming various monitoring well thicknesses (before any extraction). Figure 4-13 shows the percentage of recoverable LNAPL as a function of monitoring well thickness, and the type of soil. In this case, monitoring well thickness of 1.44 m, 80% of free LNAPL is recoverable in sand where as for the loam the recovery rate is 40 % under no flow boundary condition. Figure 4-13 also shows that LNAPL recovery is nil for low monitoring well thickness (less than 0.6 m). This is because the initial free LNAPL specific volume in low permeability soil is initially non-existing upto 0.6 m of LNAPL thickness in the well (See Figure 4-2).

Figure 4-14 shows the % removal of LNAPL for various types of soil, as a function of permeability with constant head boundary condition. The LNAPL thickness was varied from 0.08 m to 0.03 m. Figure 4-14 shows with the reduction of LNAPL thickness from 0.08 to 0.03 m, the LNAPL removal decreases from 65 to 35% for sand, and from 5 to 0.2% for the field soil. Percent LNAPL removal for sandy loam and loam also indicates a reduction of permeability of 10 times associated with reduction in percent LNAPL removal. The percent removal is not only influenced by the permeability but also

by the thickness of LNAPL. Difference in percent removal due to permeability increases with decreasing LNAPL thickness. Higher permeability leads to lower percent removal when rates are compared for 0.08 versus 0.03 m LNAPL thickness. For example, for 0.08 m thick LNAPL, the removal percentage is 2.5 times higher for sandy loam than that in loam soil. This recovery percentage becomes 6.5 times when the LNAPL thickness is reduced to 0.03 m.

Impact of Irreducible Water and LNAPL Contents

The baseline irreducible water, LNAPL and gas contents are presented in Table 4-1 for the field soil. In this analysis, each of the irreducible contents was individually varied to assess its impact on the removal of free LNAPL while keeping other two unchanged, and assuming both constant head and no flow boundary conditions.

Figure 4-15 shows the percent removal of LNAPL for 5%, 10%, 15% and 20% irreducible LNAPL content. It is observed from Figure 4-15 that LNAPL removal efficiency significantly decreases with the increasing irreducible LNAPL content. In the case of field soil, increasing irreducible LNAPL content from 5 to 20% decreases the percent removal from 52 to 0.2% for 0.08 m LNAPL thickness (assuming constant head boundary condition). Increasing irreducible LNAPL content decreases the volume of extractable LNAPL. Irreducible LNAPL content has the most significant impact of the three irreducible contents (water, LNAPL and gas) varied in this analysis.

Similarly, data in Figure 4-15 show that with the increase of irreducible water

content percent, the removable LNAPL decreases. The removal efficiency drops further when a constant head boundary is assumed as the continuous flow of wetting fluid increases the formation of blobs/ganglia of the non wetting fluid (LNAPL). This can be explained by the fact that the irreducible water content has an impact on the available initial LNAPL thickness. As shown in Figure 4-16 increasing irreducible water content from 5 to 20% decreases the LNAPL thickness from 0.08 to 0.067 m.

As LNAPL is the wetting fluid and gas is a non wetting fluid, with increasing irreducible gas content, the reduction in LNAPL recovery slightly decreases as shown in Figure 4-15. The impact of boundary condition on hydrocarbon removal in gas phase is also shown and follows the logic of faster desaturation leading to increased mass transfer into gas phase.

Impact of Loading from Hydrocarbon

Figure 4-17 shows a sensitivity analyses to evaluate the contaminant transport concentration in both water and air, as a function of loading from hydrocarbon to water and air, respectively. For soluble phase, three values, 0.0331 1/m, 0.331 1/m and 3.31 1/m, of load from hydrocarbon to soluble phase were demonstrated. Similarly, loading from hydrocarbon to gas phase was analyzed for three values, 0.745 1/m, 7.45 1/m and 74.5 1/m. In both cases, a linear relationship is observed with the variation of the respective hydrocarbon loading parameters. The significance of the finding is the hydrocarbon concentration in both extracted groundwater and vapor streams varies

directly to contaminant loading from hydrocarbon to in both aqueous and vapor phase under non equilibrium conditions. Assessment of hydrocarbon loading values with time is needed. A more robust analysis model should allow specifying these two parameters as a function of time for better representation of transfer kinetics.

SUMMARY AND CONCLUSION

The analysis presented in this paper integrates calibration and verification of a simulated model and parametric sensitivity analysis to explore the mechanics involved with extraction of LNAPL using prefabricated vertical wells installed relatively on a close spacing. BIOSLURP (a two-dimensional finite element analysis model) was used to simulate free, soluble and gas-phase LNAPL transport under the vadose-saturated condition. The analysis in this paper was mainly focused to the free LNAPL recovery since a primary concern in LNAPL-contaminated sites with low permeability soil is the removal of the source. The modeling study included two components; firstly validating the hydraulic and hydrogeologic parameters by calibrating the model with the field results and secondly, a parametric study varying the key parameters of the calibrated model.

The finite element model was calibrate with field data in terms of groundwater and LNAPL flowrate, hydraulic head distribution, and soluble and gaseous phase transport assuming LNAPL was accumulated in the 0.08 m lens. The model validation was performed in three steps. The first effort is to replicate the specific volume of LNAPL within the flow domain. The second is to compare the model output extraction flowrate

for both groundwater and LNAPL with field flowrates and the third is to compare the hydraulic head distribution between model and field. In addition, data from previous studies by Carsel et al. (1988) and Charbeneau (2000) were compared with the numerical values from the calibrated model. The groundwater and LNAPL extraction rates were compared for both the operation of one row and multiple rows in a day.

The contaminant load from a hydrocarbon source to the mobile phase H_{ga} and contaminant load from a hydrocarbon source into the gas phase $H_{\partial a}$ are the two sensitive parameters affecting model output but are not well defined in literature. Simulation showed that if H_{ga} = 0.331 1/m and $H_{\partial a}$ = 7.45 1/m, field mass extraction values are obtained.

Five key parameters were varied to determine the effect on the LNAPL flow and transport behavior. The input parameters are water extraction rate, irreducible water, LNAPL and gas content, both monitoring well and actual LNAPL thickness and impact of loading from hydrocarbon for both soluble and gas phase. Based on the result from this study, the following conclusions are advanced:

i. Analysis with different boundary conditions presents an argument against injection/extraction operational mode if LNAPL recovery is the primary focus from low permeability soil. Continuous flow in constant head boundary induces more wetting fluid (water) which entraps the non-wetting fluid (LNAPL) in the soil pores. The

surplus of wetting fluid reduces the mobility of non-wetting fluid which eventually reduces the LNAPL recovery.

ii. For a given soil type, results indicated that LNAPL removal percentage is not dependent on the water to LNAPL extraction rates as long as free LNAPL exists in the subsurface. Assuming various hydraulic characteristics (i.e. various soil permeability characteristic curves) the ratio of water to LNAPL extraction flowrate was varied from 100 to 1 keeping the LNAPL extraction rate at 0.285 L/h for all types of soil. The LNAPL percent removal rate varied from 65 to 20% due to the variability of entrapped mass as hydraulic conductivity and porosity varied.

iii. LNAPL removal efficiency was dependent on soil type (for the 4 soil types considered in this study). Assuming no flow boundary and for LNAPL thickness of 0.08 m, 65% of the LNAPL was recoverable in sand (hydraulic conductivity 8.25×10^{-3} cm/s) where as the for the field soil (silty sand hydraulic conductivity 8×10^{-6} cm/s) the recovery rate was merely 20%. This signifies the important role of saturation.

iv. The magnitude of irreducible LNAPL content has significant influence on the extraction efficiency. Increasing irreducible LNAPL from 5 to 20% decreases the percent removal from 52 to

0.2% for 0.08 m LNAPL assuming constant head boundary condition.

v. The magnitude of initial LNAPL thickness presents in the field is influenced by the irreducible LNAPL of the soil pores. For field soil, analysis results also show that increasing irreducible water content from 5 to 20% decreases the free oil thickness from 0.08 m to 0.067 m which eventually reduces removal efficiency from 20 to 10% assuming no flow boundary condition.

vi. For the same soil type, lower initial LNAPL thickness decreases LNAPL removal efficiency. Results showed that the reduction of initial actual LNAPL thickness from 0.08 m to 0.03 m decreased the free LNAPL removal from 65 to 35% for sand.

vii. The sensitivity analyses to evaluate the contaminant transport concentration, in both water and air, as a function of loading from hydrocarbon to water and air shows a linear relationship of the soluble and gaseous phase with the variation of respective load from hydrocarbon parameters. Assessment of hydrocarbon loading values with time is needed. A more robust analysis model should allow specifying these two parameters as a function of time for better representation of transfer kinetics.

REFERENCES

Adams, J.A., and Reddy, K.R. (2000). “Removal of dissolved- and free-phase benzene pools from ground water using *in situ* air sparging.” *Journal of Environmental Engineering*. 126: 697-707.

Anderson, M. P. (1984). “Movement of contaminants in groundwater: Groundwater transport-advection and dispersion.” *Groundwater Contamination, Studies in Geophysics*. Washington DC: National Academy Press. 37-45.

Bartow, G. andDavenport, C. (1995). "Pump-and-Treat Accomplishments: A Review of the Effectiveness of Ground Water Remediation in Santa Clara Valley, California," *Ground Water Monitoring Review*. 140-146.

Bedient, P. B., Rifai, H. S. and Newell, C. J. (1999). “Groundwater contamination transport and remediation.” *Sources and Types of Groundwater Contamination*. Upper Saddle River, NJ: Prentice Hall. 75-111.

BIOSLURP. (2004). *Technical documentation and user guide*. Resources and System International, Inc. Blacksburg, VA.

Carsel, R. F. and R. S. Parish. (1988). “Developing joint probability distribution of soil water retention characteristics”. *Water Resources Research*. 24(5)(May): 755-769.

Charbeneau, R. J. (2000). “Groundwater hydraulics and pollutant transport.” *Spreadsheet Calculations of LNAPL Distribution*. Long Grove, IL: Waveland Press, Inc. 550-555.

“Density of air.” <http://en.wikipedia.org/wiki/Air_density> (2008).

Gabr, M. A. (1997). “Prefabricated well injection depth extraction WIDE system for enhanced soil flushing”. *Disclosure Document No. 422400 under 37 CFR Sec 1.21 (c)*.

Gabr, M. A., Sharmin, N., Godwin, J, Quaranta, J. D. and Altobello, J. (2008). “WIDE Implementation for LNAPL Extraction Rickenbacker International Airport Area of Concern 3 (AOC – 3) Phase III – Final Report”. *Army Corps of Engineers*.

Haley, J.L., Hanson, B., Enfield, C., and Glass, J. (1991). "Evaluating the effectiveness of ground water extraction systems.” *Ground Water Monitoring Review*.119-124.

Katyal, A.K., and King, L. G. (1988). “Three dimensional upstream finite element model for reactive solute transport in variably saturated porous media.” *International*

Summer Meeting of ASAE.

Kunberger, T., Quaranta, J. D. and Gabr, M. A. (2003). "Remediation of former Lockbourne Air Force Base using well injection depth extraction (WIDE)." *12th Panamerican Conference on Soil Mechanics & Geotechnical Engineering*. Cambridge, MA. (June): 1575-1581.

Land, C. S. (1968). "Calculation of imbibition relative permeability for two and three phase flow from rock properties." *SPE Journal*. 8(2)(June): 149-156.

Langley A., Gilbey M. and Kennedy B. (2005). "Proceedings of the Fifth National Workshop on the Assessment of Site Contamination". *Environment Protection & Heritage Council*. National Environment Protection Council Service Corporation.

Lyman Warren, J., Reehl William, F., Rosenblatt and David H. (1993). "Handbook of Chemical Property Estimation Methods." McGraw-Hill, New York.

Newell, C. J., Steven D. A., Ross, R. R. and Huling, S. G. (1995). "Light Non Aqueous Phase Liquids, Groundwater Issue". *EPA/540/S-95/500*.

Oostrom, M., White, M. D., Lenhard, R. J., Geel, P. J. V. and Wietsma T. W. (2005). "A

comparison of models describing residual NAPL formation in the vadose zone." *Vadose Zone Journal*. 4:163–174.

Peignenburg, W.J.G.M. and Damborsky, J. (1996). "Biodegradability Prediction." Dordrecht, The Netherlands.

Rawls, W.J., Brakensiek, D.L. and Logsdon, S.D. (1993). "Predicting saturated hydraulic conductivity utilizing fractal principles". *Soil Science Society of America Journal*. 57(5): 1193-1197.

Rawls, W.J., Brakensiek, D.L. and Saxton, K. E. (1982). "Estimating soil water properties". *Transactions, ASAE*. 25:1316-1320 and 1328.

Remediation Technologies Development Forum (RTDF). (2005). http://www.rtdf.org/ PUBLIC /napl/training/module1.pdf.

Robertson, B.K. and Alexander, M. (1996). "Mitigating toxicity to permit bioremediation of constituents of nonaqueous phase liquids." *Environmental Science Technology*. 30: 2066–2070.

Sharmin, N., Kunberger, T., Gabr, M. A., Quaranta, J. D., Bowders, J. J.(2008).

"Performance modeling and optimization of contaminant extraction using prefabricated vertical wells (PVWs)". *Journal of Geosynthetic International.* 15(3):205-215.

Sharmin, N.; Gabr, M. A. & Quaranta, J. D. (2009). "Multiphase extraction of Light Non-Aqueous Phase Liquid (LNAPL) using Prefabricated Vertical Wells**".** To be submitted.

Steffensen, W.S. and Alexander, M. (1995). "The effect of competition for available nutrients in systems containing mixtures of substrates." *Applied Environmental Microbiology*. 61: 2859–2862.

Travis, C.C. and Doty, C.B. (1990). "Can contaminated aquifers at superfund sites be remediated?" *Environmental Science and Technology*. 24(10):1464-1466.

van Genuchten, M. Th. (1980). "A closed-form equation for pre-. dicting the hydraulic conductivity of unsaturated soils". *Soil Science Society of America Journal*. (44):892-898.

van Genuchten, M. Th., and Wierenga, P. J. (1980). "Mass transfer studies in sorbing media 1. Analytical solution". *Soil Science Society of America Journal.* (40):473-480.

Williams, D.E., and Wilder, D.G. (1971). “Gasoline pollution of a ground-water reservoir - A case history”. *Ground Water*. 9(6):50-54.

Yen, H.K., Chang, N.B. and Lin, T.F. (2003). “Bioslurping model for assessing light hydrocarbon recovery in contaminated unconfined aquifer. I: Simulation analysis”. Practical Periodical of Hazardous, Toxic, and Radioactive Waste Management. 7 (2): 114-130.

Table 4-1 Summary of formation free-product volume using parameters presented by Carsel et al. (1988).

Type of Soil	**Permeability cm/s**	**Porosity**	**S_r**	a **1/m**	**n**	**Specific Volume cm**
Sand	$8.25x10^{-3}$	0.43	0.045	14.5	2.68	43.86
Loamy Sand	$4.1x10^{-3}$	0.41	0.057	12.4	2.28	36.10
Sandy Loam	$1.23x10^{-3}$	0.41	0.065	7.5	1.89	23.63
loam	$2.9x10^{-4}$	0.43	0.078	3.6	1.56	10.61
Sandy Clay Loam	$3.64x10^{-4}$	0.39	0.1	5.9	1.48	12.83
Silt loam	$1.25x10^{-4}$	0.45	0.067	2	1.41	5.27
Clay loam	$1.25x10^{-4}$	0.45	0.067	2	1.41	5.27
Silty loam	$3.64x10^{-4}$	0.43	0.089	1	1.23	1.72
Sandy Clay	$1.94x10^{-5}$	0.38	0.1	2.7	1.23	4.00
Silty Clay	$6x10^{-6}$	0.36	0.07	0.5	1.09	0.38
Silt	$7x10^{-5}$	0.46	0.034	1.6	1.37	4.17
Clay	$6x10^{-5}$	0.38	0.068	0.8	1.09	0.65
Test Soil	$8x10^{-6}$	0.45	0.09	3	1.4	7.60

Table 4-2. Summary of Model Grid Input Parameters

Liquid surface depth (from ground surface)	4.88 m
Soil type[a]	Gray/brown silty sand (SM)
Water content, %[a]	22.8
Permeability, cm/s[a]	8×10^{-6}
Specific gravity, Gs[a]	2.73
Density of JP-4 (jet fuel or LNAPL)b	800 kg/m^3
Density of air (20^{o}C)[d]	1.2 kg/m^3
Free JP-4 -to-water dynamic viscosity ratio, h$_{ro}$[e]	0.9
Surface tension of water, σw[e]	.072 N/m
Air-free JP-4 surface tension, s$_o$[e]	0.025 N/m
LNAPL-water interfacial surface tension, s$_{owb}$	.053 N/m
Air-to-water dynamic viscosity ratio[e]	0.018
Henry's coefficient[f]**,**	0.24 gm/cc
Distribution coefficient for benzene[f]	0.83 cc/gm
Diffusion coefficient of benzene in water[f]	0.0001 m^2/d
Diffusion coefficient of benzene in air[f]	0.76 m^2/d

[a]Field and Laboratory Measured
[b]Petroleum contaminated soil, Charbeneau et. al. (2000)
[c]Carsel and Parish (1988).
[d]http://en.wikipedia.org/wiki/Air_density
[e]Oostrom, White, Lenhard, Geel, and Wietsma (2005))
[f]Lyman, Reehl, and Rosenblatt (1993)).

Table 4-3. Groundwater and LNAPL extraction rate in field for different rows.

Date	Operating time, h	Row in operation, n	Extracted Volume of FP (Free product), L	Extracted Volume of GW (Groundwater), L	FP flow rate, L/h	GW flow rate, L/h	FP flow rate, per PVW	GW flow rate, per PVW
10/18/2005	1.0	21	11.91	61.05	11.9	61.05	1.7	8.72
2/25/2006	4.0	21	11.91	464.75	2.98	116.19	0.43	16.6
3/12/2006	2.0	21	11.91	137.78	5.95	68.89	0.85	9.84
3/25/2006	0.5	2	11.91	136.7	23.8	273.4	3.4	39.06
3/25/2006	0.5	3	0	148.6	0	297.21	0	42.46
3/25/2006	0.5	4	0	148.6	0	297.21	0	42.46

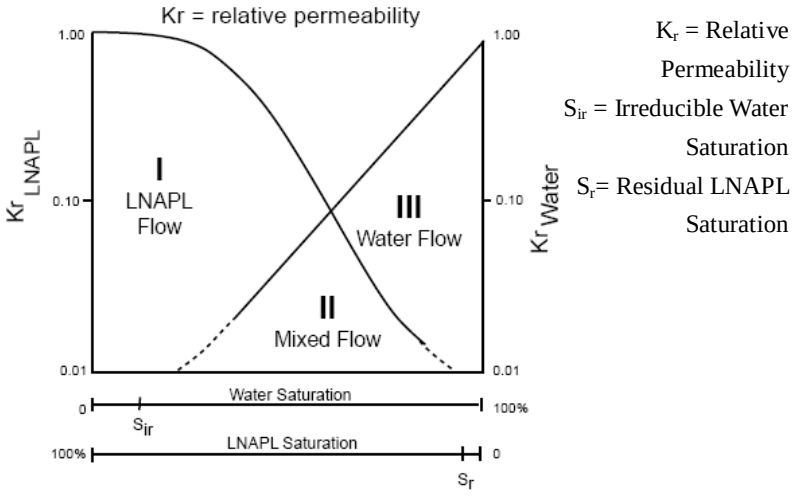

Figure 4-1 Hypothetical Relative Permeability Curve for Water and LNAPL in a Porous Medium (Newell, et al. 1995 Williams et al., 1971).

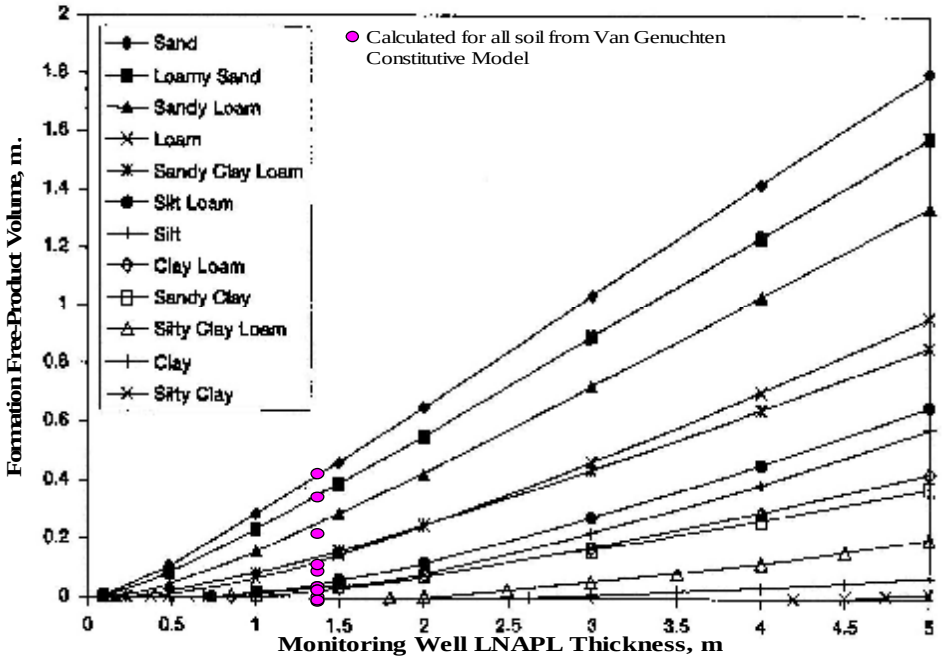

Figure 4-2 Comparison between LNAPL thickness obtained from Charbeneau (2000) and equation used for simulation using BIOSLURP simulator.

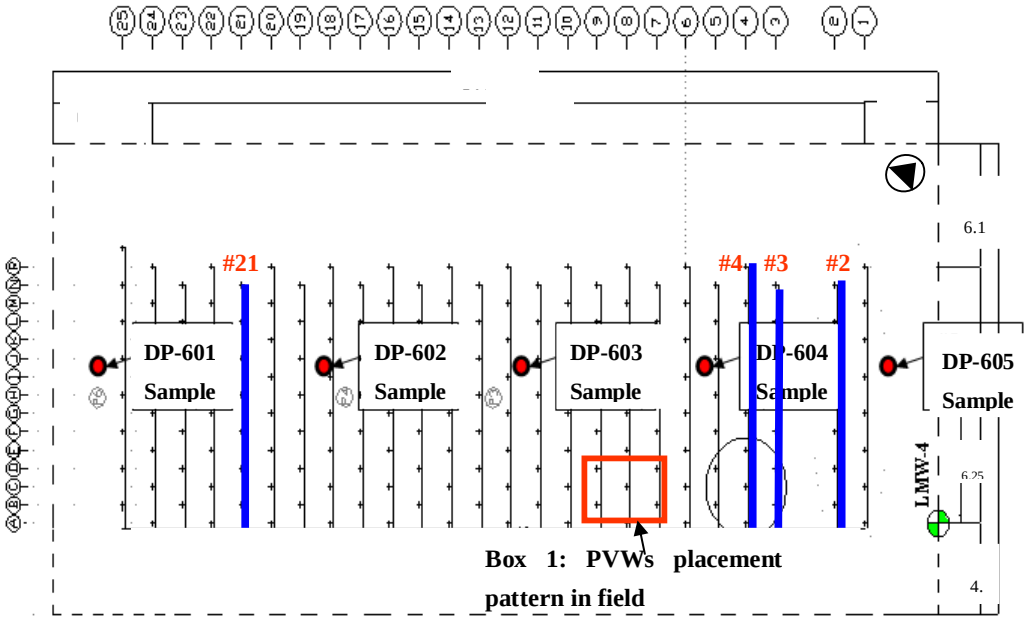

Figure 4-3 Model test pad grid for model validation

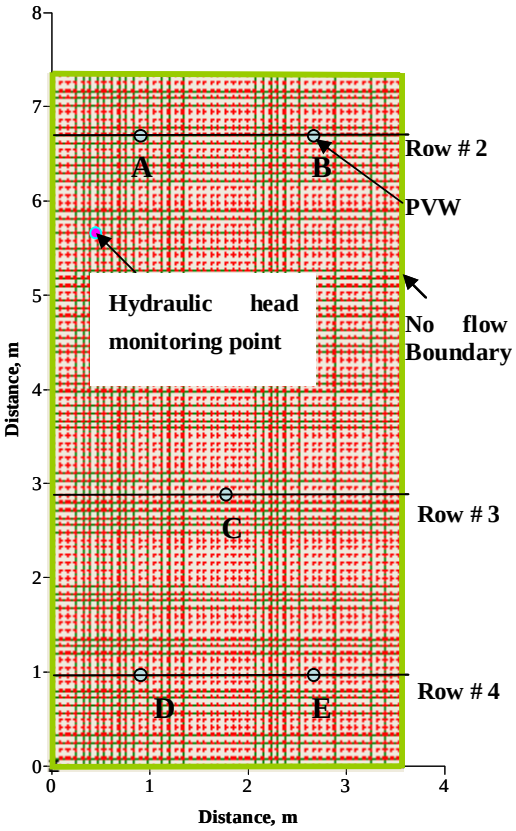

Figure 4-4 Discretized domain and model grid

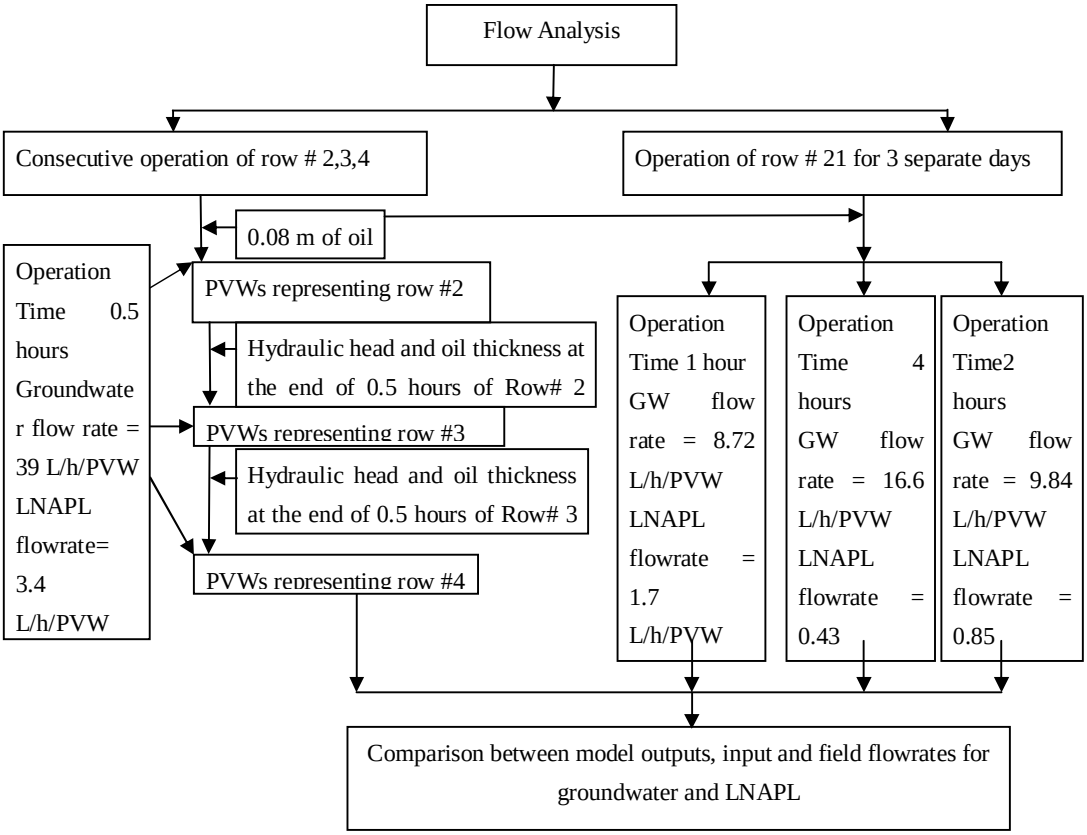

Figure 4-5 Basic steps followed validating model for flow analysis.

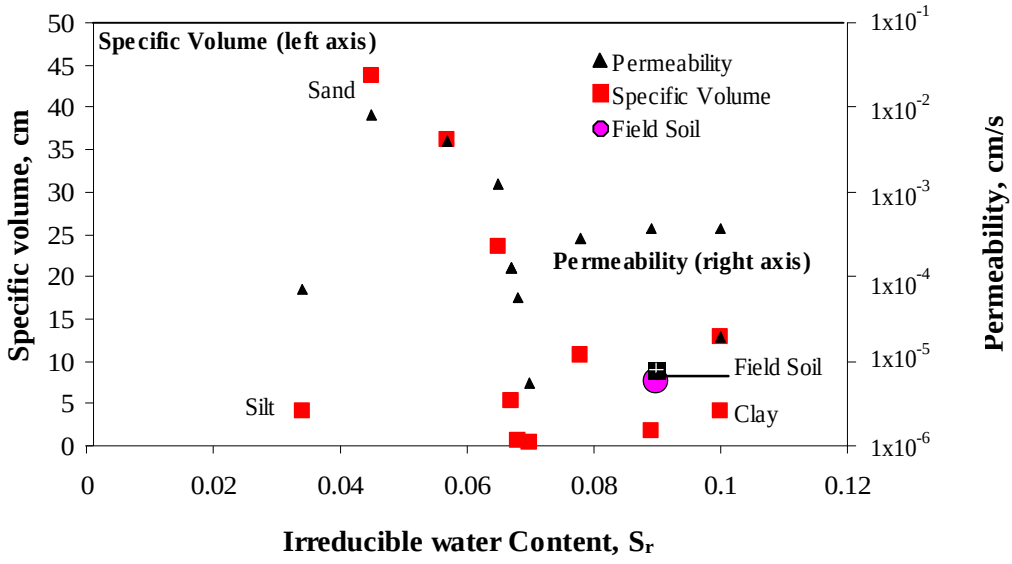

Figure 4-6 Permeability and irreducible water content for various type soil and variation of specific volume in different type of soil for the same monitoring well thickness.

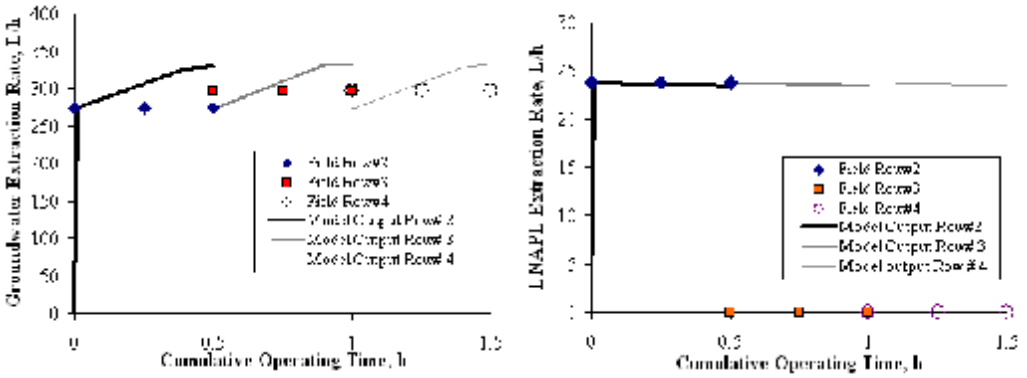

(a) Groundwater extraction rate **(b)LNAPL extraction rate**

Figure 4-7 Comparison of extraction rate of groundwater and LNAPL due to consecutive operation of row# 2, 3, 4 for field (March 25, 2006) and model.

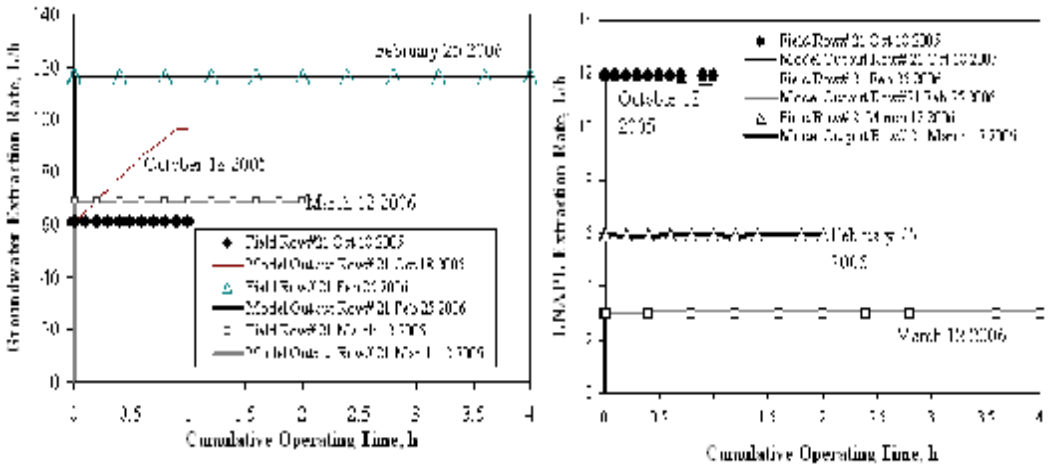

(a) Groundwater extraction rate **(b)LNAPL extraction rate**

Figure 4-8 Comparison of extraction rate of groundwater and LNAPL due to operation of row# 21 for field and model.

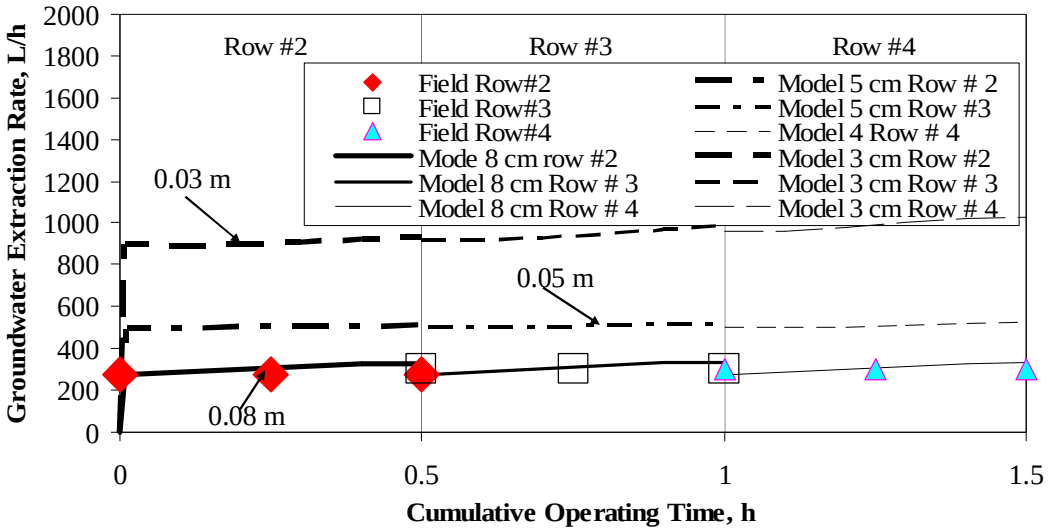

Figure 4-9 Impact of LNAPL amount present in field on groundwater extraction rate.

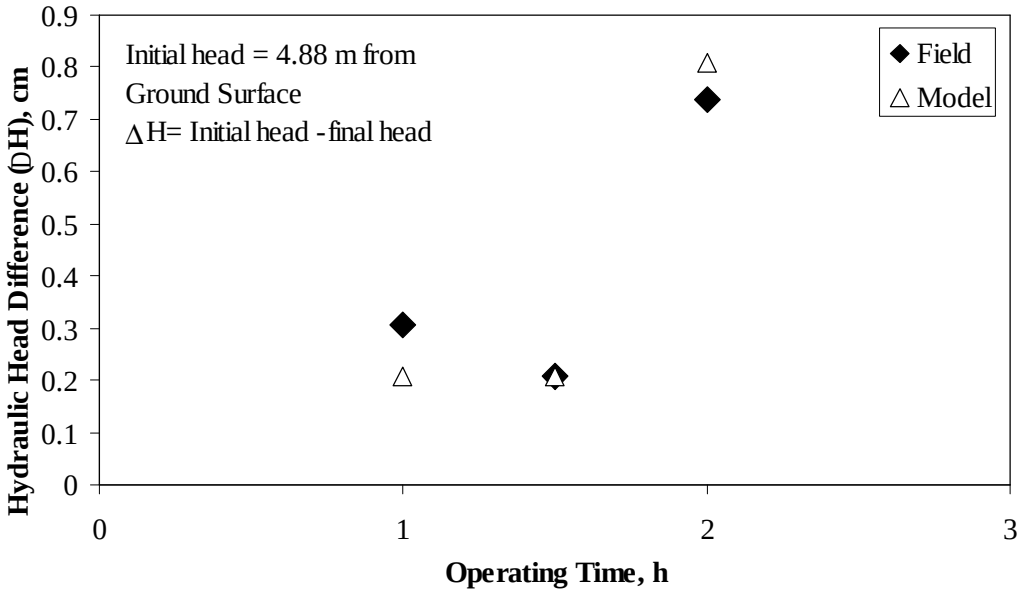

Figure 4-10 Comparison of head distribution between model and field.

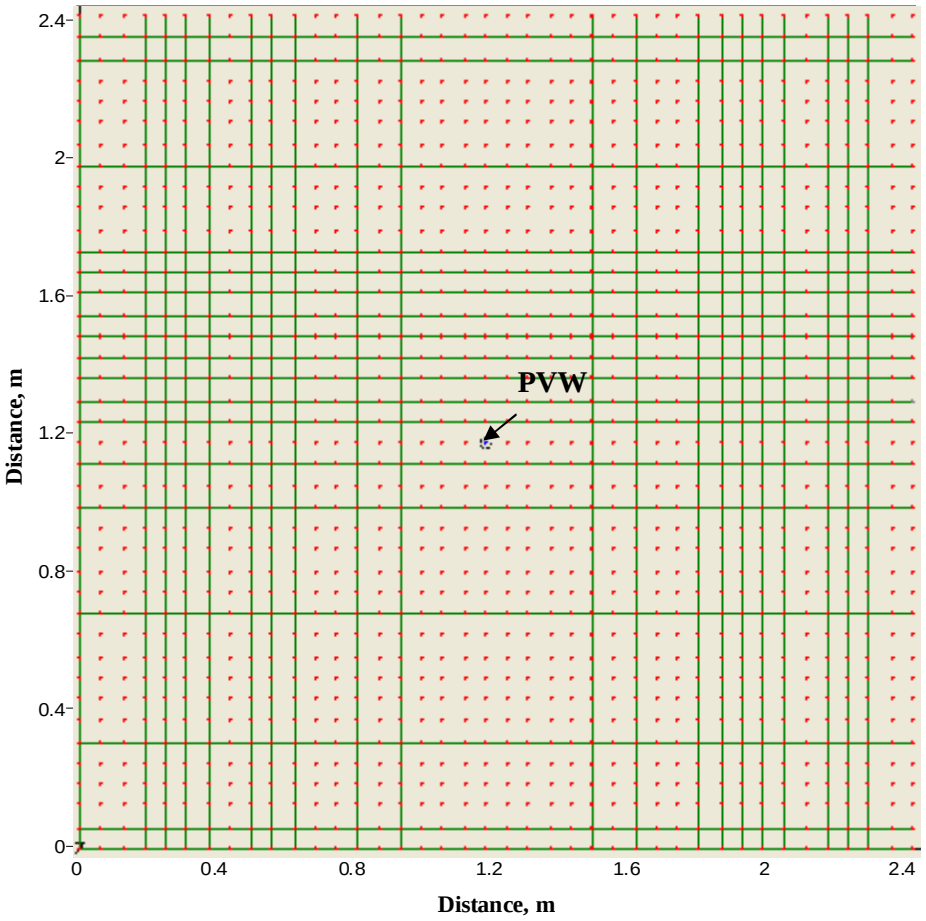

Figure 4-11 Descretized grid for parametric study.

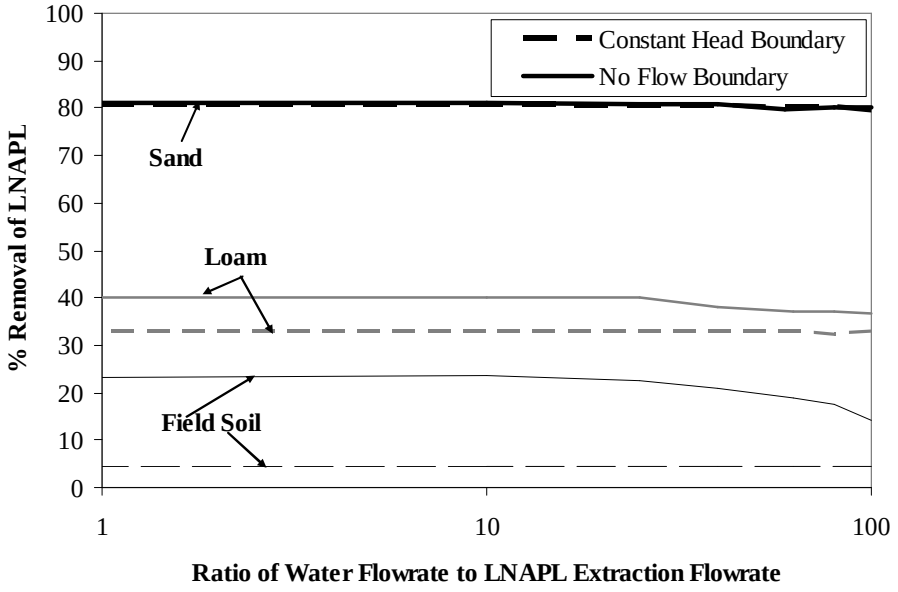

Figure 4-12 Impact of boundary type and ratio of water to LNAPL extraction flowrate on free LNAPL removal.

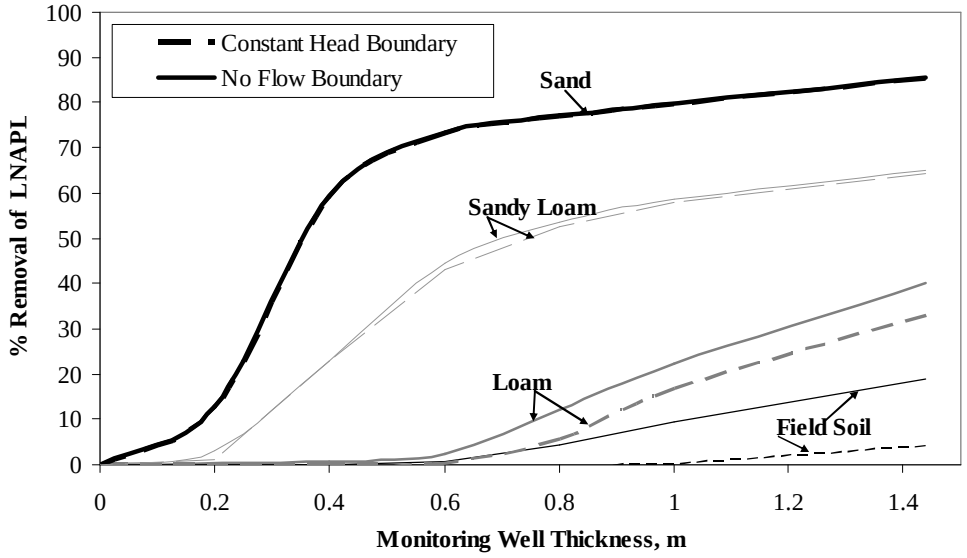

Figure 4-13 LNAPL removal from different soil textures for various monitoring well thickness.

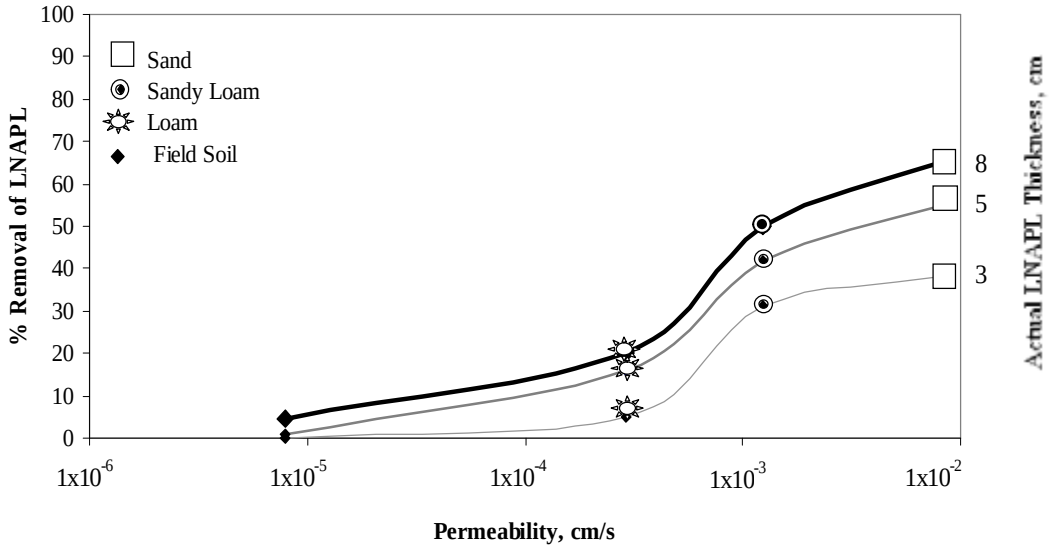

Figure 4-14 LNAPL removal from different soil textures for various actual LNAPL thickness.

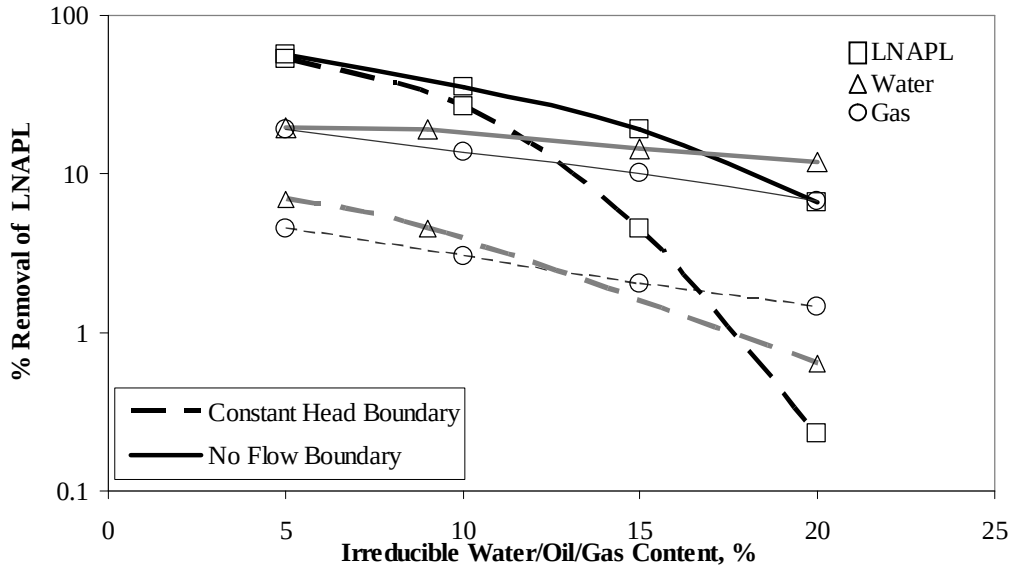

Figure 4-15 Impact of irreducible water/oil/gas content on recoverable free LNAPL for experimental soil.

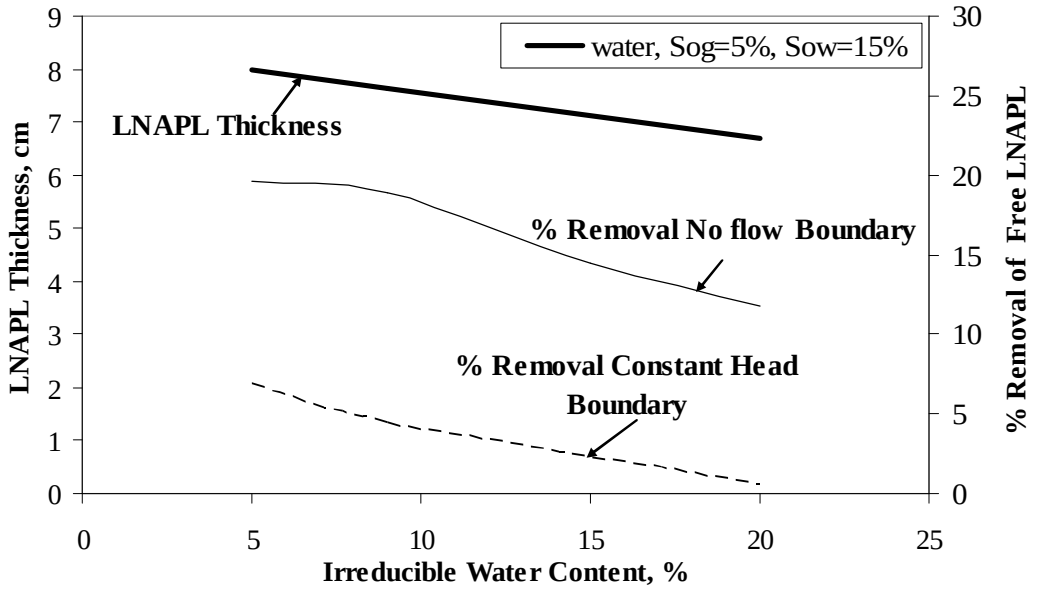

Figure 4-16 Impact of irreducible water content on available free LNAPL thickness for test soil.

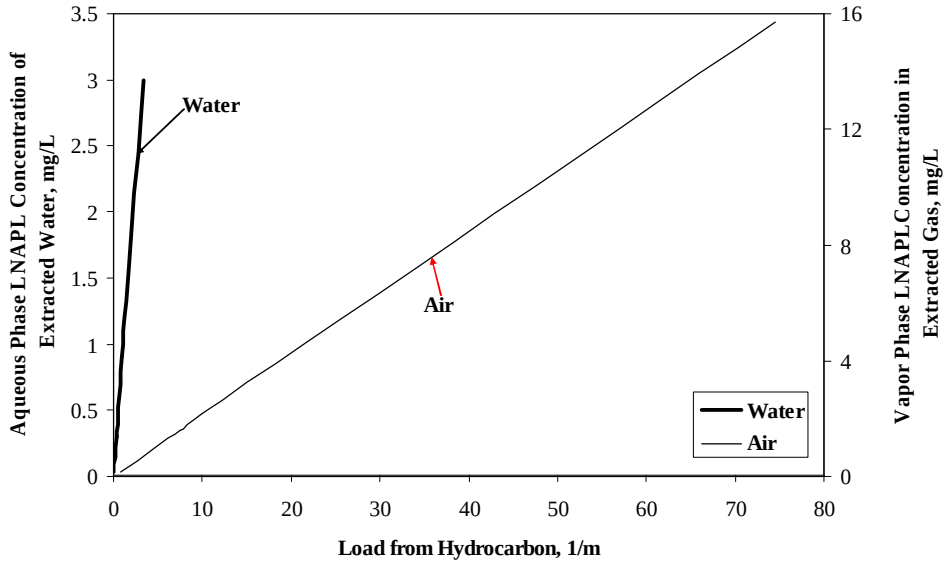

Figure 4-17 Sensitivity analyses for load from hydrocarbon both to mobile (soluble) and gas phase for experimental soil.

5. PERFORMANCE MODELING AND OPTIMIZATION OF CONTAMINANT EXTRACTION USING PREFABRICATED VERTICAL WELLS (PVWS)

Published 2008

Geosynthetics International

PERFORMANCE MODELING AND OPTIMIZATION OF CONTAMINANT EXTRACTION USING PREFABRICATED VERTICAL WELLS (PVWs)

N. Sharmin, T. Kunberger, M. A. Gabr, J. D. Quaranta, & J. Bowders

ABSTRACT

Well Injection Depth Extraction (WIDE) is a hybrid in situ subsurface remediation technology applicable for fine grained soil. A finite element model is developed to study the impact of the extraction process using WIDE on the groundwater head distribution and contaminant transport. An optimization process is employed to develop an operating schedule to control groundwater elevations and therefore the efficient removal of a given contaminant phase. The model results showed that groundwater elevation was lowered at the rate of approximately 4mm/h at an extraction rate 0.125m^3/h. The transport model is analyzed for three scenarios: (1) applying a continuous source of benzene concentration to provide information on the required time for mobilization of benzene due to the presence of a constant source at the top of the groundwater table; (2) applying an initial pulse concentration of benzene at the top of the groundwater table to show the reduction rate of soluble benzene concentration with time, once the liquid free product is removed, and the soluble phase is removed from within the sand seam but remains above it in the low permeability layer; and (3) applying a uniform distribution of the soluble phase of

benzene within the geologic medium between the wells to investigate progressive contaminant removal from the hydro-geologic domain, given that groundwater is contaminated with soluble phase. Effluent concentration equal to the initially assumed constant source of 0.3mg/L of benzene leaking to the groundwater, within a 0.08m thick sand lens was obtained after 18 h of extraction. On the other hand, once the source ceased to exist, and considering an initial pulse concentration of benzene on top of the groundwater level, 125 h of continuous system operation was needed to lower benzene concentration to less than 0.005mg/L (maximum concentration level for drinking water standards) within the flow domain. Results from the optimization study showed that an operation schedule of 3 h “on” and 21 h “off” can enhance the efficiency of WIDE extraction of subsurface contaminants in various phases.

KEYWORDS**:** Contaminant Transport; Geosynthetics, Groundwater profile; Subsurface model; Optimization; Well Injection Depth Extraction (WIDE).

INTRODUCTION

Extracting contaminant from low permeability, high clay fraction soils, poses a significant technical challenge to in situ remediation efforts. Due to geologic discontinuities and limited subsurface coverage, conventional technologies, such as pump and treat and vapor extraction systems using conventional well fields are typically ineffective in low permeability soils. In addition, the reduction in free product saturation

near the typically few recovery wells used in pump-and-treat operation leads to a decrease in porous media permeance with regard to free product mobility. These shortcomings can be potentially addressed by the WIDE (Well Injection Depth Extraction) system in which close installation spacing, depth-specific features, and vacuum-assisted point extraction provide subsurface control of hydraulic head (Gabr et al. 1995; Gabr et al. 1996; Gabr 1997; Quaranta et al.1997; Gabr et al. 1999; Kunberger et al. 2003; Warren et al. 2006). However, and as with remediation technologies introduced in the past decade, the long-term extraction-mode performance of WIDE is not fully defined. An approach to understand long term performance aspects is to perform groundwater and contaminant transport modeling as for example presented by Uddameri, and Kuchanur (2007) and Holland (1997).

Work in this paper aims at presenting the analyses of effectiveness and time dependence of the WIDE remediation approach within the subsurface environment. The modeling resulting will be used to illustrate the development of an optimized scheme of operation addressing a given contaminant phase extraction mode. Issues investigated include variation of groundwater and contaminant profile with varying extraction time as well as the possibility of lowering the groundwater in the model area such that circulation of air can be implemented to assist in the mass transfer and vapor extraction of LNAPL residual saturation. The modeling study consists of three parts: i) groundwater modeling, ii) contaminant transport modeling, and iii) optimization analysis of operating schedule.

TECHNOLOGY OVERVIEW OF WIDE

The WIDE system is a hybrid subsurface flushing/vapor-gas extraction system that uses Prefabricated Vertical Wells (PVWs) for the in situ remediation of contaminated ground-water and fine-grained soils with hydraulic conductivities ranging from 10^{-3} to 10^{-8} cm/s. (Gabr et al. 1995; Gabr et al. 1996; Gabr 1997; Quaranta et al.1997; Gabr et al. 1999; Kunberger et al. 2003; Warren et al. 2006). The major elements of the WIDE technology include the following: i) prefabricated vertical wells (PVWs), ii) groundwater and soil vapor vacuum extraction system, iii) liquid injection system, and iv) above-ground treatment system.

The WIDE system incorporates the PVWs as the mechanism for pressurized injection of a flushing solution into the *in situ* soil concurrent with vacuum extraction for removal of the contaminated solution. A PVW, 100mm wide by 4mm thick, is manufactured as a composite system of an inner core, an outer permeable filter jacket, and at specified positions, an impermeable barrier sleeve. A schematic of the PVW utilized in WIDE is displayed in Figure 5-1.

FIELD LAYOUT

The PVWs are commonly installed in a grid pattern containing separate injection and extraction rows. Each PVW row is connected to an above ground polyvinyl chloride (PVC) pipe. The piping network is designed to allow connection solely to either the injection or extraction unit, or, to both injection and extraction units in an alternating row

manner. Figure 5-2 illustrates a typical installation layout plan view of 4.5 m square (Kunberger et al. 2003). A three-dimensional schematic of the WIDE concept is presented in Figure 5-3.

TEST SITE DESCRIPTION

Modeling input parameters were based on data from a test site at a former Air Force Base (AFB), located approximately 16 kilometers south-east of Columbus, Ohio. BTEX (Benzene, Toluene, Ethylbenzene and Xylene), Jet Propellant 4 (JP-4), and Jet A petroleum hydrocarbon from leaking underground storage tanks and failure in the underground piping systems contaminated the subsurface profile. In order to investigate the feasibility of using WIDE as an in situ remediation system, three research phases were implemented. The first phase included installation of a 9.14 m by 9.75 m test pad and testing feasibility of operation which involved subsurface parameter determination. In the second phase, the test pad was re-commissioned for testing efficiency of various spacing in contaminant extraction. Phase III included the installation, operation, and monitoring of a larger-scale test pad, and modeling and optimization analysis of the with a PVW spacing of 1.83 m.

Phase III scale-up included an area measuring 13m by 44m, surface piping network consisted of 25 rows – each encompassing 7 or 8 PVWs, and a 17 m^3/min air compressor powering a 5cm diameter eductor vacuum system. A 1.5 m^3 tank was used as a means for applying vacuum pressure to the piping network, and temporarily store

extracted fluids. The extracted liquid was transferred to two 6 m^3 liquid holding tanks for subsequent disposal. The WIDE is operated in dual-phase extraction (DPE) mode to remove various combinations of contaminated groundwater, separate-phase petroleum product, and hydrocarbon vapors.

The site soils are characterized as glacial till with shale fragments, clay, silt, and sand with locally isolated layers of sand and gravel. These isolated layers are poorly connected, suggesting a lenticular morphology. Hence, the extraction of the JP-4 at this site is further compounded by such heterogeneity which not only impacts the mobilization of JP-4 but also its entrapment on micro (intra particles) and macro (intra layers) scales.

Groundwater on site was detected in a gray/brown, medium dense, silty sand layer 16-18 feet below ground level. The site is of generally flat topography with the groundwater's natural gradient less than 1% based on elevations from well data. The hydraulic conductivity values reported in the past, based on groundwater well testing, ranged from 8×10^{-6} cm/s to 2×10^{-4} cm/s.

MODEL DESCRIPTION

The computer programs used for analysis of system performance and domain idealization are SEEP/W and CTRAN/W Version 5 by Geo-Slope International. These codes are based on continuum analyses of the flow domain using the finite element approach. The advantage of this program is the ability to perform the analysis under coupled saturated and unsaturated conditions. Accordingly, as the extraction process leads

to the de-saturation of the flow domain, an accurate estimate of the head distribution is obtained

Groundwater Modeling: SEEP/W

Groundwater modeling by SEEP/W, considered the subsurface profile as an axi-symmetric media for evaluation of hydraulic head distribution and changes in saturation fronts. In this case, the subsurface profile was idealized to include major soil stratifications, groundwater table, and representation of the installed PVWs on 1.83 m spacing. The idealized profile including subsurface layers, water table, and well spacing is shown in Figure 5-4. The water table was set at a depth of 4.88 m below ground surface, as approximately measured in the field. The model domain was developed based on a 10.67 m depth and was extended to 9.14 m in width to observe variations of groundwater profile within the PVWs zone of influence. In the field, a typical PVW was installed down to 7 m from ground surface and the active extraction zone was from 4.88 m to 7m below ground surface. The soil layers are labeled, and denoted with shading, illustrating thicknesses and stratification changes (Figure 5-4). The water table is shown as a thick line above the sand lens. Figure 5-4 represents scaling based on the (0,0) coordinate. The axis passing through the (0,0) coordinate is the axis of axi-symmetric domain rotation.

Input material properties required for each of the relevant soil types include grain size distributions, volumetric water content (volume of water/total volume) functions, hydraulic conductivity functions, and anisotropic permeability ratio (if anisotropic

conditions are to be modeled.) The material properties used in the model are taken from Phase I soil characterization data (Kunberger et al.2003). The subsurface parameters are presented in Table 5-1.

SEEP/W provides the capability of defining volumetric water content and hydraulic conductivity functions based on grain size distributions. The hydraulic conductivity variation with suction head is then developed from the corresponding volumetric water content function. SEEP/W uses the Green and Corey (1971) relationship to estimate the hydraulic conductivity based on the soil-water characteristic relationships.

The mesh used for the finite-element analysis is shown in Figure 5-5. The mesh consisted of 1739 nodes and 1656 elements (quadrilaterals). Figure 5-5 also illustrates the idealized soil types, PVW locations, groundwater table location, and all boundary conditions imposed on the model. The solid triangles at the bottom and sides of the model represent “no flow” boundary conditions, while unit flux conditions are applied across the length of the PVWs located at the side, and at 1.83 m away from the side. The idealization considers the PVW at the center of the domain as the rotation point for analysis.

The program in axi-symmetric mode considers a “1 radian” thick slice of a circular domain. For this type of analysis, the program considers the y-axis (or the left side of the graph in Figure 5-5) as the rotation point, and the x-axis as the diameter of the domain. Because of the axial symmetry requirement for the input, certain adaptations to the actual field parameters were necessary. These adaptations were mainly associated with the well

spacing, and subsequent extraction volumes and rates. Flow rates from the 8 PVWs modeled were correlated to flow rates from the central well and a "ring" well (created by rotating a single injection well 2Π(rad) during the analysis). This "ring well" was placed 1.83m (6ft) from the center well. Since a PVW is approximately 10cm wide, the y axis was placed at the center well; the unit flux was applied at 5 cm from the y axis. In the "ring" well, the unit flux was applied at 1.88 m from rotation axis. Tables 2 and 3 present the modeling parameters used to idealize field conditions.

As shown in Table 5-3, a thin sand layer [0.08m thick] with high permeability was included to model the sand lens. The distribution of extraction flowrate in soil strata, determined in accordance with the permeability and the thickness of the geologic layers, showed that the relatively thin sand layer contributes 86% of the total volume of extracted water. Therefore, 100% extraction flow rate was assigned to the thin sand layer. After refining the site domain and modeling parameters, transient (or time dependent) analysis was conducted based on an extraction-only mode.

Contaminant Transport Model: CTRANW

In addition to modeling the groundwater profile resulting from the extraction process, contaminant transport modeling was performed in order to determine the contaminant removal rate and change in distribution of the soluble phase due to the PVW extraction operation. Due to the Lenticular morphology of the test site, the focus was on contaminate movement within the sand lens at depth of 4.88 m-4.95 m. Initial conditions

and contaminant concentration data were assumed based on monitoring well data. Data from the monitoring well closest to the Phase III test pad showed that the benzene concentration was on the average equal to 0.3 mg/L.

Contaminant transport was assumed to be governed by both advection and dispersion. Adsorption is accounted for later in the discussion through the presentation of a retardation coefficient. As the spacing between PVW1 and PVW2 (SEEP/W model) was 1.83 m, a value equal to 10% of the half spacing [0.914 m] was assumed as the longitudinal dispersivity [i.e. 0.0914 m]. Transverse dispersivity was chosen as 10% of longitudinal dispersivity (EPA, 2008).

The transport model is analyzed for three scenarios: i) Case 1: applying a continuous source of benzene concentration at the top of the groundwater table (shown as solid circles in Figure 5-6(a)), ii) Case 2: applying initial pulse concentrations of benzene at the top of the groundwater table (shown as rectangles in Figure 5-6(b)), and iii) Case 3: applying a uniform distribution of the soluble phase of benzene within the geologic medium in-between the modeled PVWs (as in shown in Figure 5-6(c)). Figure 5-6 represents the profile view of each scenario. Case 1 provides information on required time for mobilizing benzene due to the presence of a constant source at the top of the water table. Case 2 will illustrate the reduction in the rate of benzene concentration with time, from initial concentration, and with continuing extraction once the free product was removed.

Case 3 represents progressive contaminant removal from the hydrogeologic domain

in between two PVWs given that the groundwater is contaminated with the soluble phase (within the sand lens.) CTRAN/W uses the groundwater flow velocities as generated by SEEP/W to perform the contaminant transport analyses. The modeling results presented herein are based on 10-minute time steps (i.e. results are on the basis of a constant velocity increment within each 10-minute time step.)

Optimization Modeling

As mentioned earlier, an approach to address residual saturations is to lower the groundwater level at the site and apply a vacuum head (in the partially saturated zone) to volatilize residual saturations and extract vapor phase contaminants. The field extraction schedule from March 8th, 2006 to March 12th 2006 (Table 5-4) shows, on an average, 6 h of operation time for 5 consecutive days. Based on soil morphology at the location of test pad, and if the groundwater table is lowered 0.08 m (as sand lens thickness is 0.08 m) in between two PVWs, air can be circulated for volatilization of the residual phase. The purpose of the optimization modeling and analysis is to develop an extraction schedule to induce the lowering of groundwater table in a sustainable manner. The optimization modeling utilized MATLAB7.1 optimization tools to develop performance schedule, based on SEEP/W model predictions, by which groundwater table can be lowered efficiently.

The optimization process utilizes the head distribution from the Seep/W transient analyses (for the vadose and saturated zones) which models the extraction schedule

implemented in the field as shown in Table 5-4. The issue here is that SEEP/W indicated approximately a 0.46m lowering of the groundwater table at the end of day 5 (March 12th) using the field operation schedule. It is however more efficient from remediation perspective to lower the groundwater table by only 0.08 m as not to greatly impact the liquid flow rate or cause volumetric changes leading to reduction in hydraulic conductivity.

To optimize PVW extraction performance, the time frame for the simulation in SEEP/W was chosen initially as 1 h system operation and 23 h of system shut-down, during which groundwater table recovery is allowed takes place within the domain. During system operation a flowrate of approximately 0.125 m^3/h was applied to the model (consistent with values observed in the field.). Zero flowrate was used in the model to simulate the period of system shut-down.

The optimization program within the framework of MATLAB was linked to SEEP/W and was set up to control the operational times (input to the SEEP/W), on the basis of the head distributions (output of SEEP/W). The head distribution of each node of the VSM was considered as input parameter with the operation time schedule needed lowering groundwater table by 0.08 m is the target optimization parameter (which means the head at all nodes are lowered by 0.08 m). By definition this value interprets the inequality design constraints (MATLAB 7.1) for the optimization process in this paper. Section 5.1 shows that the SEEP/W has 1739 nodes and as mentioned earlier, the region in the sand layer is the area of concern. Since there are 11 nodes in between PVW1 and

PVW2, the number of variables for the optimization program was chosen as 11. Figure 5-5 shows the focus area of the optimization.

MODELING RESULTS

Model Validation

The SEEP/W model has been validated by comparing the groundwater depth obtained at point 1 (Figure 5-4) from model and field monitoring Well (LMW4). The model was simulated according to the field schedule. Both WIDE in the field and model was operated for 4.5, 7.75 and 7 h for 1^{st}, 2^{nd} and 3^{rd} day respectively. In field, the groundwater depth was measured after the system operation stopped. Figure 5-7 shows that, given the simulation parameters, the model is capable of replicating the field data in terms of groundwater depth.

Hydraulic Head Distribution and Permeability

Figure 5-8 shows the groundwater profile for various durations (100 minutes, 400 minutes and 800 minutes) of system operation with an extraction rate of 0.125 m^3/h,. Figure 5-8 shows that water table was lowered at the rate of approximately 4 mm/h. This is mainly due to the presence of the sand lens with a hydraulic conductivity nearly two orders of magnitude greater than that of the two layers above and below it.

Figure 5-9 illustrates the permeability variation for the vadose-saturated model

(VSM) due to varying system operation time. Figure 5-9 shows that with the increase in suction head and extraction duration, the water permeability also decreases and the air permeability increases. The decreasing rate for water permeability is nearly three orders of magnitude under suction head of 9.6 KPa. As operation time increases, the reduction rate of permeability with increasing suction declines. The air permeability reaches a steady state value of approximately of $5x10^{-6}$ cm/s. These "equivalent" permeability values can be used to estimate the rate of air circulation for gas extraction and venting.

Results from CTRAN/W Contaminant Transport

The model simulation was conducted for 10000 minutes (167 h) of extraction time. Figure 5-8 shows the position of key locations selected for the purpose of results presentation and discussion. Figure 5-10 presents the results from the simulation for the continuous source at the upper boundary of the sand layer (Case 1, Figure 5-6(a)). The simulation results are shown for 1680 minutes (28 h) of operation time and show that PVWs extraction process mobilizes the soluble phase through the silty sand layer. The concentration at point 1 (Figure 5-8) reaches the induced constant source concentration of 0.3 mg/L after 1060 minute (18 h) of extraction time.

The data in Figure 5-11 corresponds to Case 2 in which an initial concentration of benzene is applied at the top of the groundwater table (pulse source of contaminant). Data in Figure 5-11 depict the propagation and reduction of benzene over time at two points (at the top and bottom of the sand lens, points 2 and 3 of Figure 5-8) due to continuous

extraction by the PVWs. Results in Figure 5-11(a) indicate that 4300 minutes (71 h) are required to reduce benzene's soluble phase to less than 0.005 mg/l at a point 0.61 m away from PVW1, where the benzene concentration was initially 0.3mg/L. Point 2 is located at the top of the groundwater table, where the instantaneous pulse source was introduced and therefore the gradual reduction in concentration with system operation. Figure 5-11(b) shows the variation of benzene concentration at a point in-between the two PVWs, at the bottom of the sand lens (point 3 of Figure 5-8). In this case initial concentration at point 3 is zero, but increases as the contamination is mobilized and then decreases with the continuous extraction. For the first 1200 minutes (20 h) of operation, the benzene concentration increased at point 3, and then dropped to less than 0.005 mg/L after 6720 minutes (112 h) of continuous operation.

Figure 5-12 shows benzene concentration contours with increasing extraction time, assuming uniform initial concentration within the sand lens (Case 3). Figure 5-12 shows that 7,500 minutes (125 h) of continuous system operation were needed to lower benzene concentration to less than 0.005mg/L within the flow domain, whereas 10,000 minutes (167 h) of operation reduced the concentration to zero (with benzene initial concentration 0.3 mg/L).

If adsorption is considered due to the presence of organic carbon in the soil, retardation of contaminant transport may occur and lead to an increase in extraction times. For the purpose of illustration, the partitioning coefficient for benzene was assumed as log(Koc)=1.58 (ASTM, 1998), soil bulk density 1.84 gm/cc and porosity

equal to 0.4 with 1% organic carbon content. The calculated retardation factor was 3. Therefore, the impact of adsorption of the soluble phase of benzene was to increase the transport time by a factor of 3 using the assumed properties.

Optimization Results

Result from optimization indicated the ability to lower the groundwater table within the active zone of a given row by 0.08 m by using 3-h on, 21-h off optimized schedule. The optimized operational schedule is presented in Table 5-5. The schedule in Table 5-5 is developed such that lowering of the groundwater table by 0.08 m is achieved across the active flow domain based on the 1.83 m spacing. In a field setting, this operational schedule is translated into the operation of 3 lines per day assuming 9-h work days. If the process is automated, 8 lines can be then operated within 24-h period and the line rotation can be continued according to the prescribed schedule. The groundwater table can be lowered by more than 0.08 m by applying a similar optimization process, if desired. The target head values should be provided on the basis of feed back from field data with monitoring of the extracted waste stream.

Figure 5-13 shows a comparison of groundwater table levels from optimized and field operation schedules. Modeling results indicated that at the beginning of the 6^{th} day of system operation, the groundwater level is at 4.953 m from ground surface, 1.22 m away from PVW1. While field schedule employed during the modeled week fulfilled the requirement of lowering the groundwater level by 0.08 m by the second day of operation,

the continued extraction leads to an approximately 0.46 m drop in groundwater table after 5 days. This excessive drop in head may not however be advantageous for two reasons. The first is excessive drop in groundwater table may limit the amount of LNAPL to be extracted and increase the amount of trapped phase. The second is continued drop in groundwater table may increase the ratio of extracted groundwater to extracted free product volume ratio.

Figure 5-14 shows the difference in decreasing head with time as computed from the schedule implemented in the field versus that computed from the optimization modeling. As shown in Figure 5-14, the head magnitude difference between the two cases is larger during system operation as compared to when the system is shut down.

In summary, the hypothesis being advanced here, based on the model results, is the possibility of extraction process rotation through the 25 PVWs rows in an optimized manner such that extracted volume of free product as well as contaminated vapors are maximized. In this case, the shut down period per row can be utilized for vapor extraction at lower vacuum heads such that the groundwater table is not further impacted or for air injection if bioventing is implemented.

The optimization modeling provided a scheme for lowering the groundwater table by a prescribed magnitude to provide for contaminant recovery in vapor phase. As long as the extraction operation is targeting free product (i.e. free product flow rate is sustained), lowering of the groundwater table is minimized. Once no more free product is extracted in a given line (per given run period), the groundwater can then be lowered for

implementation of gas extraction and bioventing. This process is rotated throughout the system rows, and each row may have its own schedule based on feedback data, in terms of extracted aqueous and free product flow rates and mass in gas phase.

SUMMARY AND CONCLUSION

Groundwater and contaminant transport modeling were developed to investigate and analyze the performance aspects of WIDE system as an in-situ remediation technology. The modeling study consisted of three parts: i) groundwater modeling, ii) contaminant transport modeling, and iii) optimization analysis of the operating schedule. The computer programs used for the study were SEEP/W and CTRAN/W with optimization modeling performed using MATLAB tools.

The modeling study included two components; the first (modeling by SEEP/W) considered the subsurface profile as an axi-symmetric media for evaluation of hydraulic head distributions and changes in saturation fronts. The ground water model showed that the water table was lowered at the rate of approximately 4mm/h due to extraction rate $0.125 m^3$/hr. The second (modeling by CTRAN/W code) used the results from SEEP/W to determine the contaminant movement due to the extraction operation. Three cases were considered: i) applying a continuous source of benzene at the top of the groundwater table (also at the top of high permeability sand lens), ii) applying initial pulse concentrations of benzene at the top of the groundwater table, and, iii) applying a uniform distribution of the soluble phase benzene within the high permeability sand lens.

Results from Case 1 showed that, with system extraction, a constant source concentration of 0.3mg/L leaking to the groundwater within the sand lens reached the level of the source concentration after 1060 minutes (18 h) of extraction time. Case 2 analyses revealed that 4300 minutes (71 h) were required to remove benzene's soluble phase once the source ceased to exist. Results from Case 3 showed that 7,500 minutes (125 h) of continuous system operation were needed to lower benzene concentrations to less than 0.005mg/L within the flow domain, once the source ceased to exist. If adsorption is considered such as the presence of organic carbon content in the soil, retardation of contaminant transport may occur and lead to an increase in extraction times by approximately a factor of 3.

To enhance the efficiency of WIDE extraction of subsurface contaminants in various phases, and as an approach to address residual saturations, groundwater level at the site can be lowered such that it is possible to volatilize residual saturations and extract contaminants in the vapor phase. Optimization analysis was used to develop an extraction schedule to maximize system performance in terms of lowering the groundwater table by a prescribed magnitude. MATLAB7.1 optimization tools were used to manipulate the results from SEEP/W predictions with respect to a performance schedule. Optimization results indicated the ability to lower the groundwater table within the sand lens by 0.08 m using a 3-h on, 21-h off operating schedule across the active flow domain, based on the 1.83 m spacing. In a field setting, this operational schedule is translated into the operation of 3 lines/d assuming 8-h work days. If the process is automated, 9 lines are then operated

within 24-h period according to a rotation schedule. The groundwater table can be lowered by more than 0.08m by applying a similar optimization process but with different target objective. Such target values should be provided on the basis of field data with continual monitoring.

The scope involved in this paper explains the mechanics involved with the ability of controlled lowering and rising of groundwater table through system optimization. The analysis demonstrates optimization of pumping schedule through controlling groundwater elevation. This paper's contributions to the state of the art are as follows:

1) The model simulates an approach to remove "wide cut" contaminant from low permeability soil.
2) The optimization approach can be used to optimize operational parameters for maintaining regulatory limits in a timely manner.

ACKNOWLEDGEMENTS

The Rickenbacker Air National Guard Base / Rickenbacker International Airport (RIA) remedial action is led by the US Army Corps of Engineers, Louisville District Office. The field oversight was provided by the US Army Corps of Engineers, Nashville District Office. The site owner is the Rickenbacker International Airport Authority. Regulatory interface and oversight were provided by the Ohio Environmental Protection Agency, Central District Office, Ms. Diana Bynum. Maxim Technologies shared data to aid in site characterization for the WIDE system test site and their contribution is acknowledged. The system fabrication and field construction was performed by the Nilex Corporation, Denver. The West Virginia Water Research Institute was involved in project management and permitting requirement. North Carolina State University in cooperation with West Virginia Water Research Institute performed system parameters monitoring and optimization, modeling, data collection and reduction, analysis and reporting. Mr. John J. Sneberger coordinated and conducted the field work and reporting to respective organizations. The air and liquid samples were sent to Research Environmental and Industrial Consultants, Inc. for laboratory testing to determine extraction rates and masses. Dr. Kumar Mahintakumar, professor of North Carolina State University, helped to develop the optimization approach.

REFERENCES

ASTM 1998. Standard Guide for Remediation of Ground Water by Natural Attenuation at Petroleum Release Sites. American Society for Testing and Materials. (E 1943 98; 1998).

EPA (2008). EPA on-line tools for site assessment calculation United States Environmental Protection Agency, Washington, DC, USA, http://www.epa.gov/ athens /learn2model/part-two/onsite/ longdisp.htm

Gabr, M. A. (1997). "Prefabricated well injection depth extraction WIDE system for enhanced soil flushing". *Disclosure Document No. 422400 under 37 CFR Sec 1.21 (c)*.

Gabr, M. A., Bowders, J. J., Wang, J., and Quaranta, J. D. (1996). " In situ soil flushing using prefabricated vertical drains". *Canadian Geotechnical Journal.* 33(1). 97–105.

Gabr, M. A., Bowders, J. J., and Woksien, S. (1995). "Prefabricated vertical drains (PVD) for enhanced soil flushing". *Geoenvironment 2000*. 1250–1264.

Gabr, M. A., Sabodish, M., Williamson, A., and Bowders, J. J. (1999). "BTEX extraction

from clay soil using prefabricated vertical drains". *Journal of Geotechnical and Geoenvironmental Engineering*. 125(7). 615–618.

Holland, J.P. (1997). "Development of environmental quality modeling and simulation systems for the U.S. Department of Defense". *Proceedings of the 27th Congress of the International.*

Association of Hydraulic Research, IAHR. Part C, Aug 10-15 1997, : San Francisco, CA, USA, ASCE, New York, NY, USA, p. 319-324.

Kunberger, T., Quaranta, J. D. and Gabr, M. A. (2003). "Remediation of former Lockbourne Air Force Base using well injection depth extraction (WIDE)." *12th Panamerican Conference on Soil Mechanics & Geotechnical Engineering*. Cambridge, MA. (June): 1575-1581.

MATLAB 7.1 , The MathWorks Inc, www.mathworks.com (December 1, 2006)

Quaranta, J. D., Gabr, M. A., Cook, E. E., and Szabo, D. ,1997, Developments in prefabricated vertical drain enhanced soil flushing. *Proceedings from the 7th International Offshore and Polar Engineering Conference*,703–706.

SEEP/W,CTRAN/W Version 5.18 GEO-SLOPE International, Calgary, Alberta, Canada. http:/www.geo-slope.com/.

Uddameri, V., and Kuchanur, M. (2007). "Simulation-optimization approach to assess groundwater availability in Refugio County, TX". *Environmental Geology*. 51: 921-929.

Warren, K.A. , Gabr, M.A., and Quaranta, J.D. (2006). "Field study to investigate WIDE technology for TCE extraction", *Journal of Geotechnical and Geoenvironmental Engineering*. 132(9):1111-1120.

Table 5-1. Input Subsurface Characteristics for Groundwater Model

Elevation (From Ground Surface)	Soil Type	Water Content % (g/g)	Permeability	
			meter/minute	cm/sec
0m-3.66m (0'-12')	Brown to gray clayey silt, (ML)	16.5	$3.6x10^{-8}$	$6x10^{-8}$
3.66m-4.88m (12'-16')	Gray, clayey/silty sand (SC-SM)	17.6	$3.6x10^{-7}$	$6x10^{-7}$
4.88m-4.95m (16'-16.25')	Gray/brown silty sand (SM)	22.8	$4.8x10^{-6}$	$8x10^{-6}$
4.95m -6.1m (16.25'-20')	Gray, sandy, lean clay (CL)	18.1	$1.8x10^{-8}$	$3x10^{-8}$
6.1m -7.32m (20'-24')	Gray, sandy, lean clay (CL)	15.0	$3.6x10^{-8}$	$6x10^{-8}$
7.32m - 10.52m (24'-34.5')	Gray, well graded silty sand (SW-SM)	12.8	$3.6x10^{-8}$	$6x10^{-8}$

Table 5-2: Model Parameters to Idealize Field Conditions

Flowrate	m^3/hr	0.125
	gal/hr	33
Flowrate (m^3/min)		0.00021
Spacing(m)		1.83
Number of PVWs modeled		8

Table 5-3: Determination of unit flux Distribution Ratio

Layer (depth below ground surface)	Permeability k meter/minute	Layer Thickness t (m)	k·t (m^2/min or m^3/min/m)	k·t ratio $\frac{k_1 \cdot t_1}{k_2 \cdot t_2}$
4.88m-4.95m (Sand Lens)	$4.8x10^{-6}$	0.076	$3.65x10^{-07}$	18
4.95m -6.1m	$1.8x10^{-8}$	1.143	$2.1x10^{-08}$	1
6.1m-7.32 m	$3.6x10^{-8}$	1.22	$4.4x10^{-08}$	2.14

Table 5-4. Field Extraction Schedule from 8th March 2006 to 12th March 2006

Days of operation	3/8/2006 (Day 1)	3/9/2006 (Day 2)	3/10/2006 (Day 3)	3/11/2006 (Day 4)	3/12/2006 (Day 5)
Duration of operation (h)	4.5	7.75	7	8.5	7.5
Duration of System shut down (h)	19.25	16.75	15.5	17	-

Table 5-5: Optimized Operation Schedule for 5 days to lower total head 0.08m

Days of operation	(Day 1)	(Day 2)	(Day 3)	(Day 4)	(Day 5)
Duration of operation (h)	3	3	3	3	3
Duration of System shut down (h)	21	21	21	21	21

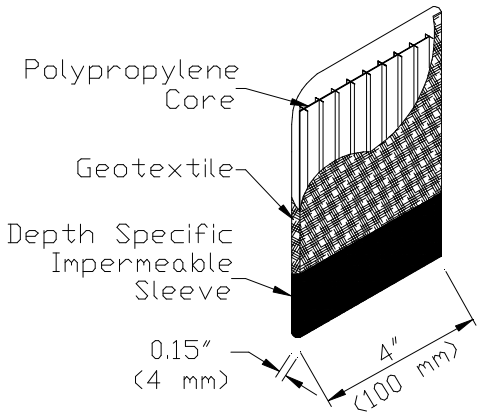

Figure 5-1 Prefabricated Vertical Well (PVW).

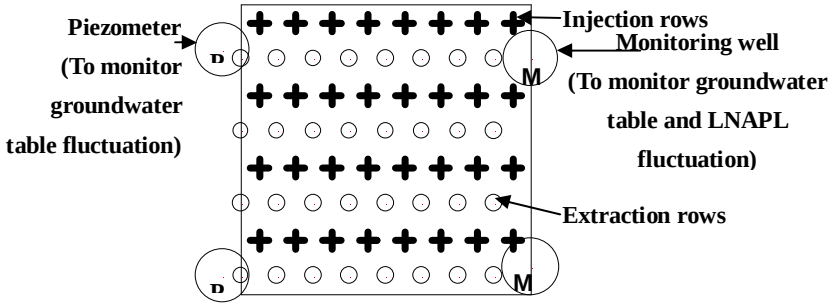

Figure 5-2. Typical WIDE test pad layout.

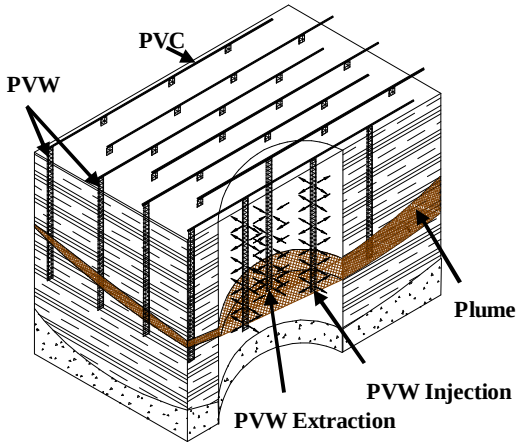

Figure 5-3. Well Injection Depth Extraction technology

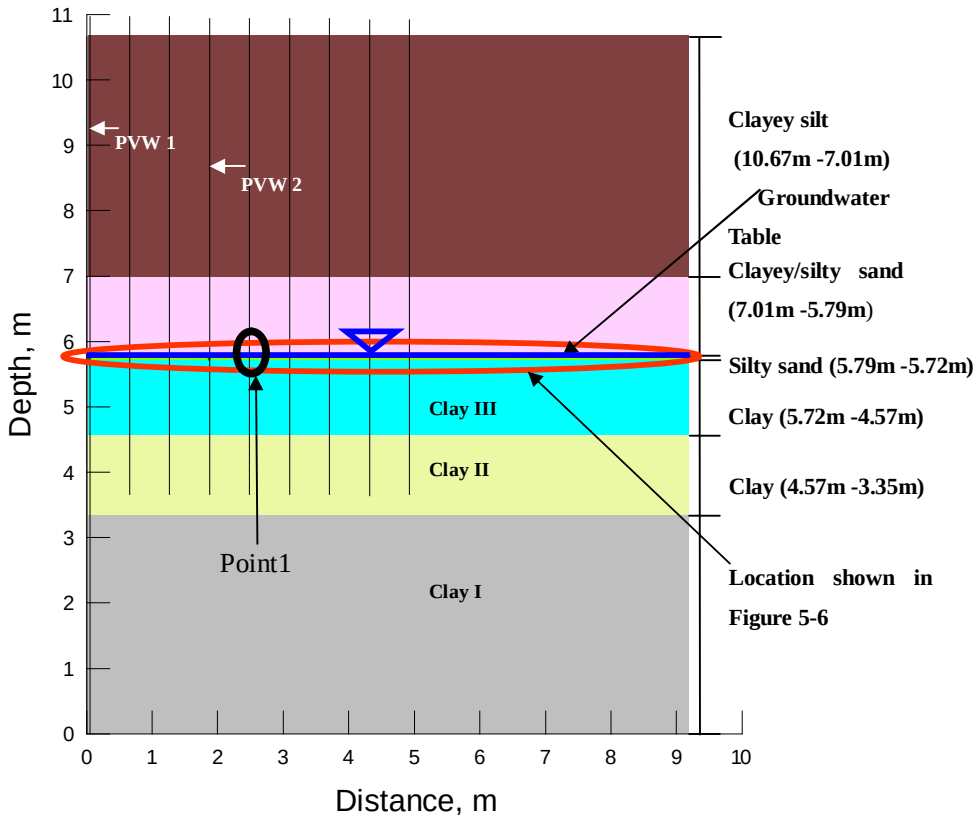

Figure 5-4. General site profile.

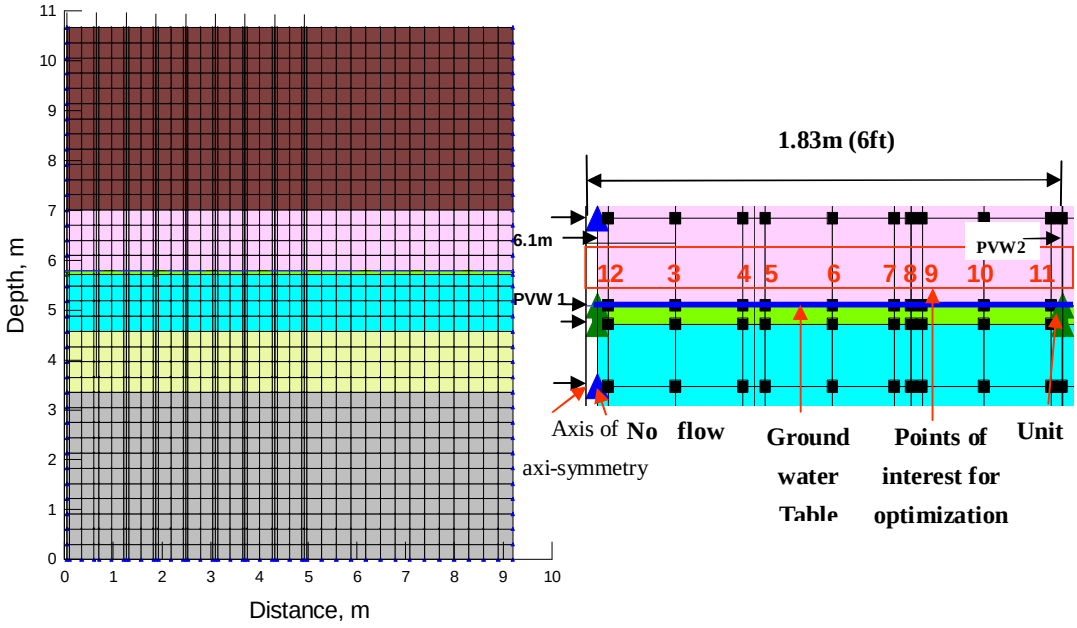

Figure 5-5. General parameters used in groundwater model.

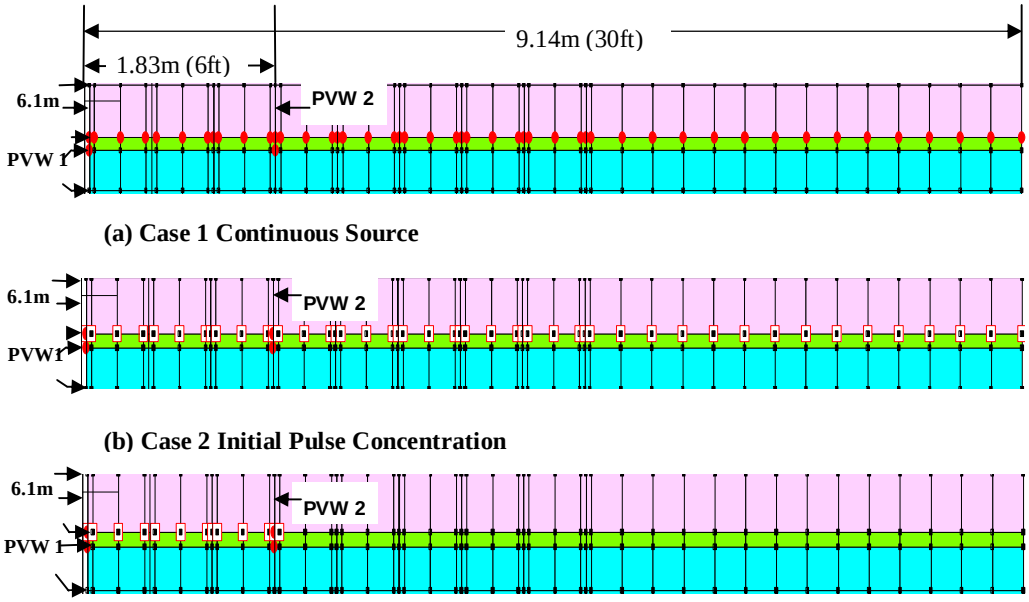

Figure 5-6 Contaminant Transport Model for Three Scenarios

(Model area denoted in Figure 5-4)

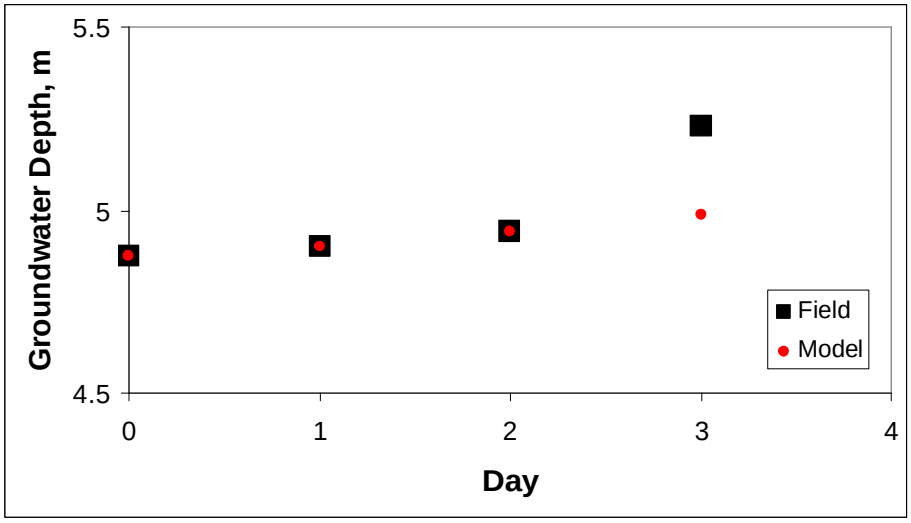

Figure 5-7. Comparison between field and model groundwater profile.

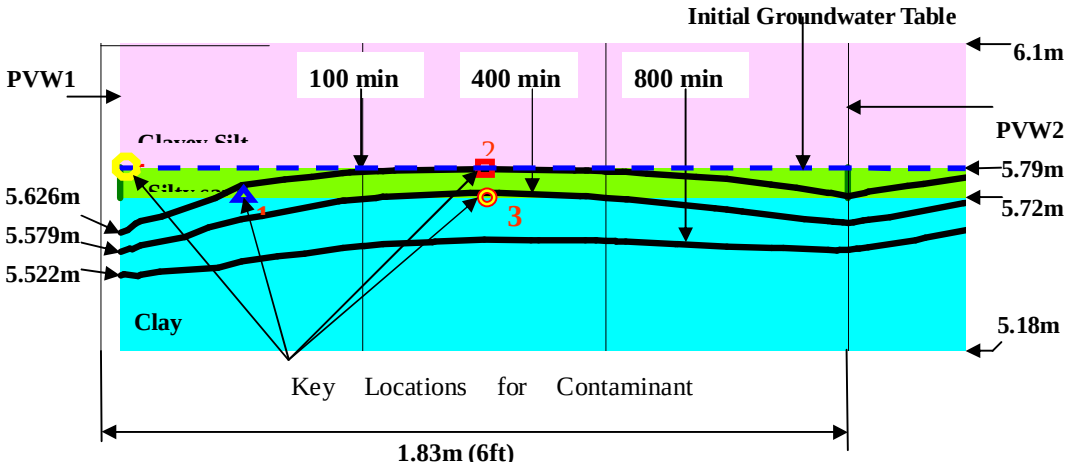

Figure 5-8 Groundwater profile after 100, 400 and 800 minutes of extraction.

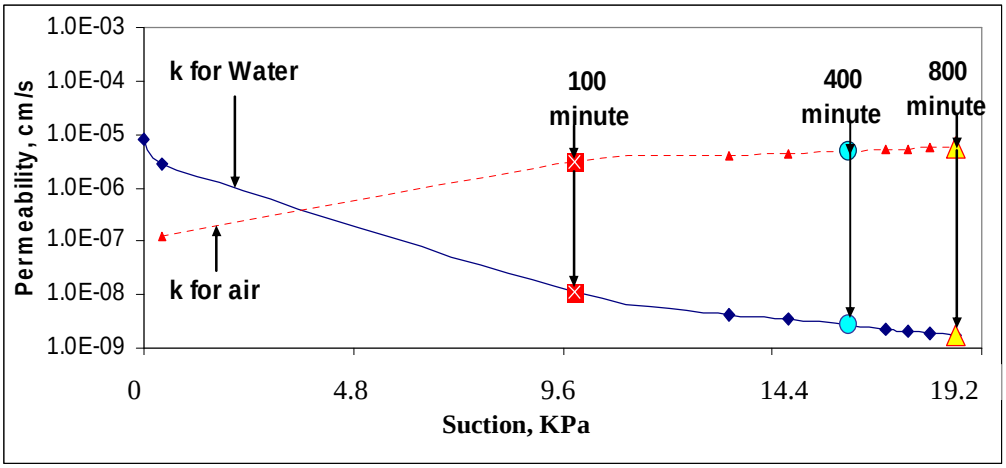

Figure 5-9 Permeability variation with suction at point 4 of Figure 5-8.

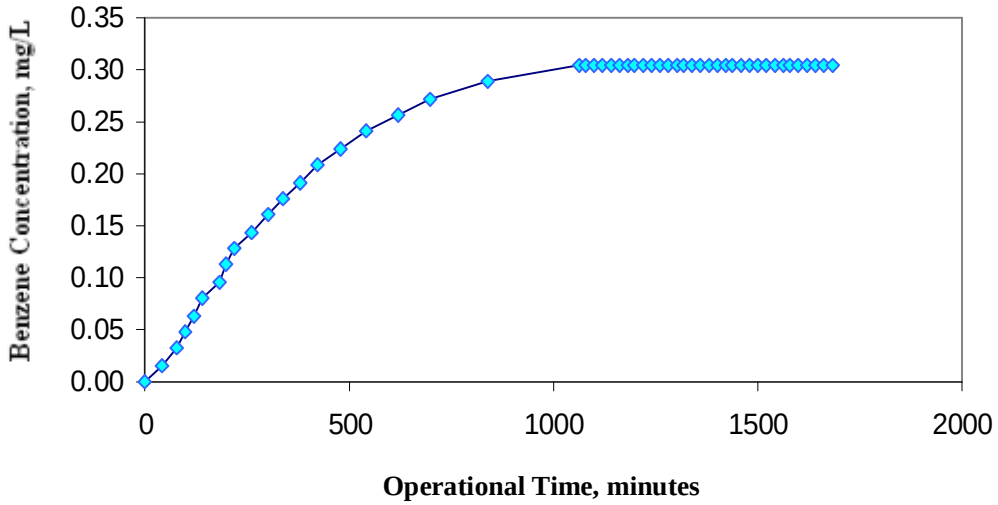

Figure 5-10 Contaminant concentration for 28 h system operation at point 1 (Figure5-7, coordinates (0.3048m, 5.72m)) at the interface of sand and clay layers

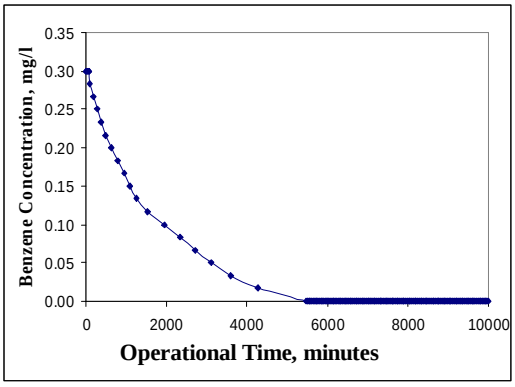

(a) Contaminant Reduction due to 10000 minute (167 h) System Operation at point 2 (Figure 5-8 coordinate (0.9144m, 5.79m (3 ft, 19 ft)))

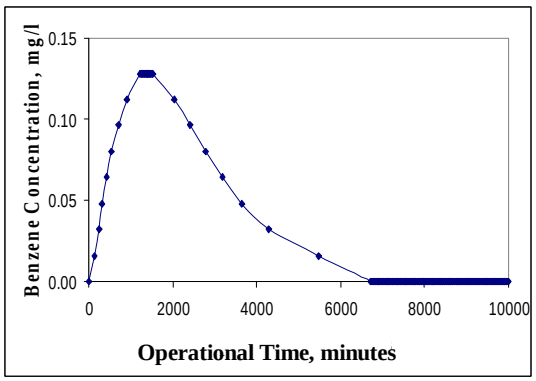

(b) Benzene Concentration at a point (co-ordinate 0.9144m, 5.72m(3ft, 18.75ft)point 3 in Figure 5- 8) in between two wells along the interface of sand and clay layer

Figure 5-11 Benzene movement pattern due to PVWs extraction-only mode operation.

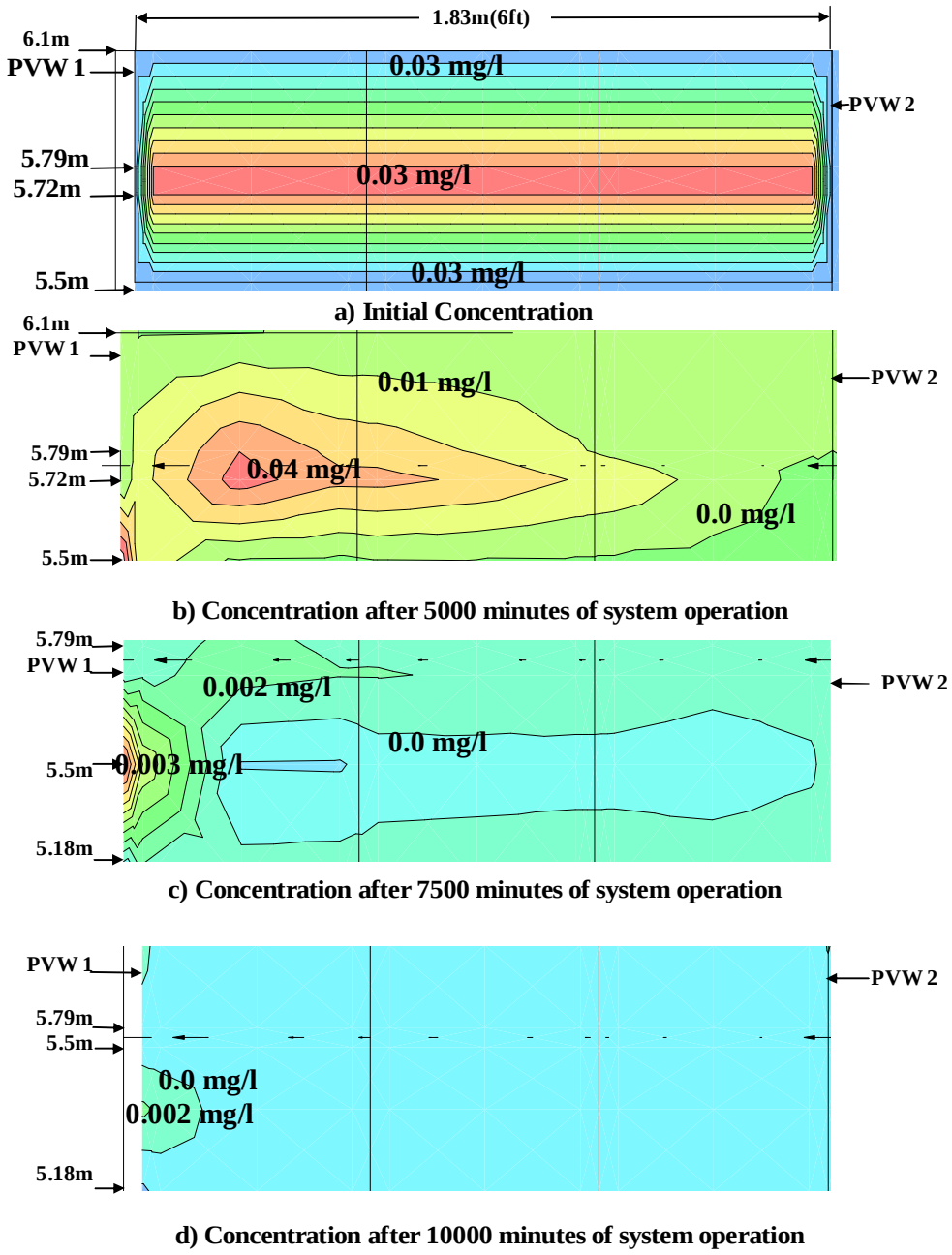

Figure 5-12 Benzene removal contours with increasing operation time.

(Scenario 3: Initial concentration in the hydraulic domain in between 2 PVWs)

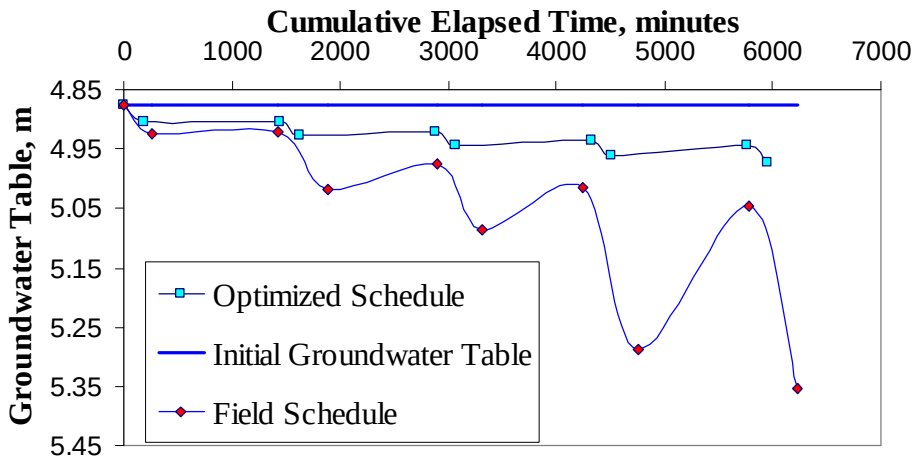

Figure 5-13 Groundwater table variations with optimized and field schedule.

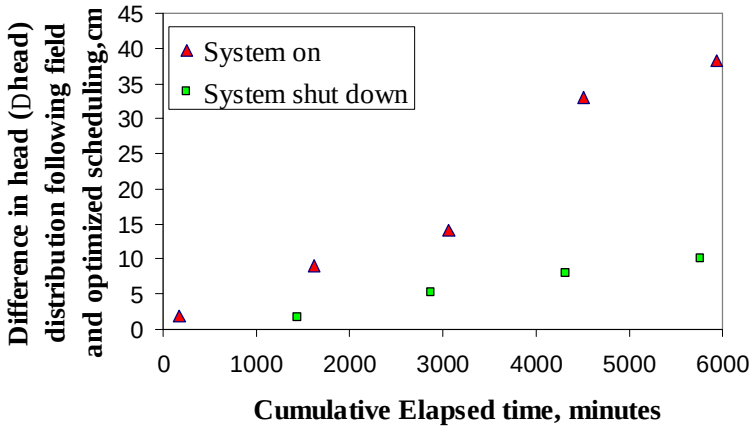

Figure 5-14 Difference in head distribution computed from field schedule and computed from optimized schedule with cumulative elapsed time.

6. OPTIMIZATION OF MULTIPHASE LNAPL RECOVERY USING PREFABRICATED VERTICAL WELLS (PVWS)

Paper to be submitted to the Journal of Soil Contamination

OPTIMIZATION OF MULTIPHASE LNAPL RECOVERY USING PREFABRICATED VERTICAL WELLS (PVWs)

N. Sharmin and M. A. Gabr

ABSTRACT

With the advent of computing power, coupling simulation and optimization algorithms to assess approaches for remediation of sites contaminated with multiphase light non-aqueous phase liquid (LNAPL) is becoming popular. Work in this paper examines optimization analysis of PVWs performance during the extraction of LNAPL in liquid and vapor phases. The focus parameters for optimization are the vacuum level and spatial distribution of the PVWs within the contaminated domain, as well as control of liquid level to the advantage of the remediation scheme. Results indicated that the relationship between the optimized times required for liquid level drop vary linearly with the amount of drop for both constant head and no flow boundary. This is not surprising for the laminar flow conditions. Targeting the free LNAPL removal, using extraction only process, is more effective than the injection-extraction mode as higher water saturation (wetting fluid) leads to lower LNAPL (non wetting fluid) relative permeability and therefore prolonged time to lower the liquid level.

It was observed that liquid level drops faster in the lower permeability zone due to the phase content as a function of pore size for a three phase fluid system. Within the

range of high and low vacuum levels achieved in the field, there is an optimized vacuum which leads to highest extraction rate in the gas phase. It is observed that higher suction than the optimized level traps more LNAPL, since it depresses the LNAPL into a lower level over a larger depth. On the other hand, more LNAPL is trapped and cannot come into contact with air at the lower vacuum level due to higher water flow rates as water passes through NAPL entrapment zone. Analysis the feasibility of optimizing PVWs spacing on the basis of LNAPL free phase extraction mode, and offers an approach for the design of PVWs with focus on PVW placement pattern, effective vacuum magnitude, and time concept of rising and rebounding liquid level to maximizes free phase extraction.

KEYWORDS**:** Air mass, Contaminant Transport, Groundwater profile, LNAPL optimized remediation technology, Optimization, Subsurface model, Vacuum.

INTRODUCTION

Recently, considerable attention has been focused on the use of optimization methods to enhance the study of groundwater remediation approaches by coupling optimization techniques to groundwater flow models (Sayeed et al. 2007, Mahinthakumar et al. 2005, Emch et al. 1998, Yeh 1992, Willis et al. 1988). Cooper et al. (1998) performed analyses in attempt to optimize time-varying (stepwise) pumping rates, while minimizing residual LNAPL volume and maximizing LNAPL recovery. Sawyer et al.

(1998) applied a “mixed-integer” programming model to determine the optimum number of wells, their locations and pumping rates for soil vapor extraction (SVE) by coupling an air flow simulation model (AIR3D) with the General Algebraic Modeling System (GAMS) optimization software. Simulation/optimization (S/O) methods have been applied to aqueous phase and miscible contaminant transport cases (e.g. Yen et al. 2003.) Yen et al. (2003) applied S/O method using BIOSLURP model and LINDO software package to develop optimal pumping schemes for 10 wells with the goal of minimizing groundwater extraction and maximizing oil and air phase extraction in a relatively high permeability soil. Sharmin et al. (2008) used SEEP/W and Matlab optimization tool to develop a systematic pumping schedule for 5 days of operation to lower groundwater table while minimizing groundwater volume extraction.

In terms of LNAPL remediation process, work in this paper involves optimization of operational parameters for multiphase (soluble, gas and free phase) extraction of LNAPL using prefabricated vertical wells (PVWs) installed on close spacing. Specifically the objectives of this paper include the following:

(1) Examining the ability to control liquid level within the subsurface profile under multiphase flow conditions,

(2) Investigating optimum vacuum level for extraction of gas phase, including the impact of permeability, on optimized extraction time and mass.

(3) Developing a technique for specifying PVW spacing, through implementation of optimization approach to target the recovery of a specific LNAPL phase.

OPTIMIZATION OBJECTIVE FUNCTION

The optimization program within the framework of MATLAB is linked to BIOSLURP, a commercially available code that was presented by Katyal et al. (1988) and Yen et al. (2003). The program is developed using finite element approach and provides a tool for continuum analyses of the multiphase flow domain. The optimization modeling utilized MATLAB 7.2 optimization tools (Mathworks 2008). The optimization program is set up to control the decision variables (input to the BIOSLURP), on the basis of the objective function (output of the BIOSLURP). The objectives of the optimization effort are (1) to determine vacuum level for maximum vapor phase mass extraction. Such objective also includes th time at which air circulation should be adopted based on liquid level within the subsurface, (2) to address impact of residual saturation on extraction processes and (3) to investigate the spatial placement of PVWs to maximize the free LNAPL extraction. While it is common that one model is capable of solving all issues or decision variables, the optimization analysis in this study was performed using air and liquid models due to the complex nature of integrating these two phases of flow into a single node within BIOSLURP.

STUDY LIMITIONS

Bioslurping, a remediation technology, that is a combination of bioventing, soil vapor extraction and vacuum-enhanced recovery, is the basis of the multiphase finite element simulator (BIOSLURP, 2004). The program's execution depends on the amount

of LNAPL present, applied vacuum level, and location of wells. On the other hand, the optimization approach is basically the implementation of function with decision rules to achieve a pre-defined objective. In this study, the optimization approach is implemented through several trial runs to meet a specific objective with respect to time, vacuum level, or PVW spatial locations within the area of concern.

One challenging aspects of modeling LNAPL is addressing its entrapment as residual phase in isolated pores. BIOSLURP becomes numerically unstable when LNAPL extraction volume is more than the volume of LNAPL present at the PVW location, irrespective of the specified time. Limitations of BIOSLURP with respect to its use in conducting optimization analysis are as follows:

§ *High pressure application to remove small thickness of oil (LNAPL in this study)*

Katyal et al. (1988) stated that the fluid level elevations, air-oil (P_{ao}) and air-water table (P_{aw}), are related to the product thickness, H_o, as

$$H_o = \frac{P_{ao} - P_{aw}}{1 - RD_{ro}}$$

Equation (1)

Where, RD_{ro}= relative density of LNAPL

$$P_{aw} = Z_{aw} - h_a$$

Equation (2)

and

$$P_{ao} = Z_{ao} - \frac{h_a}{r_o}$$

Equation (3)

Where,

ρ_o= density of oil

Z_{aw} = Air-water interface obtained from monitoring well

Z_{ao} = Air-oil interface obtained from monitoring well

h_a = Equivalent gas phase total head

Comparing Equation 1 to 3, it is clear that very high equivalent gas phase head can lead to negative LNAPL thickness for small Z_{ao} value. In addition, high Z_{aw} and low h_a can lead to negative H_o (equations 1 and 3). In this case, the simulation becomes numerically unstable for the solution of the oil phase flow and distribution. Accordingly, there is a limitation to the magnitude of a vacuum head that can be introduced with LNAPL extraction depth as not to cause a negative H_o.

§ *Boundary Sensitivity*

Constant head boundary cannot be considered in the analyses to optimize the time for lowering the liquid level. The issue is, with the water flow from the constant head boundary being more than the water extraction rate, the water saturation level increases and displaces the non-wetting fluid, which leads to LNAPL trapping. Consequently, no LNAPL will be available to extract. Therefore, in order to model the water rebounding effect, and address air circulation issues after lowering the water table, vacuum head is applied only for vapor phase extraction.

On the other hand, in the case simulating water level rebounding, a no flow boundary condition provides insufficient water to rebound the liquid level in low

permeability soil, thus the simulation becomes non-converging; this case of no-flow boundary was therefore not considered for the rebounding scenario.

§ *Specific volume*

The required input for the flow analyses consists of an initial air-LNAPL and air-water table levels. The program does not consider porosity and irreducible water content in calculating the initial volume of LNAPL. For example, if thickness of LNAPL (H_o) is present in a given area A, and the soil has porosity (n) and irreducible water content (S_{wir}), BIOSLURP calculates the initial volume of oil $V_{BIOSLURP}$= A* H_o and shows thickness of LNAPL in field as H_o. The actual initial volume should be Vactual= A* H_o *(n-S_{wir})=$V_{BIOSLURP}$*(n- S_{wir}) which is less than $V_{BIOSLURP}$. Therefore, the LNAPL-water height needs to be chosen by trial and error, if the goal is to obtain a target LNAPL thickness, and consider the irreducible water content in the analysis.

INPUT PARAMETERS

A model test grid is developed to simulate field testing conditions as shown in Figure 6-1 of this paper. A detailed description of the field testing program is presented in Sharmin et al. 2009. The hydraulic and hydraogeologic parameters and fluid properties are summarized in Table 1. The average groundwater and LNAPL extraction rates are assigned as 125 L/h and 2 L/h, respectively. These values were monitored in the field during the system operation. The field vacuum head ranged between 410 to 310 mm of Hg, based on data from the field vacuum gauges (Sharmin et al. 2009). The vacuum head

was set to 410 mm of Hg for the base case study presented herein.

Liquid Level

In this analysis, the initial LNAPL thickness was set to 0.08 m to match the thickness detected in the field (Sharmin et al. 2008, Sharmin et al. 2009). The optimization analysis is performed for two different models (these will be referred to herein as model 1 and model 2). The objective of model 1 is to establish initial conditions that match field LNAPL thickness of 0.08 m, floating on the groundwater table (liquid level is at 4.88 m from ground surface). Model 1 calculates the initial volume without considering porosity and irreducible water content. The calculated LNAPL volume in this case is thickness*Area of grid=0.08 m*$(2.44)^2$= 453 L.

In Model 2, the objective is to match the initial LNAPL volume, rather than thickness, considering the porosity and irreducible water content (a more realistic representation of site conditions). The liquid level and air-LNAPL/water table levels are the same as in Model 1. However, Model 2 gives LNAPL volume =thickness*Area of grid*(soil porosity-irreducible water content) =0.08 m*$(2.44)^2$*(0.45-0.09)=165 L. For model 2, the impact of porosity and irreducible water content on LNAPL volume is taken into account by changing the monitoring well thickness from 1.44 m to 0.7 m. The consequence of such change is that Model 2 output shows an initial thickness of LNAPL of 1.9 cm which corresponds to the field volume of 165 L, considering porosity and irreducible water content.

Since input parameters for Model 2 lead to a smaller amount of LNAPL, a slight variation of PVW location, or longer run time can make the BIOSLURP simulation numerically unstable. Therefore, Model 1 is used for parametric variation and optimization analysis, while model 2 is used to study applicability of the optimized parameters.

OPTIMIZATION ANALYSES

Optimization analyses seek to investigate aspects related to lowering liquid level within the subsurface profile, vacuum levels, gas phase extraction with rising liquid level, and feasible PVW spatial distribution to maximize free LNAPL extraction. Influence of boundary conditions and permeability are also addressed.

Liquid Level and Air Extraction

An approach to address residual non-aqueous phase saturation is to lower the groundwater level at the site in a sustainable manner, and apply a vacuum head (in the created partially saturated zone) to volatilize residual saturation and extract mass in the vapor phase. The optimization modeling is used to investigate lowering the liquid level by 0.08 m, 0.11 m and 0.15 m at 0.61 m radial distance away from the location of the PVW while maximizing mass removal in gas phase. For this part of analysis, the model grid presented in Figure 6-1 is used, and only one well is assumed in the middle of the grid. With no flow boundary conditions, the analysis assumes repeating units of the grid; the

0.61 m represents half-way distance between the boundary and the extraction well.

The optimization program within the framework of MATLAB, was set up to control the operation times (input to BIOSLURP), on the basis of the head magnitude (output of BIOSLURP). The objective function was to maximize the free product removal in air phase. Time was the only user-specified decision variable. The head distribution at a radial distance of 0.61 m from the PVW (allowing for saturated-unsaturated flow conditions) was checked as the constraint in the optimization program. The constraint of the program is lowering the liquid level by 0.08 m, 0.11 m and 0.15 m respectively. Figure 6-2 presents a summary of the different scenarios of liquid level lowering assessed within the scope of the study.

In addition, the impact of permeability on lowering liquid level is assessed, but only for the no flow boundary case. As mentioned earlier in program limitations, the case of constant head boundary led to numerical instability. A no flow boundary condition is representative of "repeating" PVWs units. The same optimization approach is followed for Model 2 (where a porosity and irreducible water content were considered). The optimization approach is also used to obtain times to raise liquid level to 4.88 m depth (initial level) under applied vacuum head of 410 mm of Mercury. For the scenario of raising the water table, the decision variable is time, and the objective function is to maximize the extracted air mass. The constraint is the liquid level from ground surface should be more than or equal to 4.88 m.

Optimized Vacuum Application

The optimization approach is applied to investigate the vacuum level as a function of extraction duration. Time and vacuum level are the two analysis variables. The optimization approach is run twice for two different objective functions. The first objective function is to maximize the air mass extraction rate. This objective function minimizes the required time (which is one of the decision variable). The second objective function is to maximize the cumulative extracted mass. In both cases, the constraint is having extracted air mass greater than zero. This scenario provides information on system performance when no liquid extraction is being induced, and applied vacuum head is less than depth to liquid level (i.e. air extraction during time of groundwater level recovery when no liquid is being extracted).

Spacing of PVW

Flexibility of specifying PVWs spacing is one of the advantages related to the ease of their installation using direct push technology. The objective of this analysis is to assess the optimum spacing to extract maximum free LNAPL. Targeting the free product would reduce the remediation cost (since free LNAPL acts as a source of continuous contamination). As Newell (1995) stated "Multiple wells pumping water and LNAPL at lower rates may ultimately recover more LNAPL than fewer wells pumping water at higher rates." This means PVWs installed on a spacing leading to lower extraction rate per PVW may increase mobile LNAPL recovery potential. On the other hand, very

closely spaced PVWs can cause significant drawdown in water levels which may not be desirable for recovery of LNAPL in free product form (recovery of LNAPL in free product form is specially desirable when it is recycled to power the extraction system.) Clearly, spacing configuration needs to be practical and economical, and it is one of the most important parameters in implementation of in situ field technology for remediation through wells.

In this analysis, PVWs locations are the decision variables. The optimization program is set up to control the PVW locations (input to the BIOSLURP), on the basis of the head magnitude of liquid and height of air-LNAPL table (output of the BIOSLURP). The objective function is to maximize the free product removal. The hydraulic head distribution and depth of air-LNAPL interface at PVW locations are checked as the constraint in the optimization program. If the difference between air-water table and air-LNAPL level is such that the total extraction rate is less than the extraction rate of a single PVW, a penalty of high value of head, is assigned to make sure that the PVW is located at a point where enough LNAPL exists. Another constraint is to check that two PVW locations are not identical.

The numbers of PVWs are modified in the test grid as shown in Figure 6-1. For PVW spatial optimization, 6 PVWs are randomly assigned to nodes within the grids. The total average groundwater and free LNAPL extraction rates, 125 L/h and 2 L/h respectively, are distributed equally among the six PVWs.

The model grid has 1600 nodes. Therefore, for the first run, the upper and lower

limits for all six PVWs locations are chosen as 1600 and 1 respectively. As mentioned earlier, if no LNAPL exists at a node and a pump is assigned at that node, BIOSLURP becomes numerically unstable and execution stops. Using several trials, and based on the amount of initial LNAPL, the extraction time is chosen as 1.45 h to keep BIOSLURP from experiencing numerical instability. Once the optimized spacing locations for 6 PVWs are determined, the locations of the PVWs are confirmed by running BIOSLURP outside the optimization scheme for a longer time period. If the program fails to execute for a longer time period (i.e. more than 1.45 h, therefore indicating unfeasible filed implementation), the upper and lower limits of the PVW locations are changed, and the optimization process is repeated. Figure 6-3 displays the flow diagram followed to study the optimized spacing.

OPTIMIZATION RESULTS

Lowering Liquid Level

Figure 6-4 shows the impact of boundary conditions on the extraction time for lowering the liquid level by 0.08 m, 0.11 m and 0.15 m at 0.61 m radial distance from the location of the PVW (assuming location in Model 1). Extraction time is higher for the constant head boundary than that of the no flow boundary, given that the same extraction flowrates are used for both (water extraction rate is 125 L/h and LNAPL extraction rate is 2 L/h). The relationship between the optimized times required for liquid level drop vary linearly with the amount of drop for both cases. This is not surprising for the laminar

flow condition given a coefficient of permeability as low as $8x10^{-6}$ cm/s. Figure 6-4 shows a no flow boundary condition requires less time for lowering liquid level than the constant head boundary. The schematic of relative permeability change with water and LNAPL saturation, embedded in Figure 6-5, defines types of multiphase flow regimes that may exist at a particular site. Data in Figure 6-5 shows 30 L and 14 L of trapped LNAPL are obtained for constant head and no flow boundaries, respectively, for the case of lowering the liquid level by 0.15 m. Higher trapped LNAPL (30 L) induces lower flow of LNAPL which leads to a situation represented by Zone III, water flow zone (area with higher water relative permeability but lower relative LNAPL's permeability) as shown in Figure 6-5. Therefore, with a constant head boundary, higher water saturation due to the continuous flow of water from the boundary leads to lower LNAPL relative permeability, and therefore the need for more time to lower the liquid level, as compared to the no flow boundary.

Figure 6-6 shows the impact of permeability on extraction time for lowering the liquid level; no flow boundary condition is assumed and permeability of $8x10^{-6}$ cm/s is used as representative of the field soil (Sharmin et al. 2009). The two other permeability values used in the analyses are $8x10^{-5}$ cm/s and $8x10^{-4}$ cm/s. To lower the liquid level by 0.08 m at a radial distance 0.61 m away from the PVW, the extraction times for permeability of $8x10^{-6}$cm/s, $8x10^{-5}$ cm/s and $8x10^{-4}$ cm/s are 1.23, 55 and 100 h respectively. For one order of magnitude difference in permeability ($8x10^{-6}$ cm/s versus $8x10^{-5}$ cm/s) the extraction time is 45 times higher, where as for the $8x10^{-5}$ cm/s versus

$8x10^{-4}$ cm/s permeability, also a one order of magnitude difference, the extraction time nearly doubles. While this finding sounds counterintuitive, the qualitative phase diagram as a function of pore size for a three-phase fluid system, presented by Charbennau (2000) and inserted in Figure 6-6, may provide an explanation. The insert in Figure 6-6 defines that water flow is dominant in smaller pore sizes, while medium pores are dominated by two-phase flow type (water and oil). A three-phase flow type (water-oil and air) exists in larger pores. Assuming pore size is related to the permeability, then soil represented by permeability of $8x10^{-6}$ cm/s is dominated by water flow as the wetting fluid, while soil represented by $8x10^{-4}$ cm/s is mainly dominated by the flow of the three phases. Accordingly, a longer time is needed to lower the liquid from the soil with $8x10^{-4}$ cm/s permeability as compared to the case of permeability equal to $8x10^{-6}$ cm/s.

Rebounding Liquid Level

Following the same procedure as for Model 1, results for Model 2 configuration show that it takes 1 h for lowering the groundwater table 0.08 cm at a radial distance 0.61 m away from the PVW with a permeability $8x10^{-6}$ cm/s and constant head boundary. At the end of 1 h of liquid extraction, a total of 7.54 gm of hydrocarbon mass is present in the vapor phase. After lowering the groundwater table, simulations are run to assess extraction of hydrocarbon gas phase assuming model 2 conditions. In this case, 410 mm of Mercury vacuum is applied with a gas phase extraction flow rate of 527 m^3/h (based on the field data monitored in the field, Sharmin et al. 2009). Optimization results show that

5.1 h are needed to raise the liquid level to its initial condition (4.88 m from ground surface). In parallel, Figure 6-7 shows the reduction in mass in gaseous and aqueous phases as a function of operational time when liquid level rebounding was taking place. Figure 6-7 shows after 50 h of operation, the total mass in aqueous phase reached a constant value of 20 gm, and the gaseous phase rate of reduction accelerated with the continued vapor extraction (as the mass distribution within the subsurface reached an equilibrium). Data in Figure 6-7 show the vapor phase mass can be extracted in 160 h of continuous operation with rebounding liquid level.

Optimized Vacuum Level

Figure 6-8 shows that highest rate of mass extraction in air phase is obtained for the 276 mm (11 inches) of Mercury (3.8 m H_2O) of vacuum head. Two other vacuums 129 mm and 515 mm of mercury are used to study the impact of the applied vacuum on mass extraction rate. In parallel, and compared to the initial specific volume of 0.08 m, the trapped LNAPL specific volume at a distance 0.61 m away from PVW is found to be 0.0179, 0.0273 and 0.1158 m for 276, 129 and 515 mm Hg of vacuum level, respectively. Higher suction traps more LNAPL, since it depresses the LNAPL into lower levels over larger depth. This leads to redistribution of LNAPL over a larger volume, which leads to reduction in its saturation level. On the other hand, at the lower vacuum level of 129 mm of Hg, LNAPL is trapped due to higher water flow, and wetting fluid , and cannot come into contact with air to induce volatilization. Therefore, in the wide range of high and low

vacuum levels, there is an optimized vacuum which leads to a best extraction rate in gas phase.

PVW Spatial Distribution

Figure 6-9 shows the six PVW locations within the modeled domain as obtained from several optimization runs. The PVWs are organized in triangular (Figure 6-9(a)) and rectangular (Figure 6-9(b)) patterns. From a triangular pattern, the average spacing is 1.23 m and for a rectangular pattern the average spacing 1.12 m. Figure 6-9 shows that PVW "E" falls on "FD line" in the PVWs network. Therefore, the lower limit of PVW "E" is modified and the optimization process is run again. For the revised optimization, Figure 6-10 shows the new position of PVW "E" as "E'" for both triangular ((Figure 6-10 (a)) and rectangular (Figure 6-10(b)) patterns. The final analysis yielded a spacing for the triangular configuration of 1.18 m and for rectangle configuration of 1.12 m. Assuming hundreds of repeating units may be installed in the field for a specific project, more traditional configurations of triangular and rectangular patterns using the optimized spacing, are shown in Figure 6-11(a) and Figure 6-11(b) respectively.

Impact of Spacing

Figure 6-12 presents the extracted volume as a function of spacing for both rectangular and triangular configurations. The total flowrate (125 L/h for groundwater and 2L/h for LNAPL) were distributed equally among four PVWs in rectangular pattern and among three PVWs in triangular pattern. Accordingly, higher flowrate for both

groundwater and LNAPL are assigned to each PVW in the triangular pattern than in the rectangular pattern. Another analysis was performed by assigning flowrate of each PVW in rectangular pattern to each PVW in the triangular pattern.

For comparative results, two more spacing values are chosen (using typical values selected in the past field studies; see Gabr et al. 1999) such that one is higher than the "optimized" one is lower for both rectangular and triangular configuration. For the rectangular pattern, four PVWs with 1.83 m and 0.5 m are simulated. Figure 6-12 shows 1.12 m spacing (optimized spacing) extracts 251 L in 123 h and 1.83 m spacing extracts 220 L in 113 h. The difference of 31 L of free product is in the residual phase, and remains to act as a source of continuous contamination. Using the rectangular pattern, both of 1.12 m and 1.83 m spacings are used for vapor phase extraction at the end of LNAPL removal. In both cases, the extraction airflow rate is 527 m^3/h and the applied vacuum head is 410 mm of Hg (as monitored in the field, Sharmin et al. 2009). On the other hand, in triangular set, PVW with flowrate equal to the rectangular pattern extracts 220 L of LNAPL in 143 h. Despite of same flowrate, for LNAPL and water, assigned to each PVW in both rectangular and triangular set, longer operating time increases higher LNAPL entrapment in the triangular set.

With the smallest spacing of 0.5 m, results indicated that 236 L are extracted in 118 h. In this case, the LNAPL extraction stopped after 118 h because the liquid level dropped below the pump level. The four PVWs installed at 0.5 m spacing cause rapid drawdown over a short period of time. The liquid flow (groundwater+LNAPL) rate

towards PVWs is unable to sustain the rate of extraction. In this analysis, the 1.12 m spacing is the optimum spacing as it provides a balance between the dual phase liquid flow rates in the $8x10^{-6}$ cm/s permeability, for full removal of free phase in a sustainable manner.

Figure 6-13 shows rectangular patterns entrapped 146 L of LNAPL in 123 h whereas triangular pattern entrapped 203 L of LNAPL in 60 h. As the liquid flow is limited by the given permeability of $8x10^{-6}$ cm/s, the rectangular pattern extracts more LNAPL than the triangular pattern even with a lower flowrate per well. One obvious reason is extracting LNAPL from four, versus three, different locations, albeit with a lower extraction rate. But another reason is the lower LNAPL entrapment in the model with rectangular configuration due to lower rate of LNAPL desaturation**.** On the other hand, in triangular set, PVW with flowrate equal to the rectangular pattern entrapped 174 L of LNAPL in 143 h. In addition to longer operating hours, LNAPL entrapment in the triangular set is higher through out the operating time albeit with the same flowrate per PVW in the rectangular set. The reason is the triangular set extracts three-fourth of LNAPL volume extracted in rectangular set in each hour which leaves more LNAPL in the flow domain at the end of each operating hour. The wetting fluid (water) gets in contact with more non-wetting fluid (LNAPL) at the end of each operating hour which entraps more LNAPL.

SUMMARY AND CONCLUSION

Work in this paper aimed at developing a process for optimization of field parameters affecting the performance of Prefabricated Vertical Wells (PVWs) installed on close spacing for the purpose of LNAPL remediation. Two sets of initials conditions with respect to LNAPL volume were utilized in the study. The first initial condition matched field LNAPL thickness of 0.08 m, floating on the groundwater table. In this case, the calculated LNAPL volume is 453 L. The second matched the initial LNAPL volume, rather than thickness, considering the porosity and irreducible water content (a more realistic representation of site conditions). In this case, the LNAPL thickness is 0.019 m corresponding to volume of 165 L. The focus parameters for optimization were the target liquid level for promotion of vapor phase extraction, the vacuum level, and the spatial distribution of the wells. These parameters are the most difficult to specify during a design phase, and are usually specified on the basis of groundwater flow characteristics. Other aspects investigated in the study include effect of boundary conditions and permeability values. Based on the results of this study, the following conclusions are advanced:

i. Analyses results showed that to lower the liquid level by 0.08 m with a constant head boundary, the extraction time is 1.75 h for the case of 453 L LNAPL within the subsurface, and 1 h for the case of 165 L of LNAPL. The relationship between the optimized times required for liquid level drop vary linearly with the amount of drop

for both constant head and no flow boundaries. This is not surprising due to the laminar flow condition given the coefficient of permeability is as low as $8x10^{-6}$ cm/s.

ii. Targeting free LNAPL removal using extraction only process (represented by no flow boundary) is more effective than an injection-extraction mode (represented by constant head boundary.) With a constant head boundary, higher water saturation due to the continuous flow of water (wetting fluid) from the boundary leads to lower LNAPL (non-wetting fluid) relative permeability. Therefore, more time is needed to lower the liquid level, as compared to the case of no flow boundary.

iii. Liquid level drops faster in the lower permeability zone (a case of multiphase flow.) For one order of magnitude difference in permeability ($8x10^{-6}$ cm/s versus $8x10^{-5}$ cm/s) the extraction time was 45 times higher for the higher permeability soil, whereas for the $8x10^{-5}$ cm/s versus $8x10^{-4}$ cm/s permeability (still one order of magnitude difference), the extraction time nearly doubled for the higher permeability soil. While this finding is counter intuitive, it may be explained by phase content as a function of pore size for a three-phase fluid system, as presented by Charbennau (2000). It is hypothesized that water flow is dominant in smaller pore sizes, two-phase (water and oil) flow is dominant in medium size pores, and the three-phase flow (water-oil and air) exist in larger pores. Assuming pore size is related to the permeability value; results indicated that in $8x10^{-6}$ cm/s case flow is dominated by water as the wetting fluid, while the $8x10^{-4}$ cm/s case is mainly

dominated by the flow of three phases. Therefore a longer time is needed to lower the two-phase liquid in the soil with $8x10^{-4}$ cm/s permeability.

iv. In the range of high and low vacuum levels achieved in the field, there is an optimized vacuum level which leads to highest extraction rate in the gas phase. In this study this value is 276 mm Hg (~3.8 m H_2O). Higher suction traps more LNAPL, since it depresses the LNAPL into a lower level over a larger depth. This leads to redistribution of LNAPL over larger volume, which in turn leads to reduction in its saturation level. On the other hand, lower vacuum level allows higher water flow rates. As water passes through NAPL entrapment zone, more LNAPL is trapped and cannot come into contact with air.

v. Analysis showed that 1.12 m is the optimum spacing for rectangular placement of PVWs, and 1.18 m is the optimum for triangular placement, in order to extract maximum mass of LNAPL. Rectangular configuration was the more effective of the two and it was evident that lower flow rates with more wells leads to lower LNAPL entrapment, and higher free LNAPL extraction.

This paper offers an approach for the design of PVWs with focus on PVWs placement pattern, effective vacuum magnitude, and with the concept of lowering and rebounding liquid level to maximize LNAPL extraction rather than a design based merely on groundwater flow analysis. However, a typical run for one of the analysis cases varied between approximately 7 h (liquid level control) to 14 h (PVW spatial placement). The scope of this paper shows that incorporation of optimization method not only requires that

integration of simulation and optimization algorithms in a computing-intensive environment, but also the availability of a cyber infrastructure where computations can be achieved expediently.

ACKNOWLEDGEMENTS

Dr. Kumar Mahinthakumar, professor of North Carolina State University, helped to develop the optimization approach. His knowledge of the subject and contributions to the work are greatly appreciated.

REFERENCES

BIOSLURP. (2004). *Technical documentation and user guide*. Resources and System International, Inc. Blacksburg, VA.

Cooper, G. S. Jr., Peralta, R. C., Kaluarachchi, J. J. (1998). "Optimizing separate phase light hydrocarbon recovery from contaminated unconfined aquifers**"**. *Advances in Water Resources*. 21(5) (April):339-350.

Emch, P. G., Yeh, W. G. (1998). ''Management model for conjunctive use of coastal surface water and groundwater''. Journal of Water Resources. Planning and Management. 124 (3):129–139.

Gabr, M. A., Sabodish, M., Williamson, A., and Bowders, J. J. (1999). "BTEX extraction from clay soil using prefabricated vertical drains". *Journal of Geotechnical and Geoenvironmental Engineering*. 125(7). 615–618.

Katyal, A.K., and King, L. G. (1988). "Three dimensional upstream finite element model for reactive solute transport in variably saturated porous media." *International Summer Meeting of ASAE*.

Mahinthakumar, G.; Sayeed, M. (2005). “Hybrid genetic algorithm - Local search methods for solving groundwater source identification inverse problems.” *Journal of Water Resources Planning and Management*. v 131(1):45-57

“Petroleum contaminated soil.” <http://www.com.state.oh.us/SFM/pub/bust_1301_7-9-16.pdf> (Dec. 5, 2007).

Sawyer, C. S., Kamakoti, M. (1998). “Optimal flow rates and well locations for soil vapor extraction design”. *Journal of Contaminant Hydrology.* 32(1-2)(July):63-76.

Sharmin, N., Kunberger, T., Gabr, M. A., Quaranta, J. D., Bowders, J. J.(2008). “Performance modeling and optimization of contaminant extraction using prefabricated vertical wells (PVWs)”. *Journal of Geosynthetic International.* 15(3):205-215.

Sharmin, N.; Gabr, M. A. & Quaranta, J. D. (2009). “Multiphase extraction of Light Non-Aqueous Phase Liquid (LNAPL) using Prefabricated Vertical Wells**”.** To be submitted.

Sharmin, N., Gabr, M. A. (2010). “Parameters affecting multiphase LNAPL recovery using WIDE.” To be submitted.

Sayeed, M., Mahinthakumar, K.; Karonis, N. T. (2007). “GRID-enabled solution of groundwater inverse problems on the TeraGrid network.” Simulation. 83(6): 437-448

Willis, R., Finney, B. A. (1988). ‘‘Planning model for optimal control of saltwater intrusion.’’ *Journal of Water Resources. Planning and Management. Journal of Water Resources. Planning and Management.* 114(2): 163–178.

Williams, D.E., and Wilder, D.G. (1971). “Gasoline pollution of a ground-water reservoir - A case history”. *Ground Water*. 9(6):50-54.

Yeh, W. G. (1992). ‘‘Systems analysis in ground-water planning and management.’’ *Journal of Water Resources. Planning and Management.* 118 (3): 224–237.

Yen, H. Y., Chang, N. B. (2003). ‘‘Using the bioslurping model to assess the light hydrocarbon recovery in contaminated unconfined aquifer. I: Simulation analysis.’’ *Practice Periodical of Hazardous, Toxic, and Radioactive Waste Management.* 7(2) (April):114-130.

Yen, H. Y., Chang, N. B. (2003). ‘‘Using the bioslurping model to assess the light hydrocarbon recovery in contaminated unconfined aquifer. II: Optimization analysis.’’

Practice Periodical of Hazardous, Toxic, and Radioactive Waste Management. 7(2) (April):131-138.

Table 6-1 Summary of Model Grid Input Parameters

(Sharmin et al. 2010)

Liquid surface depth (from ground surface)	4.88 m
Soil type	Gray/brown silty sand (SM)
Water content, %	22.8
Permeability, cm/s	8×10^{-6}
Specific gravity, Gs	2.73
Density of JP-4 (jet fuel or LNAPL)	800 kg/m^3
Density of air (20°C)	1.2 kg/m^3
Free LNAPL-to-water dynamic viscosity ratio, h**ro**	0.9
Surface tension of water, σ_w	.072 N/m
Air-free JP-4 surface tension, s_o	0.025 N/m
LNAPL-water interfacial surface tension, s_{ow}	.053 N/m
Air-to-water dynamic viscosity ratio	0.018
Henry's coefficient	0.24
Distribution coefficient for benzene,	0.83 cc/gm
Diffusion coefficient of benzene in water	0.0001 m^2/d
Diffusion coefficient of benzene in air	0.76 m^2/d

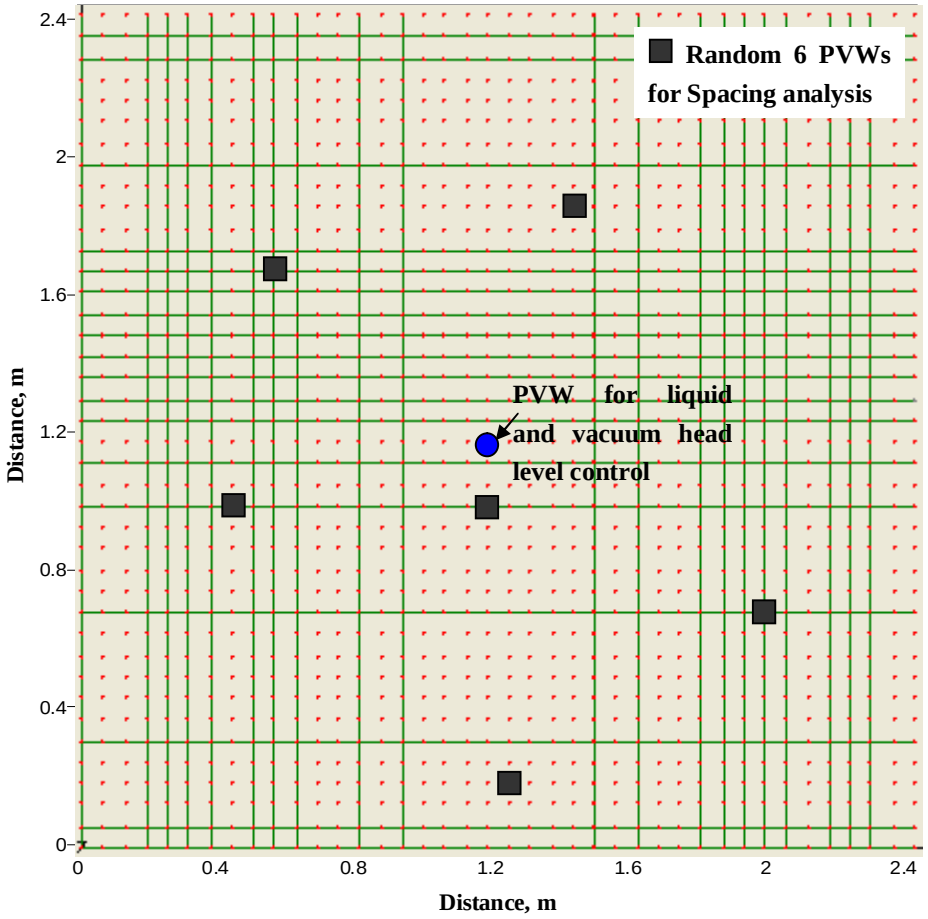

Figure 6-1 Discretized grid.

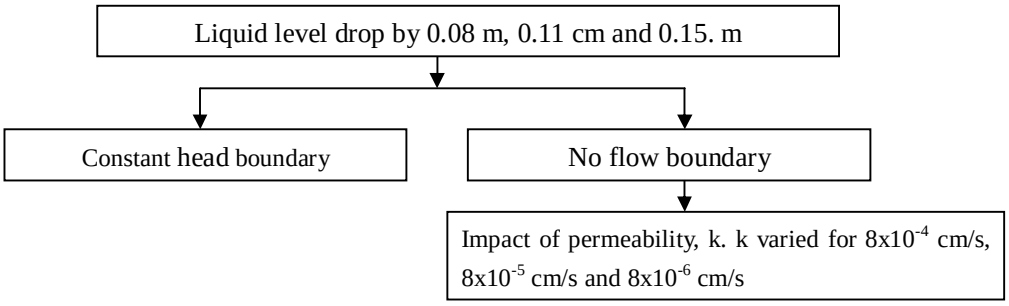

Figure 6-2 Flow chart showing the aspects addressed in lowering liquid level.

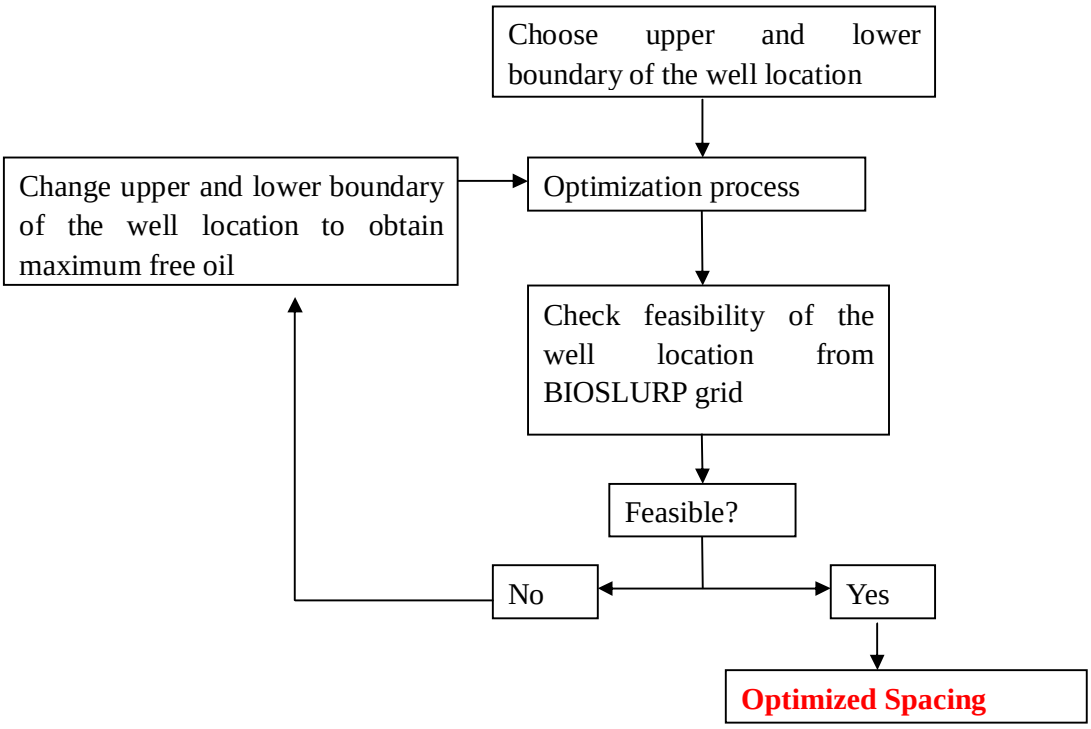

Figure 6-3 Process flow diagrams to determine optimized spacing combining optimization and trial-error process.

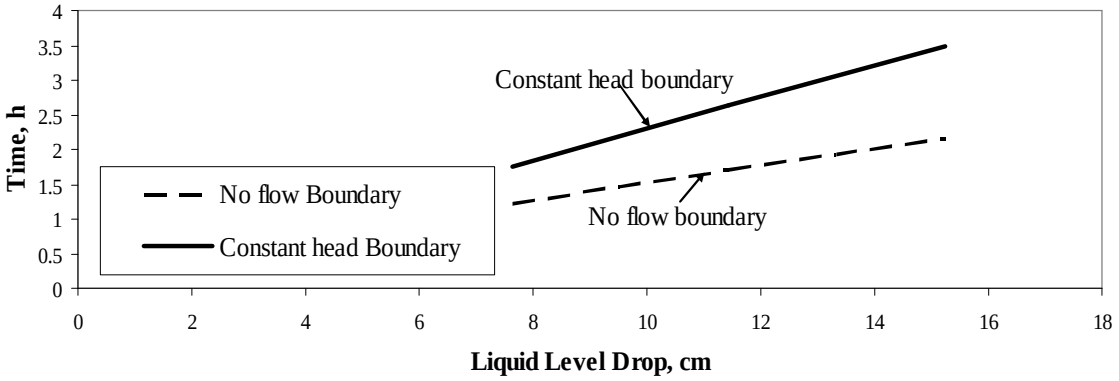

Figure 6-4 Impact of boundary condition on lowering liquid level.

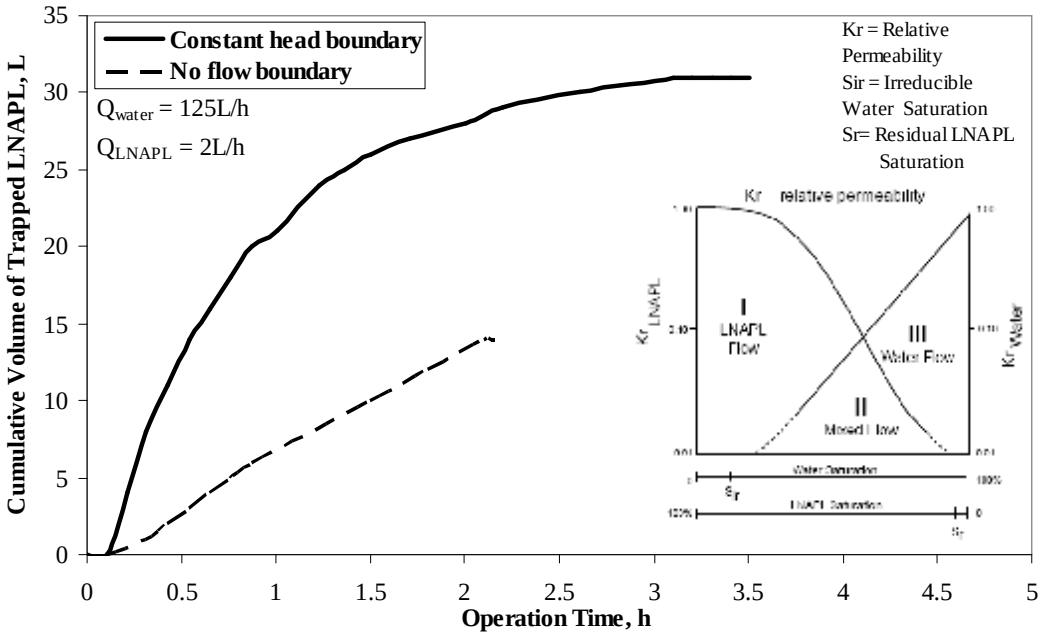

Figure 6-5 Impact of variation of boundary condition for lowering liquid level by 0.15 m (Inset Figure: Hypothetical Relative Permeability (Newell, et al. 1995 Williams et al., 1971).

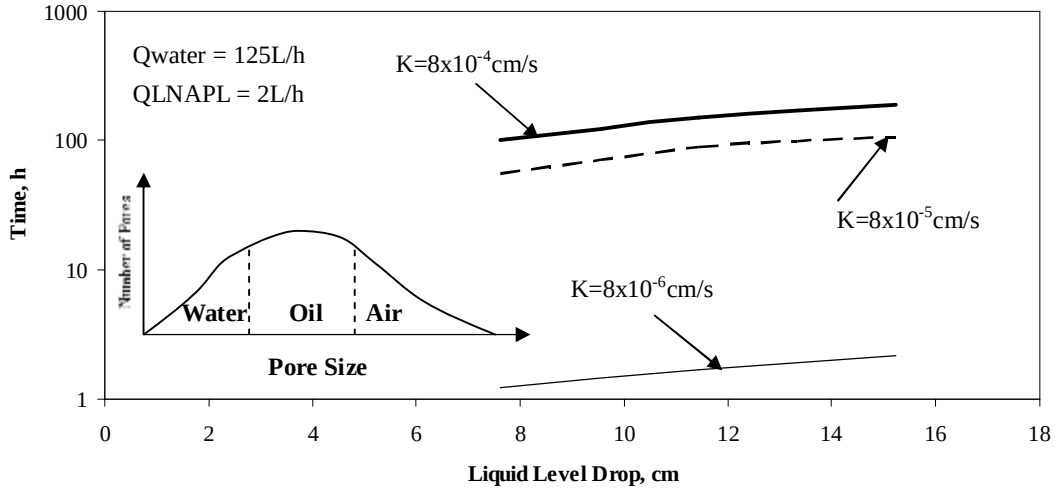

Figure 6-6 Impact of permeability on extraction time (No flow boundary) (Inset Figure: Phase content as a function of pore size for a three phase fluid system (Charbennau 2000)).

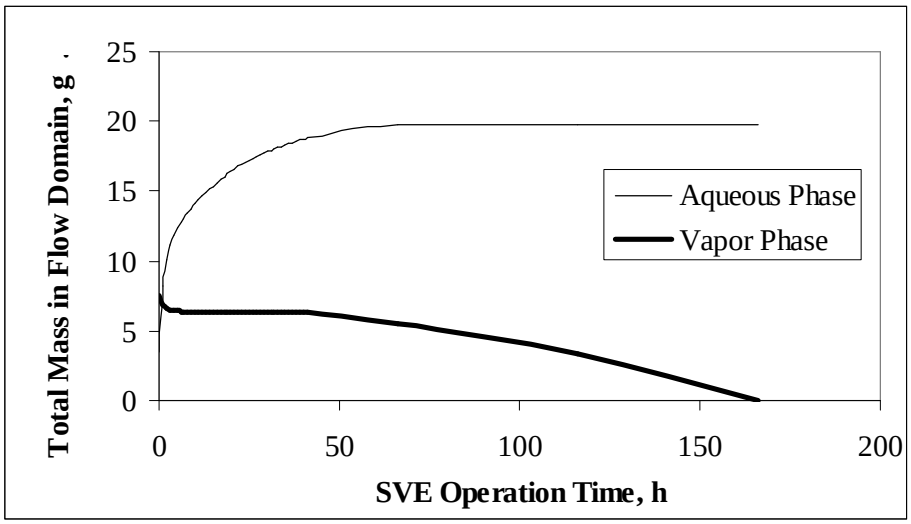

Figure 6-7 Available mass in vapor phase at flow domain (constant head boundary and Vacuum=410 mm of Mercury).

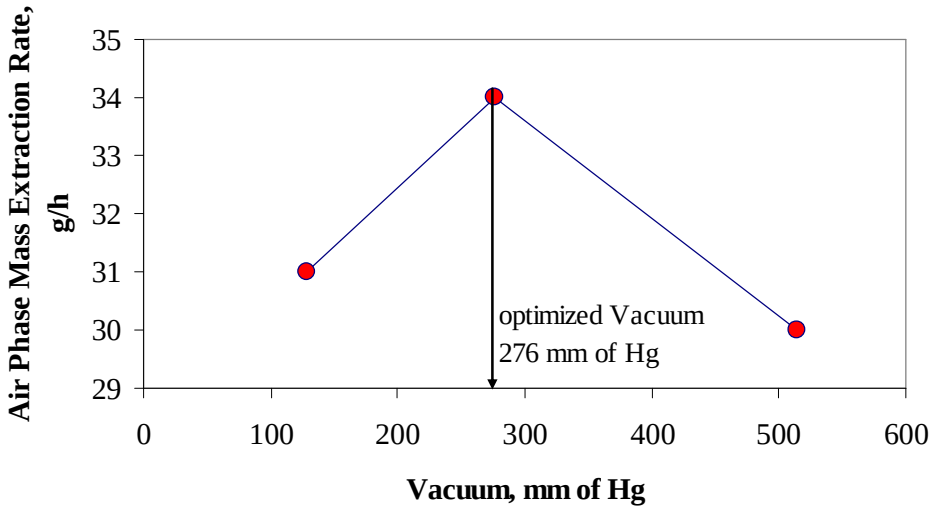

Figure 6-8 Optimized applied vacuum to maximize the air phase mass extraction rate.

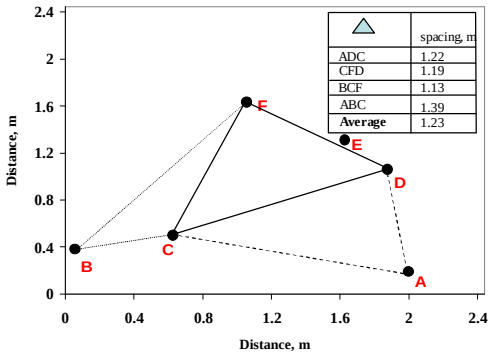

(a) Triangular

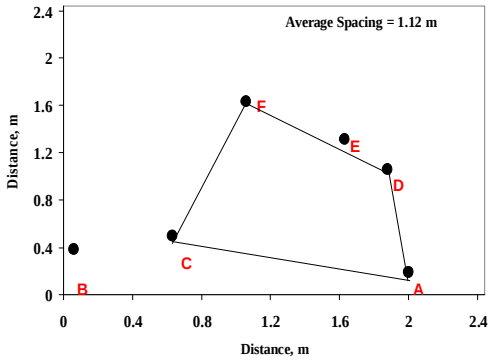

(b) Rectangular

Figure 6-9 PVW Locations (●) _Step-1.

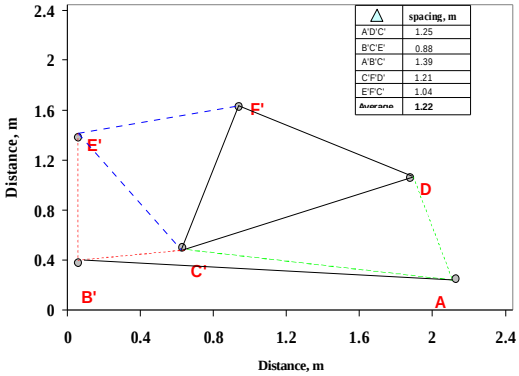

(a) Triangular

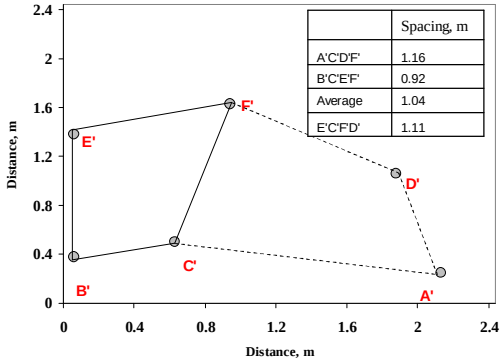

(b) Rectangular

Figure 6-10 PVW locations (⬢) _Step-2.

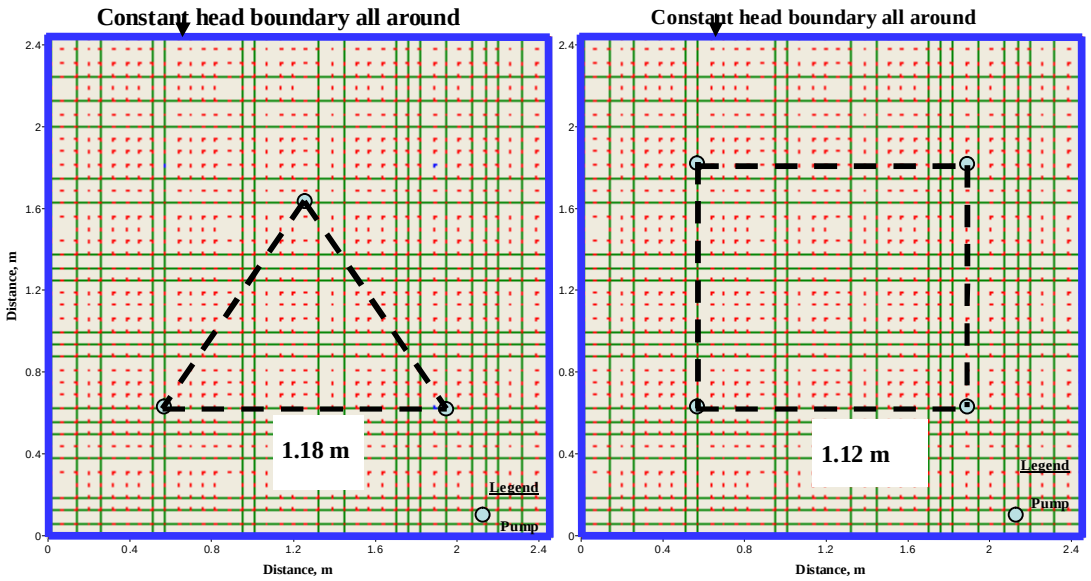

(a) Triangular **(b) Rectangular**

Figure 6-11 PVW locations in grid Step-3.

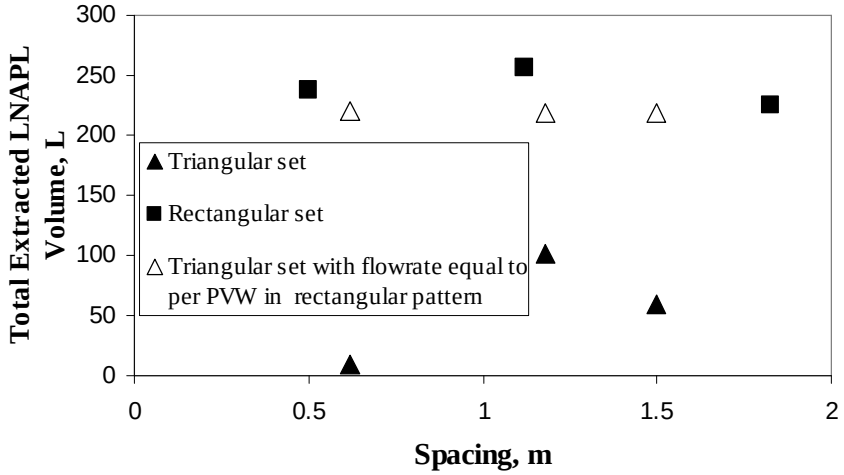

Figure 6-12 Impact of spacing on the extracted volume of oil

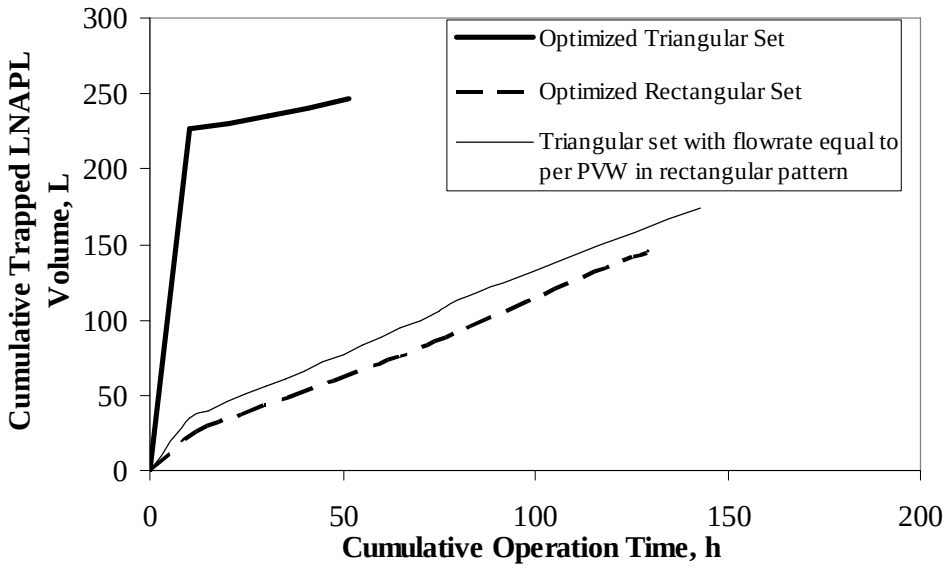

Figure 6-13 Impact of PVW placements on the LNAPL trapping with operation.

7. SUMMARY AND CONCLUSION

SUMMARY

Work in this study is performed to investigate aspects related to LNAPL extraction mechanism using prefabricated vertical wells (PVWs) installed on a relatively close spacing. The study approach encompassed field-experiments and numerical analyses. The field study, the first to report on the use of prefabricated vertical wells for extraction of LNAPL, provided data on the extraction rates in liquid, soluble, and gas phases. The field data were also used to calibrate input parameters for the numerical models. The numerical analyses investigated aspects related to optimized schedule to lower groundwater level to promote volatilization, affect of hydraulic conductivity and residual LNAPL saturation on phase extraction, and case optimization of PVWs' spatial configuration and vacuum levels to target multiphase removal.

The field demonstration was conducted at the former Lockbourne Air Force Base, currently known as the Rickenbacker International Airport (RIA). The site soils are characterized as glacial till with shale fragments, clay, silt, and sand with locally isolated lenses of silty sand. The installed test area measured 12.8 m by 43.9 m, and consisted of 25 rows – each encompassing 7 or 8 PVWs (Prefabricated Vertical Wells), and 16990 L/m air compressor powering a 5.08 cm diameter eductor vacuum system. The PVWs are operated in dual-phase extraction (DPE) mode to remove various combinations of free-phase petroleum product, hydrocarbon vapors, and contaminated groundwater.

Numerical modeling was utilized for the analysis of system performance at the test site. The modeling study consisted of from parts: i) groundwater modeling, ii) soluble phase transport modeling, iii) multiphase flow and transport modeling and iv) optimization scheme to study scenarios associated with system performance. The computer programs used in this study are SEEP/W and CTRAN/W by Geo-Slope and BIOSLURP by Resources and System International, Inc. Groundwater modeling is used to assess hydraulic head distributions and changes in saturation front. Soluble phase transport modeling was used to study contaminant movement due to the extraction operation with a focus on the impact of the silty sand lens of the subsurface on the extraction scenarios of the soluble phase.

Multiphase transport modeling was performed to provide an analysis of the extraction process in liquid, gas, and soluble phases, and investigate the effect of key parameters (hydraulic conductivity and LNAPL saturation) on multiphase removal. The model was calibrated using field data.

An optimization process was linked to the numerical groundwater and transport model to investigate a possible configuration of PVWs to target LNAPL removal. The optimization program, within the framework of MATLAB, was used to control the decision variables (input to the simulated model by both SEEP/W and BIOSLURP), on the basis of an objective function (output of the simulated model by both SEEP/W and BIOSLURP). The optimization process yielded results on demonstrating the development of an operating schedule to control groundwater elevations, and therefore the efficient

removal of volatile contaminant phase. In addition, the optimization analysis of the multiphase LNAPL was used to study the air and LNAPL phase extraction, and investigate an optimum well spacing.

CONCLUSIONS

Based on the filed and model properties, used in this study and associated results, the following conclusions are advanced:

1. The main contribution from the field study is documenting the performance of LNAPL extraction using PVWs.
    i) Over 185 operating h, a total of 133 L of free JP-4 was removed from the subsurface in conjunction with 467 kg of organics in the vapor phase as volatilization took place due to the application of vacuum heads range from 310 to 410 mm of Hg. This mass is equivalent to LNAPL volume of approximately 567 L (150 gal).
    ii) The average LNAPL extraction rate -was 0.72 L/h, and the average extracted mass in the gas phase was 2.54 kg/h.
    iii) When free LNAPL was present, it was usually indicated by relatively high photo-ionization detector (PID) readings (approximately >500 ppmv), but typically within one to two h the PID readings are significantly reduced.

iv) In general, the higher liquid removal rates were achieved when the groundwater table was elevated. The average extraction rates varied between 75 L/h and 285 L/h.

2. Multiphase modeling provides an explanation of phase extraction as a function of key parameters, and impact of those parameters on residual saturation.

   i. Calibration of multiphase model indicated the importance of selecting the value, describing the contaminant load from a hydrocarbon source to the mobile phase (H_{ga}) and the contaminant load from a hydrocarbon source to the gas phase $(H_{\partial a})$, when equilibrium is not reached. Specifying H_{ga} = 0.331 1/m yielded benzene concentration in water of 0.3 mg/l in soluble phase, as was measured in the field. Similarly specifying $H_{\partial a}$=7.45 1/m, yielded benzene concentration was 1.6 mg/L in extracted vapor after 0.5 h of run time (similar to what was measured in the field). Other than matching with field data, guidelines for selecting these values needs to be developed in literature.

   ii. Analysis with different boundary conditions presents an argument against injection/extraction operational mode if LNAPL recovery is the primary focus from low permeability soil. Continuous flow in constant head boundary induces more wetting fluid (water) which

entraps the non-wetting fluid (LNAPL) in the soil pores. The surplus of wetting fluid reduces the mobility of non-wetting fluid which eventually reduces the LNAPL recovery.

iii. For a given soil type, results indicated that LNAPL removal percentage is not dependent on the water to LNAPL extraction rates as long as free LNAPL exists in the subsurface. Assuming various hydraulic characteristics (i.e. various soil permeability characteristic curves) the ratio of water to LNAPL extraction flowrate was varied from 100 to 1 keeping the LNAPL extraction rate at 0.285 L/h for all types of soil. The LNAPL percent removal rate varied from 65% to 20% due to the variability of entrapped mass as hydraulic conductivity and porosity varied with porosity.

iv. LNAPL removal efficiency was dependent on soil type (for the 4 soil types considered in this study). Assuming no flow boundary and for LNAPL thickness of 0.08 m, 65% of the LNAPL was recoverable in sand (hydraulic conductivity 8.25×10^{-3} cm/s) where as the for the field soil (silty sand hydraulic conductivity 8×10^{-6} cm/s) the recovery rate was merely 20%. This signifies the important role of saturation.

v. The magnitude of irreducible LNAPL content has significant influence on the extraction efficiency. Increasing irreducible

LNAPL from 5% to 20% decreases the percent removal from 52 to 0.2% for 0.08 m LNAPL assuming constant head boundary condition.

vi. The magnitude of initial LNAPL thickness presents in the field is influenced by the irreducible LNAPL of the soil pores. For field soil, analysis results also show that increasing irreducible water content from 5% to 20% decreases the free oil thickness from 0.08 m to 0.067 m which eventually reduces removal efficiency from 20 to 10% assuming no flow boundary condition

vii. For the same soil type, lower initial LNAPL thickness decreases LNAPL removal efficiency. Results showed that the reduction of initial actual LNAPL thickness from 0.08 to 0.03 m decreased the free LNAPL removal from 65 to 35% for sand.

viii. The sensitivity analyses to evaluate the contaminant transport concentration, in both water and air, as a function of loading from hydrocarbon to water and air shows a linear relationship of the soluble and gaseous phase with the variation of respective load from hydrocarbon parameters. Assessment of hydrocarbon loading values with time is needed. A more robust analysis model should allow specifying these two parameters as a function of time for better representation of transfer kinetics.

ix. Results from BIOSLURP multiphase modeling showed that the concentration in the vapor phase at the location of the pad based on the 1.83 m of PVW spacing is below regulated thresholds values after 2.5 years of extraction. The results of the model indicate that the soluble phase in the groundwater at the end of 4.25 years of system operation is at or below 0.005 ppm.

3. Soluble phase modeling scheme establishes an approach for assessing scenarios for clean-up times in lenticular morphology.
    i. The findings of transport under transient conditions are important to understand system performance with respect to clean up times once the source has been removed.
    ii. For PVWs installed on 1.83 m spacing, results from soluble phase modeling showed that, with system extraction, a constant source concentration of 0.3mg/L leaking to the groundwater within the sand lens reached the level of the source concentration after 1060 minutes (18 h) of extraction time.
    iii. Analyses also revealed that 4300 minutes (71 h) were required to remove benzene's soluble phase once the source, 0.3 mg/L initial pulse concentration of benzene at top of groundwater table, ceased to exist.

iv. In addition, 7,500 minutes (125 h) of continuous system operation were needed to lower 0.3 mg/L of initial benzene concentrations to less than 0.005mg/L within the flow domain of 1.83 m, once the source ceased to exist.

4. Optimization analyses presents framework for developing operational parameters of active remediation, and specifying spatial configuration of PVWs location.
    i. Optimization results demonstrated the ability to develop operation scheme in the field to lower the groundwater table within a specific zone. In this study, groundwater was lowered by 0.08 m (3 inches) using a 3-h on, 21-h off operating schedule across the active flow domain, based on the 1.83 m spacing. In a field setting, this operational schedule is translated into the operation of 3 lines/d assuming 8-h work days.
    ii. Optimization results demonstrated the ability to control the liquid level (a case of multiphase flow) within a specific zone. Analyses results showed that to lower the liquid level by 0.08 m with a constant head boundary, the extraction time is 1.75 h for the case of 453 L LNAPL within the subsurface, and 1 h for the case of 165 L of LNAPL. The relationship between the optimized times required for liquid level drop vary linearly with the amount of drop for both

constant head and no flow boundaries. This is not surprising due to the laminar flow condition given the coefficient of permeability is as low as $8x10^{-6}$ cm/s.

iii. Targeting free LNAPL removal using extraction only process (represented by no flow boundary) is more effective than an injection-extraction mode (represented by constant head boundary.) With a constant head boundary, higher water saturation due to the continuous flow of water (wetting fluid) from the boundary leads to lower LNAPL (non-wetting fluid) relative permeability. Therefore, more time is needed to lower the liquid level, as compared to the case of no flow boundary.

iv. Liquid level drops faster in the lower permeability zone (a case of multiphase flow.) For one order of magnitude difference in permeability ($8x10^{-6}$ cm/s versus $8x10^{-5}$ cm/s) the extraction time was 45 times higher for the higher permeability soil, whereas for the $8x10^{-5}$ cm/s versus $8x10^{-4}$ cm/s permeability (still one order of magnitude difference), the extraction time nearly doubled for the higher permeability soil. While this finding is counter intuitive, it may be explained by phase content as a function of pore size for a three-phase fluid system, as presented by Charbennau (2000). It is hypothesized that water flow is dominant in smaller pore sizes,

two-phase (water and oil) flow is dominant in medium size pores, and the three-phase flow (water-oil and air) exist in larger pores. Assuming pore size is related to the permeability value; results indicated that in $8x10^{-6}$ cm/s case flow is dominated by water as the wetting fluid, while the $8x10^{-4}$ cm/s case is mainly dominated by the flow of three phases. Therefore a longer time is needed to lower the two-phase liquid in the soil with $8x10^{-4}$ cm/s permeability.

v. In the range of high and low vacuum levels achieved in the field, there is an optimized vacuum level which leads to highest extraction rate in the gas phase. In this study this value is 276 mm Hg (~3.8 m H_2O). Higher suction traps more LNAPL, since it depresses the LNAPL into a lower level over a larger depth. This leads to redistribution of LNAPL over larger volume, which in turn leads to reduction in its saturation level. On the other hand, lower vacuum level allows higher water flow rates. As water passes through NAPL entrapment zone, more LNAPL is trapped and cannot come into contact with air.

vi. Analysis showed that 1.12 m is the optimum spacing for rectangular placement of PVWs, and 1.18 m is the optimum for triangular placement, in order to extract maximum mass of LNAPL. Rectangular configuration was the more effective of the

two and it was evident that lower flow rates with more wells leads to lower LNAPL entrapment, and higher free LNAPL extraction.

CONTRIBUTIONS TO THE STATE OF THE ART

The following contributions are imparted based on the performed research. The contributions to the state of art are discussed on the basis of field performance, numerical and optimization modeling results. These are:

1. The field demonstration presented first documented case of PVWs installed for multiphase LNAPL removal. The field demonstration provided field performance data to assess screening of the future WIDE system design, implementation and performance measures at a similar site.
2. This research approach provides insight for initial screening of WIDE effectiveness to remediate LNAPL multi-phases in terms of soil hydrogeologic parameters. The model study provides an explanation of phase extraction as a function of hydro-gelogic key parameters, and impact of those parameters on multiphase LNAPL removal efficiency in low permeability subsurface environment.
3. This research addresses lenticular morphology. This study explores the groundwater control scheme to address lenticular morphology in terms of

addressing disconnected thin layers that may serve as conduit for contaminant migration.

4. Optimization linked modeling of PVWs installed on close spacing demonstrated the possibility of setting system operation schedule and achieving regulatory limits for any single/multi phase contaminant. The modeling approach involved in this study demonstrated the capability of a) controlled lowering/raising groundwater table, b) developing pumping schedule to maximize WIDE efficiency in multiphase LNAPL removal and c) understanding favorable operational parameters in terms of vacuum levels for the gas mass extraction through system optimization.
5. A combination of optimization and physical modeling demonstrated the possibility of development of spatial configuration of PVWs based on performance matrices. Results from this study are the first to document specification of spatial distribution based on multiphase extraction rate rather than based on merely groundwater extraction rates.

DIRECTIONS TO FUTURE RESEARCH

Subsurface contamination with immiscible petroleum hydrocarbon products presents a formidable challenge to the nation and the world. Among others, sources of contamination include leaking underground pipelines, underground storage tanks, and

non-point source spills. The interest in remediation of contaminated land has increased with the introduction of programs such as brown field revitalization by EPA, and Base Closure and Realignment (BRAC) by the Department of Defense. Field work in this thesis was focused on advancing the state of art for remediation of LNAPL in soils with low hydraulic conductivity. Generally, advancement of the state of the art in this area requires the implementation of field testing to obtain representative performance data since laboratory studies often have scale limitations. Even then, the field testing also suffers from limited operational period to reach end points of remediation. Based on work performed in this thesis, the following recommendations for future studies are advanced:

i. Laboratory columns studies need to be performed to assess critical key transfer parameters under partially saturated conditions. These are the transfer coefficients depicting contaminant load from a hydrocarbon source into the gas phase, and soluble phase, respectively. Using various soil composition, but with emphasis on percent clay content and clay mineralogy, these parameters need to be evaluated considering factors such as air-oil capillary pressure, and oil-water interfacial surface tension.

ii. Given the limitation of time duration of field testing, limited mass-transfer rates may not be captured by the field data. Expanded modeling, coupled with laboratory experimental program is needed to investigate the residual LNAPL saturation with the cyclic dewatering/ recharge that occurs with the operation of the extraction system. It was observed in the field that LNAPL is extracted

in its free phase after a period of shutdown where the groundwater was allowed to recover. As such data from a further study is needed to provide information on hysteresis behavior between capillary pressure and LNAPL saturation.

iii. The work presented in the thesis showed an advantage of an optimization scheme to target the free phase of LNAPL. Unfortunately, it was not possible to implement the findings from the model study in the field due to timing constraints. A future study can be to optimize spatial configuration of the prefabricated vertical wells to target a specific phase of contamination (given site and contaminant parameters) and then implement the findings in the field to investigate the extent of successful implementation. This is an important issue since, as was the case in this study, the main concern is the removal of the source, for expedient development of property.

iv. One larger issue to consider is the availability of a comprehensive numerical model to represent subsurface conditions with accuracy. Such model is not commercially available. Such a model will need to be based on unsaturated flow, capable of accommodating layered subsurface strata, has provisions for multiphase flow, including free phase, has provisions for application of vacuum head to induce both air and liquid flow, and also has a 3-D capability to account of areal and depth variations. It may be rather ambitious to strive toward the development of such numerical simulator, but incremental progress

toward such a goal is important, especially starting with the understanding the interaction of air and multiphase liquid flow under applied vacuum pressures.

APPENDICES

APPENDIX A. FIELD CHARACTERIZATION

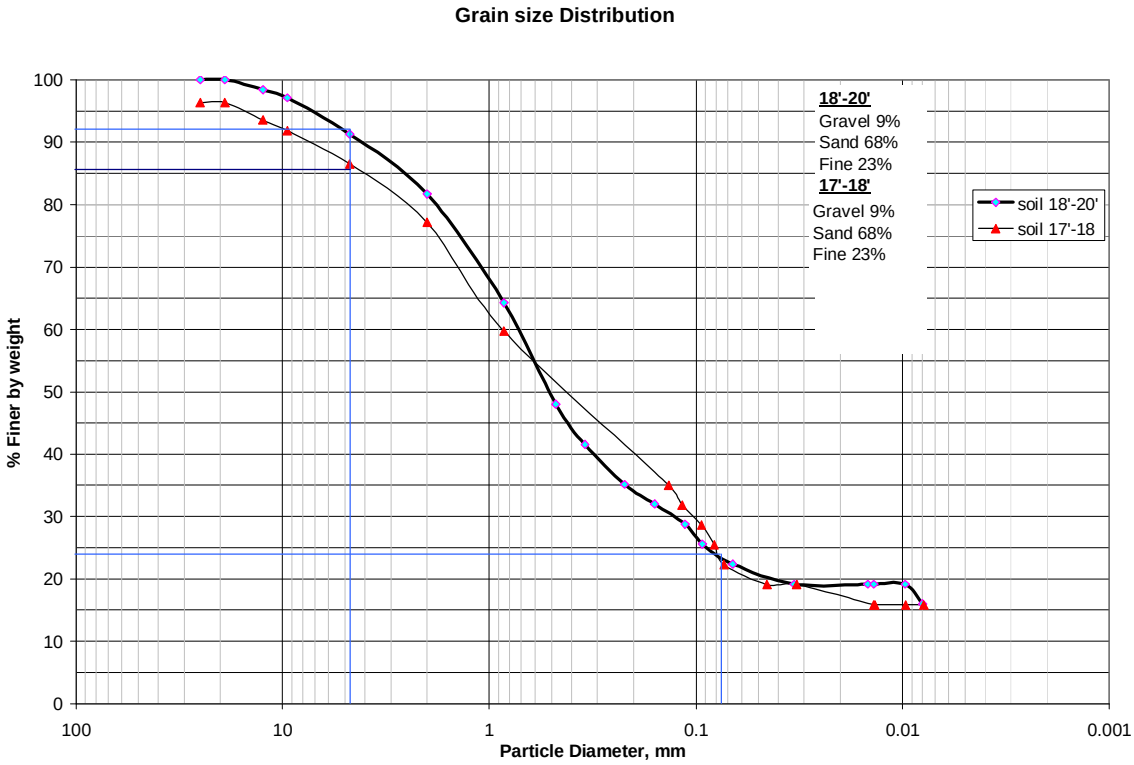

Figure A.1. Grain Size Distribution of Site Soils

West Virginia University Water Research Institute						
BORING LOG						
Project:	Lockbourne AFB-Ph 3			Boring No.	DP-601	
Boring #	**DP-601**			Sheet	1 of 3	
Method:	**Direct Push, Rig: SIMCO 2400**	**Run Length: 4'-0"**				
Inspector:	John Quaranta		Date Started:	15 Nov 06	Date Completed:	15 Nov 06
Driller:	Belasco Drilling Co., Mr. Alan Swisher		Boring Location:	North of Row 25		
EPA Method: 8015 Mod. Wide Window,			Coordinates:	**39.82908 N, 82.92200 W**		

Depth (ft)	Description	Rec. (ft)	Analytical Sample No.	Field Screening Result (ppm)	Remarks
0.0	Vegatation, Fill, Brown clay CH,				
1.3	high plasticity, moist, med. Stiff				
2.0					
2.5	SC sand w/clay; Fuel odor				
2.6	Brown clay CH, high plasticity,				
3.0	moist, med. Stiff				
3.5					
4.0		2.6			Push #1
4.5					
5.0					
5.5					
6.0					
7.0	Brown clay w/sand, CL, gavel 1/8"				
7.5	to 1/4" ; Fuel odor	3.0			Push#2
8.0				PID:	
8.5	Clay w/small gravel, sand, fuel			VOC=2050	
9.0	odor			LEL=7%	
10.0					
10.5					
11.0					
12.0	Firm brown clay, small stones, CL	4.0			Push #3
12.1					
12.5	No recovery, compacted tube				
13.0				PID: VOC=185 LEL=4%	
13.5					
14.0			**DP-601-14**		
14.5					
15.0					
16.0	Brown sandy clay SM, fuel odor	3.5			Push #4
16.1					
16.5	No recovery, compacted tube				
16.6					
17.0	Gravel w/sand SM, fuel odor, low			Soil Bag to Mo	
18.0	plasticity				
19.0			DP-601-19		
20.0	Brown clay w/sand, SC, fuel odor	3.5			Push #5
20.1					
21.0					
22.0					
23.0	Gravel w/sand SP, fuel odor, wet,		DB-601-23		
24.0	cobbles w/small stones	4.0			Push #6
24.1					
25.0					
25.5	No recovery, compacted tube				
25.6					
26.5	Brown, silty sand SM, wet				
27.0	Brown, wet, SP gravel w/fines, 1"				
28.0	stones, less odor	2.5			Push #7

Figure A.2 Boring Log 601 located North of Row 25 (See Figure 1 of Paper 1)

West Virginia University Water Research Institute						
BORING LOG						
Project:	Lockbourne AFB-Ph 3			Boring No.	DP-602	
Boring #	**DP-602**			Sheet	1 of	2
Method:	**Direct Push, Rig: SIMCO 2400**	**Run Length: 4'-0"**				
Inspector:	John Quaranta		Date Started:	15 Nov 06	Date Completed:	15 Nov 06
Driller:	Belasco Drilling Co., Mr. Alan Swisher		Boring Location:	North of Row 18, PVW Col K		
EPA Method: 8015 Mod. Wide Window,			Coordinates:	**39.82895 N, 82.92183 W**		

Depth (ft)	Description	Rec. (ft)	Analytical Sample No.	Field Screening Result (ppm)	Remarks
0.0					
2.5	No recovery, compacted tube				
3.0	Brown clay, low plas, SC, low				
4.0	water, wet	1.5			Push #1
4.1					
5.8					
5.9					
6.0	No recovery, compacted tube				
7.0	Clay, firm high plastic, SC, odor,				
8.0	moist, small stones	2.2			Push#2
8.1					
8.5					
9.0	No recovery, compacted tube				
10.0					
10.5					
11.0	Clayey sand SC, plastic, moist				
12.0	small angular gravel, fuel odor	2.0			Push #3
12.1					
13.0	No recovery, compacted tube				
14.0				PID, VOC=90.8, LEL=0%	
14.1					
15.0	Brown, high plastic clay, SC, high		**DP-02-15**		
16.0	odor, 1/4" rounded stones	2.5			Push #4
16.1					
16.5					
17.0					
17.5	Brown, high plastic clay, SC, high				
18.0	odor, 1/4" rounded stones				
19.0	Gravel w/sand SP, fuel odor, wet,		**DP-02-19**		
20.0	cobbles w/small stones	4.0			Push #5
20.1	SM, brown sandy small gravel				
22.0	1/4", fuel odor				
22.1					
23.0					
24.0	SP, roun small gravel	4.0			Push #6
24.1					
25.0					
26.0					
26.1					
26.5					
27.0	SP, saturatd, no odor, 1/2" -				
28.0	1"gravel	4.0			Push #7

Figure A.3 Boring Log 602 located North of Row 18 (See Figure 1 of Paper 1)

West Virginia University Water Research Institute						
BORING LOG						
Project:	Lockbourne AFB-Ph 3			Boring No.	DP-603	
Boring #	**DP-603**			Sheet	1 of	3
Method:	**Direct Push, Rig: SIMCO 2400**	**Run Length: 4'-0"**				
Inspector:	John Quaranta		Date Started:	15 Nov 06	Date Completed:	15 Nov 06
Driller:	Belasco Drilling Co., Mr. Alan Swisher		Boring Location:	North of Row 11, Column J		
EPA Method: 8015 Mod. Wide Window,			Coordinates:	**39.82888 N, 82.92175 W**		

Depth (ft)	Description	Rec. (ft)	Analytical Sample No.	Field Screening Result (ppm)	Remarks
0.0					
1.8	Compacted, no recovery				
2.0					
2.5					
2.6					
3.0					
3.5	SC sand w/clay;fill, low odor, very				
4.0	firm, 1/8" gravel	2.2			Push #1
4.1					
5.0					
5.5	Compacted, no recovery				
6.0					
7.0	SC sand w/clay;fill, no odor, very				
7.5	firm, 1/8" gravel	2.0			Push#2
8.0					
8.5					
9.0	Compacted, no recovery				
10.0					
10.5					
11.0	SM, Clay grey w/large 1" gravel				
12.0	high plasticity	2.0			Push #3
12.1					
13.4	No recovery, compacted tube				
13.0					
13.5					
14.0					
14.5					
15.0	SC, clay, firm moist, light odor,				
16.0	gravel to 1/4"	2.5			Push #4
16.1					
16.5	No recovery, compacted tube				
16.6					
17.0			DP-603-17	PID, VOC=1099, LEL=0	
18.0					
19.0	Gravel w/sand SM, high fuel odor,				
20.0	low plasticity, gravel 1/2"	3.5			Push #5
20.1					
21.0					
22.0					
23.0	Gravel w/sand SP, low fuel odor,				
24.0	wet, gravel 3/4"	3.5			Push #6
24.1					
25.0					
25.5	No recovery, compacted tube				
25.6					
26.5					
27.0					
28.0	GM, gravel no odor	2.5			Push #7

Figure A.4 Boring Log 603 located North of Row 11 (See Figure 1 of Paper 1)

West Virginia University Water Research Institute						
BORING LOG						
Project:	Lockbourne AFB-Ph 3			Boring No.	DP-604	
Boring #	**DP-604**			Sheet	1 of	3
Method:	**Direct Push, Rig: SIMCO 2400**	**Run Length: 4'-0"**				
Inspector:	John Quaranta		Date Started:	15 Nov 06	Date Completed:	15 Nov 06
Driller:	Belasco Drilling Co., Mr. Alan Swisher		Boring Location:	North of Row 5, Column J		
EPA Method: 8015 Mod. Wide Window,			Coordinates:	**39.82880 N, 82.92165 W**		

Depth (ft)	Description	Rec. (ft)	Analytical Sample No.	Field Screening Result (ppm)	Remarks
0.0					
1.8	Compacted, no recovery				
1.9					
2.5	SC sand w/clay;fill, low odor, very				
2.6	firm, 1/8" gravel				
3.0					
3.5					
4.0		2.5			Push #1
4.1					
5.0					
7.0	Compacted, no recovery				
7.1					
7.0	SC sand w/clay;fill, no odor, very				
7.9	firm, 1/8" gravel	1.0			Push#2
8.0					
9.0					
10.0					
11.0			DP-604-10	VOC=2017	
11.5	SC sat, odor, plastic clay, 1/2"			LEL=7%	
12.0	rounded gravel	2.0			Push #3
12.1					
13.4	No recovery, compacted tube				
13.0					
13.5					
14.0					
14.5					
15.0	SC, clay, firm moist, light odor,		DP-604-15	VOC=2030	
16.0	gravel to 1/4"	3.3		LEL=9%	Push #4
16.1					
16.5	No recovery, compacted tube				
16.6					
17.0					
18.0					
19.0	SC, clay, firm moist, light odor,				
20.0	gravel to 1/4"	3.5			Push #5
20.1					
21.0	No recovery, compacted tube				
22.0					
23.0					
24.0	GM, gravels light odor	3.5			Push #6
24.1					
25.0					
25.5					
25.6					
26.5					
27.0					
28.0	GM, gravel no odor	3.5			Push #7

Figure A.5 Boring Log 604 located North of Row 5 (See Figure 1 of Paper 1)

West Virginia University Water Research Institute						
BORING LOG						
Project:	Lockbourne AFB-Ph 3			Boring No.	DP-605	
Boring #	**DP-605**			Sheet	1 of 3	
Method:	**Direct Push, Rig: SIMCO 2400**	**Run Length: 4'-0"**				
Inspector:	John Quaranta		Date Started:	15 Nov 06	Date Completed:	15 Nov 06
Driller:	Belasco Drilling Co., Mr. Alan Swisher		Boring Location:	east of LMW4		
EPA Method: 8015 Mod. Wide Window,			Coordinates:	**39.82910 N, 82.92230 W**		

Depth (ft)	Description	Rec. (ft)	Analytical Sample No.	Field Screening Result (ppm)	Remarks
0.0					
2.5					
3.0					
4.0	fill	2.0			Push #1
4.1					
5.8					
5.9					
6.0					
7.0	ML, brown clay, lean 1/8" rounded				
8.0	gravel	2.0			Push#2
8.1					
8.5					
9.0	No recovery, compacted tube				
10.0			**DP-605-10**	VOC=234 ppm	
10.5				LEL=7%	
11.0	Grey clay, ML firm, moist, Strong				
12.0	fuel odor	2.5			Push #3
12.1					
13.0					
14.0					
14.1					
15.0	No recovery, compacted tube		**DP-605-16**		
16.0	CL, strong odor, clay very plastic	0.7			Push #4
16.1					
16.5					
17.0					
17.5	No recovery, compacted tube				
18.0	CL, strong odor, clay very plastic				
19.0	odor, 1/4" rounded stones				
20.0		3.0	**DP-605-20**	VOC=1.4	Push #5
20.1					
21.0					
21.5	stones				
23.0					
24.0		3.0			Push #6
24.1					
25.0					
26.0					
26.1					
26.5					
27.0	GP, sat, well sorted gravel, no				
28.0	odor	4.0			Push #7

Figure A.6 Boring Log 605 located East of LMW-4 (Closest Line is #1; See Figure 1 of Paper 1)

APPENDIX B. MULTIPHASE GOVERNING EQUATIONS

Multiphase flow

The mass conservation equations for water (*w*) and NAPL (*o*) for incompressible liquids and compressible gas (a) are displayed in Equation 1 to Equation 3 (Katyal et. al. 1988, Yen et. al. 2003).

$$f\frac{\partial S_w}{\partial t} = -\frac{\partial q_{wi}}{\partial x_i} + \frac{R_w}{r_w}$$

Equation (1)

$$f\frac{\partial S_o}{\partial t} = -\frac{\partial q_{oi}}{\partial x_i} + \frac{R_o}{r_o}$$

Equation (2)

$$f\frac{\partial r_a S_a}{\partial t} = -\frac{\partial r_a q_{ai}}{\partial x_i} + R_a$$

Equation (3)

The Darcy velocities in the p-phase (p = w,o,a for water, oil, and gas phases) are defined by Equation 4 (Katyal et al. 1988, Yen et al. 2003).

$$q_{pi} = -K_{pij}\frac{\partial y_p}{\partial x_j} + r_{rp}u_j$$

Equation (4)

where K_{pij} = p-phase conductivity tensor; $\psi p=(p_p /g\rho_w$* is the water equivalent pressure head for phase p; P_p=p-phase pressure; g=gravitational acceleration; ρ_w*=density of pure water; $\rho_{rp}=(\rho_p /\rho_w$* is the p-phase specific gravity; ρ_p= p-phase density; $u_j=(\partial z/\partial x_j)$ is a unit gravitational vector measured positive upwards; z=elevation; Φ=porosity; S_p=p-phase saturation; Rp=net mass transfer per unit porous media volume

into (+) or out of (-) phase p; and t=time. Equation 4 integration in the Z direction between the lower bound of the aquifer (Z_L) and the upper bound equal to the top elevation of the capillary fringe (Z_U) under the assumption of vertical equilibrium gives the horizontal, vertically integrated, fluxes (L^2T^{-1}) as in Equation 5, 6 and 7 (Katyal et al. 1988, Yen et al. 2003).

$$Qwx_i = -Tw_{ij}\frac{\partial Zaw}{\partial x_j}$$

Equation (5)

$$Qox_i = -To_{ij}\frac{\partial Zao}{\partial x_j}$$

Equation (6)

$$Qax_i = -Ta_{ij}\frac{\partial Zaa}{\partial x_j}$$

Equation (7)

where Q_{wxi}, Q_{oxi}, and Q_{axi}=horizontal vertically integrated fluxes (L^2 T^{-1}) for water, oil, and gas, respectively, in the x_i (i=1,2) directions; $Tw_{i\ j}$ =water transmissivity tensor; To_{ij}

= oil transmissivity tensor; and Ta_{ij}=gas transmissivity tensor. Equation 8 and 9 (Katyal et al. 1988, Yen et al. 2003) describes the phase transmissivities for water-oil and gas respectively.

$$Tp_{ij} = \int_{Z_L}^{Z_u} k_{rp} Ksp_j dz$$

Equation (8)

$$Ta_j = \int_{Z_L}^{Z_u} k_{ra} Kso_{ij} dz$$

Equation (9)

Krp=relative permeability of phase P; Ksw_{ij} =saturated hydraulic conductivity tensor; Kso_{ij} =($\rho_{ro}Ksw_{ij}/n_{ro}$), Ksa_{ij}=($\rho_{ro}Ksw_{ij}/n_{ra}$); Zu and ZL=lower and upper integration limits for the water and oil phases; Zs=ground surface elevation; n_{ro}=oil to water dynamic viscosity ratio; n_{ra}=air to water dynamic viscosity ratio; Rp=source/sink rate (LT^{-1}); p=w, o, and a for the water, oil, and gas phases; and Pao=elevation of the air-oil interface.

The vertically integrated volume balance equation for the water, oil, and gas phases are displayed in Equation 10, 11 and 129 (Katyal et al. 1988, Yen et al. 2003), where Vw=specific volume (L) of water; Vo=specific volume (L) of NAPL; and Va=specific volume (L) of gas.

$$\frac{\partial Vw}{\partial t} = \frac{\partial}{\partial x_i}[Tw_{ij}\frac{\partial Zaw}{\partial x_j}] + R_w$$

Equation (10)

$$\frac{\partial Vo}{\partial t} = \frac{\partial}{\partial x_i}[To_{ij}\frac{\partial Zao}{\partial x_j}] + R_o$$

Equation (11)

$$\frac{\partial Va}{\partial t} = \frac{\partial}{\partial x_i}[Ta_{ij}\frac{\partial Zaa}{\partial x_j}] + R_a$$

Equation (12)

Constitutive Relationship between water and LNAPL

Relationships between phase saturations and pressures are described by a three-phase extension of the Van Genuchten (1980) model which takes into account the effects of LNAPL entrapment. Prior to the occurrence of oil at a given location, the system is treated as a two-phase air-water system described by the Van Genuchten (1980) function.

$$\bar{S}_w = \left[1 + (a y_{aw})^n\right]^{-m}$$

Equation (13)

Where

$\bar{S}_w = \dfrac{(S_w - S_m)}{(1 - S_w)}$ is the effective water saturation,

S_m is the irreducible water saturation,

$y_{aw} = h_a - y_w$ is the air-water capillary pressure,

α [L^{-1}] and n are porous medium parameters, and

$m = 1 - \dfrac{1}{n}$

Following the occurrence of oil at a location, the system is described by the three phase relations.

$$\bar{\bar{S}}_w = \left[1 + \left(a \frac{s_w}{s_{ow}} y_{ow}\right)^n\right]^{-m}$$

Equation (14)

$$\overline{S}_t = \left[1 + \left(a \frac{s_w}{s_o} y_{ao}\right)^n\right]^{-m}$$

Equation (15)

Where

$\overline{\overline{S}}_w$ is the apparent water saturation,

$\overline{S}_t$ is the effective total liquid saturation,

$y_{ow} = y_o - y_w$ is the oil-water capillary pressure,

$y_{ao} = h_a - y_o$ is air-oil capillary pressure,

s_w is the surface tension of water,

s_o is the surface tension of oil,

s_{ow} is the oil-water interfacial surface tension.

The apparent water saturation is given by

$$\overline{\overline{S}}_w = \overline{S}_w + \overline{S}_{ot}$$

Equation (16)

Where

$\overline{S}_{ot}$ is the effective trapped oil saturation which can be estimated using an empirical relationship given by Land, 1968 as

$$\overline{S}_{ot} = \frac{1-\overline{S}_w^{\min}}{1+R_{ow}(1-\overline{S}_w^{\min})} - \frac{1-\overline{\overline{S}}_w}{1+R_{ow}\left(1-\overline{\overline{S}}_w\right)} \; for \overline{\overline{S}}_w > \overline{S}_w^{\min}$$

$$= 0 \; for \overline{\overline{S}}_w \le \overline{S}_w^{\min}$$

Equation (17)

where,

$$R_{ow} = \frac{1}{\overline{\overline{S}}_{or}} - 1$$

Equation (18)

where

$\overline{S}_{or}$ is the maximum effective residual oil saturation where effective oil saturations are expressed in the form of $S_o * (1 - S_m)^{-1}$.

$\overline{S}^{min}$ is the minimum effective water saturation which is defined as the historical minimum

effective water saturation at a given location since changing from a two-phase air-water to a three phase air-oil-water system. Actual water and oil saturation may be computed as

$$S_w = (1 - S_m)(\overline{\overline{S}}_w - \overline{S}_{ot}) + S_m$$

Equation (19)

and

$$S_o = (1 - S_m)\overline{S}_t + S_m - S_w \; for Z_{ow} < Z < Z_u$$

$$S_o = 0 \; for Z \le Z_{ow} or Z > Z_u$$

Equation (20)

Where,

Z_{ow} = oil-water interface

Zu = top elevation of the capillary fringe

The vertical integration of phase saturation profiles gives specific volume of water, V_w and specific volume of oil V_o.

$$V_w = \int_{Z_L}^{Z_u} f S_w(Z) dz$$

Equation (21)

$$V_o = \int_{Z_{ow}}^{Z_u} fS_o(Z)dz$$

Equation (22)

Transport model

The general transport equation for a species in is expressed by Van Genuchten et al. (1976)) as

$$\frac{\partial}{\partial t}(q_m C_{am}) + \frac{\partial}{\partial t}(q_{im} C_{aim}) + \frac{\partial}{\partial t}(frP_{am}) + \frac{\partial}{\partial t}[(1-f)rP_{aim}] = \frac{\partial}{\partial x_i}(q_m D_{mij} \frac{\partial C_{am}}{\partial x_i}) - \frac{\partial}{\partial x_i}(q_{mi} C_{am}) - q_s C_{as}$$

Equation (23)

where θ_m and θ_{im} =soil fractions filled with mobile and immobile water, respectively; $C_{\alpha m}$ and $C_{\alpha im}$=concentrations (ML^{-3}) of species a in mobile and immobile water, respectively; q_{mi}=Darcy velocity (LT^{-1}); $P_{\alpha m}$ and $P_{\alpha im}$=species adsorbed phase concentration α in the mobile and immobile phase (MM^{-1}), respectively; f=sorption site fraction in direct contact with the mobile liquid; ρ=soil bulk density (ML^{-3}); qs=fluid injection volumetric flow rate (or withdrawal) per unit volume of porous medium; and $C_{\alpha s}$=species a concentration in the injected fluid. D_{mij}=hydrodynamic dispersion tensor, defined in Equation 24 (Katyal et. al. 1988, Yen et. al. 2003).

$$q_m D_{mij} = d_L |q| d_{ij} + (d_L - d_T)\frac{q_{mi} q_{mj}}{|q|} + q_m t D_c d_{ij}$$

Equation (24)

where d_L and d_T=longitudinal and transverse dispersivities, respectively; δ_{ij}=Kronecker delta; t5tortuosity; D_c=molecular diffusion coefficient; and |q|=absolute value for the

Darcy velocity.

The mass transfer terms between: (1) mobile water and immobile water $|I_{m\text{-}im}|$; and (2) mobile water and gas phase $|I_{m\text{-}g}|$ is defined as first-order processes in Equation 25 and 26 (Katyal et al. 1988, Yen et al. 2003) respectively.

$$I_{m-im} = X[C_{aim} - C_{am}]$$

Equation (25)

$$I_{m-g} = Xl[\frac{C_{aa}}{H} - C_{am}]$$

Equation (26)

where *X*=overall mass transfer coefficient between the mobile and immobile groundwater; and *X*l=overall mass transfer coefficient between the mobile groundwater and gas phase in the unsaturated zone. H is the dimensionless Henry's law constant. Incorporating these mass transfer terms into Equation 23 gives Equation 27 (Katyal et al. 1988, Yen et al. 2003).

$$\frac{\partial}{\partial t}(q_m C_{am}) + \frac{\partial}{\partial t}(frP_{am}) = \frac{\partial}{\partial x_i}(q_m D_{mij}\frac{\partial C_{am}}{\partial x_i}) - \frac{\partial}{\partial x_i}(q_{mi} C_{am}) - q_s C_{as} + I_{m-im} + I_{m-g}$$

Equation (27)

The vertical governing equation (Equation 23) integration in the z direction between the lower bound of the aquifer (Z_L) and the upper limit (Z_u) and assuming linear

adsorption ($P=k_dC$), decay losses $\lambda_{\alpha m}$ [T^{-1}] and the contaminant load from a hydrocarbon source to the mobile phase $H_{g\alpha}$ [L^{-1}] results in Equation 28 (Katyal et. al. 1988, Yen et. al. 2003).

$$\frac{\partial C_{\alpha m}}{\partial t_i}[V_{wm}+frBK_d]=\frac{\partial}{\partial x_i}(V_{wm}D_{mij}\frac{\partial C_{\alpha m}}{\partial x_j})-Q_{wi}\frac{\partial C_{\alpha m}}{\partial x_i}-q_s(C_{\alpha s}-C_{\alpha m})B_l-l_{\alpha m}B_l+B_lH_{g\alpha}+I_{m-im}B_l+I_{m-g}B_l$$

Equation (28)

where V_w=specific volume of water; V_{wm}=specific volume of water in the mobile phase $\cong V_wS_m$; Q_{wi} and Q_{wj}=horizontal, vertically integrated flux (L^2 T^{-1}). Similarly, the vertically integrated transport equation for species α in the unsaturated zone gas phase is displayed in Equation 29 (Katyal et al. 1988, Yen et al. 2003).

$$\frac{\partial}{\partial t}[V_aC_{\alpha a}]=\frac{\partial}{\partial x_i}[V_aD_{aij}\frac{\partial(C_{\alpha a})}{\partial x_j}]-\frac{\partial}{\partial x_i}[Q_{azj}C_{\alpha a}]+b_{ui}H_{\partial a}+l_{\alpha a}B_{ui}-I_{g-mw}B_{ui}-I_{g-imw}B_{ui}-Q_aC_{\alpha as}$$

Equation (29)

where Va=specific volume of air in the unsaturated zone; Daij=hydrodynamic dispersion tensor in the gas phase; $H_{\partial a}$ =contaminant load from a hydrocarbon source into the gas phase; Q_{azj}=vertically integrated gas flux; B_{ui}=unsaturated zone thickness; $\lambda_{\alpha a}$=decay term for the unsaturated zone; and the last term is the source/sink for the gas phase.

APPENDIX C. SELECTED SIMULTAION INPUT

Table C.1. Parameter Values Used in Simulation Analysis.

Parameters	Selected value	Recommended range
Time weighting factor	0.5	0.5-1.0
Absolute convergence limit for all phases [m]	0.005	0.001-0.2
Relative convergence limit for all phase	0.0001	0.0001–0.005
Thickness of capillary zone [m]	0.3	
Density of water [g/m3]	$1x10^{6}$	
Density of oil [g/m3]	$8x10^{5}$	
Density of air[g/m3]	1200	
Ratio of oil to water phase density[g/m3]	0.8	
Ratio of air to water dynamic viscosity	0.018	
Highest elevation of Zao fluid table likely to occur[m]	4.88 (BGS)	
Lowest elevation of Zao fluid table likely to occur[m]	9.17 (BGS)	
Soil Properties		
Permeability, Ksx [cm/s]	$8x10^{-6}$	
Permeability, Ksy [cm/s]	$8x10^{-6}$	
Porosity	0.45	
Alpha [m^{-1}]	3	
Parameter n	1.4	
Permeability, Ksz [cm/s]	$8x10^{-6}$	
Bulk density for soil type [g/m3]	1.5	
Soil Properties Variable		
Residual water	0.09	
Residual oil	0.15	
Residual gas	0.05	
Transport Parameters		
Number of species	1	
Name of species	Benzene	
Solubility[mg/L]	1780	
Species mole fraction in hydrocarbon	1%	
Longitudinal dispersivity [m]	1.83	
Transverse dispersivity [m]	0.183	
Henry's coefficient	0.24	
Distribution coefficient [1/g/m3]	0.83	
Initial concentration[mg/l]	0.3	
Transport Parameters Variable		
Loading from hydrocarbon in water [/m]	0.371	
Loading from hydrocarbon in gas [/m]	7.45	

APPENDIX D. A SAMPLE OPTIMIZATION PROGRAM

Genetic Algorithm program to determine the time for raising groundwater table

```
function [X,FVAL,REASON,OUTPUT,POPULATION,SCORES] =  gtest7
%%    This is an auto generated M file to do optimization with the
Genetic Algorithm and
%      Direct Search Toolbox. Use GAOPTIMSET for default GA options
structure.
clear;
tic
%%Fitness function
fitnessFunction = @final_opt_LLB;
%%Number of Variables
nvars =1;
lb=[6];
ub=[100];
%Start with default options
options = gaoptimset;
%%Modify some parameters
options = gaoptimset(options,'PopulationSize' ,40);
options = gaoptimset(options,'Generations' ,20);
options = gaoptimset(options,'EliteCount' ,1 );
options = gaoptimset(options,'StallGenLimit' ,1000);
options = gaoptimset(options,'StallTimeLimit' ,Inf);
options  =  gaoptimset(options,'MutationFcn'  ,{  @mutationgaussian  1   1
});
options = gaoptimset(options,'Display' ,'diagnose');
%%Run GA
[X,FVAL,REASON,OUTPUT,POPULATION,SCORES]                                =
ga(fitnessFunction,nvars,[],[],[],[],lb,ub,[],options);
toc

function[TOA]=final_opt_LLB(dv) %
[total_node_number,air_rate]=T_write(dv);
[Zao_output,Zaw_output]=T_read(total_node_number);
TOA=0;
TOA=-(TOA+air_rate*dv(1));
        %if Zaw_output(1)>5.79
        if Zaw_output(1)<Zaw_output(2)
            TOA=TOA+1e6*Zao_output(1)^4;  %give    a  high  penalty  and
return
            return
```

```
        end
            if Zaw_output(1)>Zaw_output(2)
            TOA=TOA+1e6*Zao_output(1)^4;  %give    a  high  penalty  and
return
            return
        end
return

% input sub function-2 to write the input file
function[total_node_number,air_rate]=T_write(dv)
air_rate=52.7;
time(1)=1.223;
file_prefix={'noflowboundarykair'};
file_type={'.dat'};
for i=1;%:time_no%2*time_no-1 % %-1 %5 % %nvars
        time(i+1)=time(i)+dv(i);%(i);%0.5;
    a=num2str(i);
    data_f1(i)=strcat(file_prefix,a,file_type);
    fid_read_input=fopen(char(data_f1(i)),'rt');
    ii=0;
    while feof(fid_read_input)==0
        ii=ii+1;
        readline(ii)={fgetl(fid_read_input)};
        if cell2mat(strfind(readline(ii),'99999   15'))>0
            node_info_line=ii;
        end
        if cell2mat(strfind(readline(ii),'1780.'))>0
            solubility=ii;
        end
    end
    node_info=(readline(node_info_line));
    [d1 d2 d3 d4 irow kcol d5 d6 d7 d8 d9 d10]=...
        strread(strvcat(node_info),'%f  %f  %f  %f  %f  %f  %f  %f  %f  %f  %f
%f');

    time_info_line=node_info_line+4;
    time_info=(readline(time_info_line));
    [d1 d2 previous_Time d3 d4 d5]=...
        strread(strvcat(time_info),'%f %f %f %f %f %f');
    fclose(fid_read_input);
    total_node_number=irow*kcol;
```

```
    fid_write_input=fopen(char(data_f1(i)),'wt+');
    for k=node_info_line-2:time_info_line-1
        fprintf(fid_write_input,'%s\n', cell2mat(readline(k)));
    end
    for k=time_info_line
        fprintf(fid_write_input,'%10.3f',time(i)); %time(i)
        fprintf(fid_write_input,[blanks(5) '0.005']);
        fprintf(fid_write_input,'%10.3f',time(i+1)); % time(i+1)
        fprintf(fid_write_input,[blanks(6) '0.05' blanks(6) '1.03'] );
        fprintf(fid_write_input,'%10.2f\n',(time(i+1)-
time(i))/2);%time(i+1)-time(i)
    end
        for  k=time_info_line+1:ii  %solubility-13  %  This  is  the  first
line of air boundary condition
            fprintf(fid_write_input,'%s\n', cell2mat(readline(k)));
        end
        fclose(fid_write_input);
end
return

% out put Subfunction-3 to run the file and read the output

function[Zao_output,Zaw_output]=T_read(total_node_number)%,time_no)
%file_prefix={'kair','k'};
file_prefix={'noflowboundarykair','noflowboundaryk'};
file_type={'.dat','.out','.aux'};
    i=1;%:time_no %2*time_no-1%time_no
        a=num2str(i);
        %b=num2str(i-1);
    data_f2(i)=strcat(file_prefix(1),a,file_type(1));
    out_f2(i)=strcat(file_prefix(1),a,file_type(2));
    auxf2(i)=strcat(file_prefix(1),a,file_type(3));
    file=fopen('C:\DAEM\BIOSLURP\daem.bat','wt+');
        auxf2_p=strcat(file_prefix(2),a,file_type(3));
        fprintf(file,'%s\n',char(data_f2(i)));
        fprintf(file,'%s\n',char(out_f2(i)));
        fprintf(file,'%s\n',char(auxf2_p));
        fprintf(file,'%s\n',char(auxf2(i)));
        fprintf(file,'%s\n','BIOSLURP.REC');
    fclose(file);
    dos('bioslurp.bat');
```

```
    % This is to read out put
    fid_read_output=fopen(char(out_f2(i)),'rt');
    iii=0;
    while feof(fid_read_output)==0
        iii=iii+1;
        readline(iii)={fgetl(fid_read_output)};
        if cell2mat(strfind(readline(iii),'NODE |- - - - - -- HEADS - -
-|  |- - SPECIFIC VOLUMES  - - - - -|'))>0
            read_head=iii;
        end
    end
    for hw=1:total_node_number %;1600
        head(hw)=(readline(read_head+5+hw));
        [node_no(hw)    Zaw(hw)    Zao(hw)    VW(hw)    VO(hw)    SOT(hw)
SOTO(hw)]=strread(strvcat(head(hw)),'%f %f %f %f %f %f %f');
    end
 Zao_output(1)=Zao(780);
 Zaw_output(1)=Zaw(780);
 Zaw_output(2)=Zaw(760);
fclose(fid_read_output);
return
```